

Università degli studi di Padova  
Corso di Laurea MAGISTRALE in Ingegneria Energetica  
Dipartimento di Ingegneria Industriale



## Analysis for the assessment of the wave energy and ISWEC productivity along the argentinian coast

Relatore: Prof.ssa. Giovanna Cavazzini

Correlatore: Prof.ssa Giuliana Mattiazzo  
Prof. Giovanni Bracco

Laureando:  
Garbin Davide, matricola 1134289

Anno Accademico 2017-2018



*Alla vita, alle mille opportunità che ci dá,  
alle mille che ci toglie.  
Al futuro, al progresso.  
A tutte le persone che aiutandomi hanno contribuito a questo lavoro.  
L'unico limite é dentro di noi.*



# Contents

<b>Acknowledgements</b>	<b>3</b>
<b>Abstract</b>	<b>5</b>
<b>1 World global energy resources</b>	<b>9</b>
1.1 World Energetic mix today and a future perspective . . . . .	11
1.1.1 Renewables . . . . .	12
1.2 "Paris agreement", COP21 . . . . .	14
1.3 Argentine country . . . . .	16
1.3.1 Climate and biodiversity . . . . .	16
1.3.2 Economy and industry . . . . .	16
1.3.3 Argentine energetic mix . . . . .	17
1.3.4 Renewable development . . . . .	19
1.3.5 Policy measures relating to climate change and low carbon infras- tructure . . . . .	22
<b>2 Wave energy</b>	<b>23</b>
2.1 Wave energy converters classification . . . . .	26
2.1.1 Types . . . . .	27
2.1.2 Modes of operation . . . . .	29
2.2 Europe state of the art . . . . .	31
2.2.1 Market status . . . . .	31
<b>3 Mathematical view</b>	<b>35</b>
3.1 Introduction . . . . .	35
3.2 The simple linear wave . . . . .	36
3.2.1 Influence of water depth . . . . .	37
3.2.2 Orbital motion of wave particles . . . . .	38
3.3 Superposition theory: real ocean waves . . . . .	39
3.4 Wave records . . . . .	41
3.5 Wave spectrum . . . . .	41
3.6 Balance equation and WAM model . . . . .	44
3.6.1 Sources and sinks description . . . . .	45

<b>4</b>	<b>ISWEC device</b>	<b>49</b>
4.1	Reference frames . . . . .	51
4.2	Working principle . . . . .	52
4.3	Mathematical view . . . . .	52
4.3.1	Available power . . . . .	53
4.4	Device control . . . . .	56
4.4.1	PTO stiffness . . . . .	56
4.4.2	Flywheel speed $\dot{\phi}$ . . . . .	57
4.4.3	Wave frequency . . . . .	57
4.5	Power matrix . . . . .	58
4.6	Mooring system . . . . .	59
4.6.1	Geometry and relation with depth . . . . .	60
4.7	ISWEC in numbers . . . . .	63
<b>5</b>	<b>Analysis of the marine resource</b>	<b>65</b>
5.1	Reanalyses dataset . . . . .	66
5.1.1	Differences between measured data and assimilated data . . . . .	66
5.1.2	Uncertainty estimation . . . . .	67
5.1.3	Availables datasets . . . . .	67
5.2	ERA5 brief description . . . . .	70
5.2.1	Ocean waves . . . . .	71
5.3	IFS quick view . . . . .	72
5.4	Considered parameters and how they're obtained . . . . .	73
<b>6</b>	<b>Argentinian resource mapping</b>	<b>75</b>
6.1	Introduction . . . . .	76
6.2	Sea state study: wave resource map . . . . .	77
6.3	Device rank on the sea state: productivity map . . . . .	78
6.4	Validation for Mediterranean basin . . . . .	81
6.5	Results . . . . .	82
<b>7</b>	<b>Site selection and tecno-economic evaluation</b>	<b>83</b>
7.1	Bathymetry database . . . . .	84
7.2	Distance to power grid . . . . .	84
7.3	Presence of Natural Parks or Marine Protected areas . . . . .	87
7.4	Cost of kWh for a 10 device farm . . . . .	88
<b>8</b>	<b>Conclusions</b>	<b>93</b>
8.1	Afterwards . . . . .	94
	<b>Bibliography</b>	<b>95</b>

# Acknowledgements

Ringrazio la mia relatrice professoressa Giovanna Cavazzini, che mi ha dato la possibilità di scrivere questa tesi; professoressa Giuliana Mattiazzo del Politecnico di Torino per l'opportunità offertami di lavorare su questo progetto al fianco di persone di grande competenza e professionalità; Giovanni Bracco in primis per l'infinita pazienza nel seguirmi; Vincenzo Orlando e Stefano Roveda per i dati ed il supporto.





# Abstract

World's thirst of energy is constantly growing and in the last 20 years someone realized that the World needs something more than just energy: it needs a sustainable development of the whole society, not only the energy sector. Developing countries like India, China and others are on the way to reach European industrialization levels but to do this aren't tanking care of the climate change related to, the most famous picture that spread many times ago is the following: a classical Beijing sunrise covered by pollution.



*Figure 1: Beijing sunrise covered by pollution*

In particular, the current global warming trend is found to be related with intense human consumption of fossil fuels, being used as primary energy source for different activities such as industrial production, goods and people transportation and electricity generation. In fact the combustion of fossil fuels causes the emission of several gases, carbon dioxide and methane among the others. These gases, once released in the atmosphere, increase the Earth natural greenhouse effect, thus generating an anthropic-led, uncontrolled and unpredictable increase of our planet surface temperatures.

The United Nations Framework Convention on Climate Change (UNFCCC) is the main international agreement on climate action. It was one of three conventions adopted at the Rio Earth Summit in 1992. To date, it has been ratified by 195 countries. It started as a way for countries to work together to limit global temperature increases and climate change, and to cope with their impacts. After that, Kyoto Protocol and Paris Agreement are the two most important International agreements to set targets mainly on global warming

temperature and secondly on renewable slice of national power mix.

All future energy outlook says that the renewable sources will get a bigger slice of national energetic mix year by year, driven by governments incentives to witness that renewables represent a solution to reduce GHG emissions, at least the ones by electric production.

The present thesis want to propose an application of a new renewable energy harvesting device along the coast of a country that has many good reasons to use this technology, analysing before Argentinian country on Chapter 1 and why it needs "green" projects; than the ocean source review on Chapter 2, presenting how it's composed and today's most important devices to harvest it. On Chapter 3 will be presented the mathematical model build up behind the natural phenomenon with an important section dedicated to describe how Chapter 5 dataset is made up. This thesis device, ISWEC, thanks to Politecnico di Torino for its important support, is showed in Chapter 4 and its mathematical model used in Chapter 6 is analysed and explained. Finally in Chapter 7 has been done an "exclusion siting criteria" (called ESC) to highlight areas suitable for an installation of the device (a farm of it). The interest for harvest energy from waves recently increased, first of all due to the enormous potential offered and then for the continuity of the source, compared for example with the solar source. Besides, forecasts for sea state conditions are quite good compared to forecasts for wind state or solar state.

This thesis work want also to give a standard procedure to get installation maps (with several informations like yearly productivity, bathymetry, wave potential, distance to coast, etc) of ISWEC for different areas, procedure that, before this thesis, had been done only for small areas like an island or a marine site near a port, using sea status data beginning from wavemeter buoys.





# Chapter 1

## World global energy resources

It doesn't matter the country you are looking at, in the whole World the energy demand and the consequent electrification is constantly growing up and the reasons are several and out of this context. Since the end of the Second World War the society has evolved without stopping and until a few years ago without taking care of our planet. In the following chart is showed the growing energy demand from 2000 to 2014 with pointed the GDP (gross domestic product), clearly highlighting what said before.

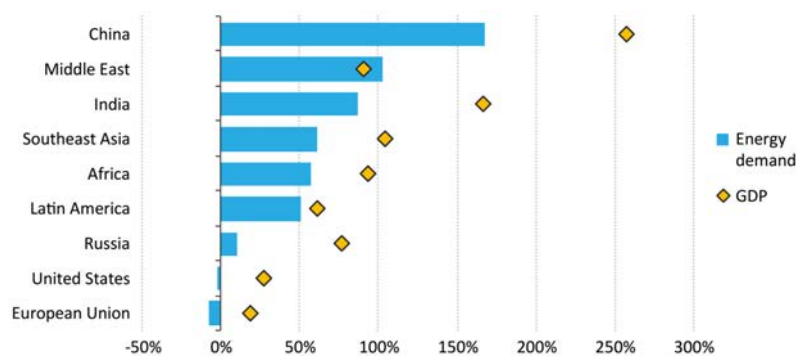


Figure 1.1: Energy demand change from 2000 to 2014 for many countries

Fortunately someone has realized and with someone one can not fail to mention, Gro Harlem Brundtland, which with the definition of *Sustainable development* born with its report «Our common future» in 1987, has fixed the guide line of today's renewable sources: "Sustainable development is development that meets the needs of the present without compromising the ability of future generations to meet their own needs.". The most important pointer that reflects what Brundtland wanted to mark-up is the  $CO_2$  emissions, the prince of the green-house gas emitted by combustions. Looking at its trend in the last 20 years and what could happen in the future with today's trend:

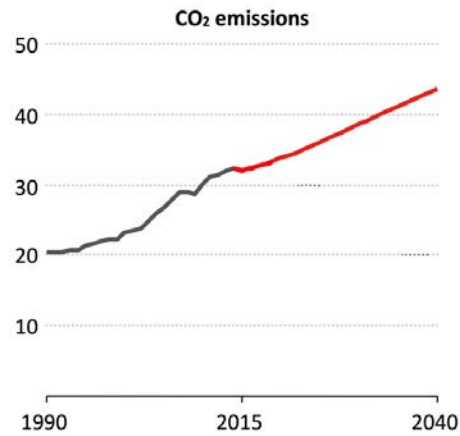


Figure 1.2: CO<sub>2</sub> trend

It's evident that World development is not going parallel to Brundtland sustainable concept. Giving a view of what could happen in the future energy demand using many different scenarios (according to what explained in [8]), the constant grow in energy demand is the minimum common denominator for each scenario:

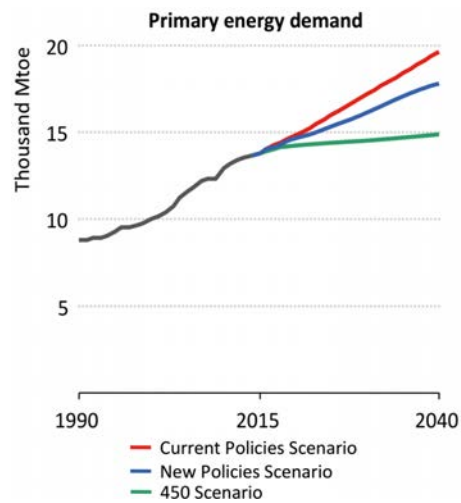


Figure 1.3: Global primary energy demand by scenario to 2040

## 1.1 World Energetic mix today and a future perspective

Up to 2014 ([8]) the World's energetic mix is governed by Coals and Oils technologies, due mainly to the low price of that sources and also to a strong consolidated engineering.

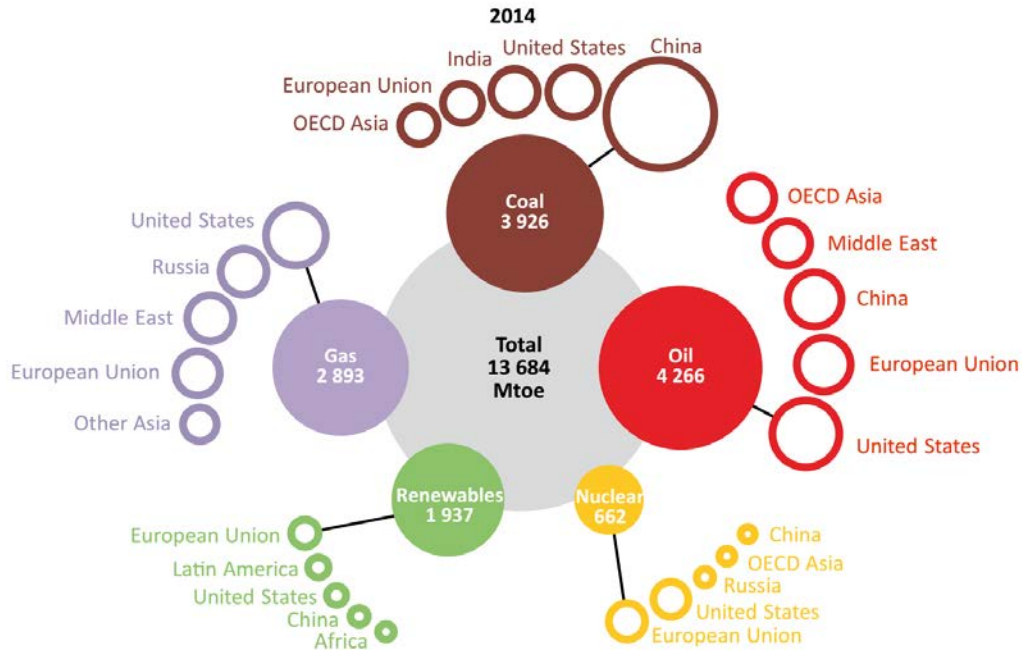
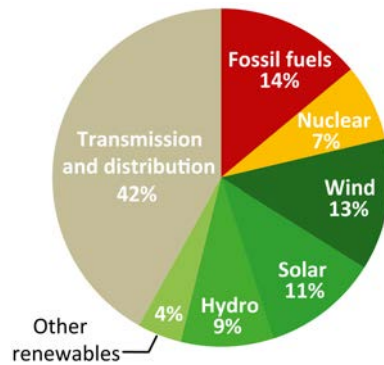


Figure 1.4: Global primary energy mix, 2014, [8]

An authoritative source ([8]) said that electricity demand is projected to grow at 2% annually, increasing by two-thirds to 2040, compared with global economic growth of 3.4%, a marked change from the period 1990-2014 when they grew at almost the same pace. Energy efficiency measures but also macroeconomic and demographic factors slow electricity growth in several mature economies. Almost half of total global electricity demand growth is in China and India, mainly in buildings (23%) and industries (21%). Electricity supply worldwide is set to diversify and decarbonise, with low-carbon generation overtaking coal before 2020. Coal-fired power's share of generation is projected to fall from above 40% now to 28% in 2040. By then, wind, solar and bioenergy-based renewables combined increase their market share from 6% to 20%. China generates almost all its incremental power from renewables, nuclear and natural gas. Globally, by 2040 producing a unit of electricity is projected to emit one-third less  $CO_2$  than today; but emissions from the power sector still rise by 6%.

The power sector (emissions from which currently account for 42% of energy-related carbon-dioxide  $CO_2$  emissions) is in the vanguard of efforts to decarbonise the energy system. Electricity provides the means to use non-fossil fuels, e.g. hydropower, nuclear and, increasingly, non-hydro renewables such as wind and solar, to produce low-carbon final energy and to contribute to the decarbonisation of final uses previously dependent on fossil fuels, for example by means of electric vehicles in transport and efficient heat pumps in industry.

For the first time in 2015, additions of renewables-based generating capacity worldwide exceeded those from all other energy sources taken together, and total installed renewables capacity passed that of coal, this can be showed in the following picture that shows the investments in global power sector.



*Figure 1.5: Investments by source in global power sector*

The global energy mix does not change easily. Although government policies, relative prices, changing costs and consumer needs all create incentives to switch fuels or to introduce a new technology in order to obtain a better energy service, in practice the energy system has a great deal of inertia. Light bulbs and office equipment might be replaced every few years, but the lifetimes of vehicles, factories, power plants and buildings are much longer, and each bit of infrastructure locks in certain patterns of energy use. So, in the absence of a concerted policy push or a dramatic change in relative prices, the positions of the different fuels and technologies in worldwide energy use tends to be fairly stable.

### 1.1.1 Renewables

Any credible path to achieving the world's climate objectives must have renewable energy at its core. The global transition to a low-carbon future is one of the most fundamental and comprehensive challenges ever faced by the energy sector, with every part of the energy system affected. The necessary effort will last for decades and the picture is evolving every day. The political commitments made at COP21 have reinforced the position of renewables as the dominant energy growth story. The power sector is leading the change, with the renewable component regularly breaking its own records for investment and deployment. But, in a decarbonised world, renewables must also permeate other fields of energy use in industry, buildings and transport, where supportive policies are often fewer and adoption has been slower. Renewables bring environmental, economic and energy security benefits. But the challenges that they face are large. While some renewables are already competitive in existing markets, others teeter on the line between needing support and being competitive, while others clearly cannot survive without financial support.



## Renewable energy resources and technologies

Renewable energy encompasses a broad range of energy resources and technologies that have differing attributes and applications. Renewable resources include solar, wind, bioenergy, hydropower, geothermal and marine energy. They are abundant (the collective energy potential being very many times greater than world demand) and widely distributed; but they are not equally easy to harness. Some examples include hydro and wind resources for electricity generation, bioenergy resources for road transport fuels (liquid biofuels) and biomass, solar and geothermal resources to produce electricity and/or heat. While renewable energy may be harnessed to provide a range of energy services (powering appliances and motors, space/water heating and cooking in buildings, transport etc.), not all types are able or suited to provide all types of energy service. Some important distinctions when discussing renewable energy are:

- **Variable or dispatchable renewables** - Due to the fluctuating nature of some resources (such as wind and solar), variable renewables cannot always be called upon when desired. Dispatchable renewables (e.g. hydropower or bioenergy) can be controlled to a greater extent and be called upon to help meet either fluctuating demand or to complement variable forms of supply. Energy storage can blur the line between variable and dispatchable renewables, enhancing the flexibility of variable renewables, but also increasing the capital cost. Hydropower comes in different forms, all of which are dispatchable over the short-term (except in extreme drought); but those without reservoirs are more exposed to seasonal variations;
- **Centralised or distributed generation** - Electricity may be supplied on a large scale by utilities through the grid or from smaller scale, distributed assets, such as rooftop solar on homes or businesses, which may or may not be connected to the main grid;
- **Direct or indirect renewable energy** - Renewable energy may be used in a relatively direct way to provide an energy service (such as solar thermal for heat) or indirectly from renewables-based electricity or renewables-based heat that is then used to provide an energy service (such as to run heat pumps or electric vehicles, or district heating);
- **Traditional or modern use of bioenergy** - The traditional use of solid bioenergy refers to the use of solid biomass for cooking or heating, using very basic technologies, such as a three-stone fire, often with no chimney or one that operates poorly. The modern use of bioenergy refers to biomass use in improved cookstoves or modern technologies using processed biomass, such as pellets, liquid biofuels or biogas.

In 2014, the global supply of renewable energy increased by 2.7% over the previous year (in energy-equivalent terms), while overall primary energy demand rose 1.1% (and coal by around 1%). Collectively, all forms of renewable energy, including the traditional use of biomass, account for 14% of the global energy mix (8% if the traditional use of biomass is excluded). Wind and solar photovoltaics (PV) have led recent growth in renewables-based

capacity, although hydropower (for electricity) and bioenergy (mainly biomass used for cooking and heating in the world's poorest communities) are by far the largest sources of renewables-based energy supply today.

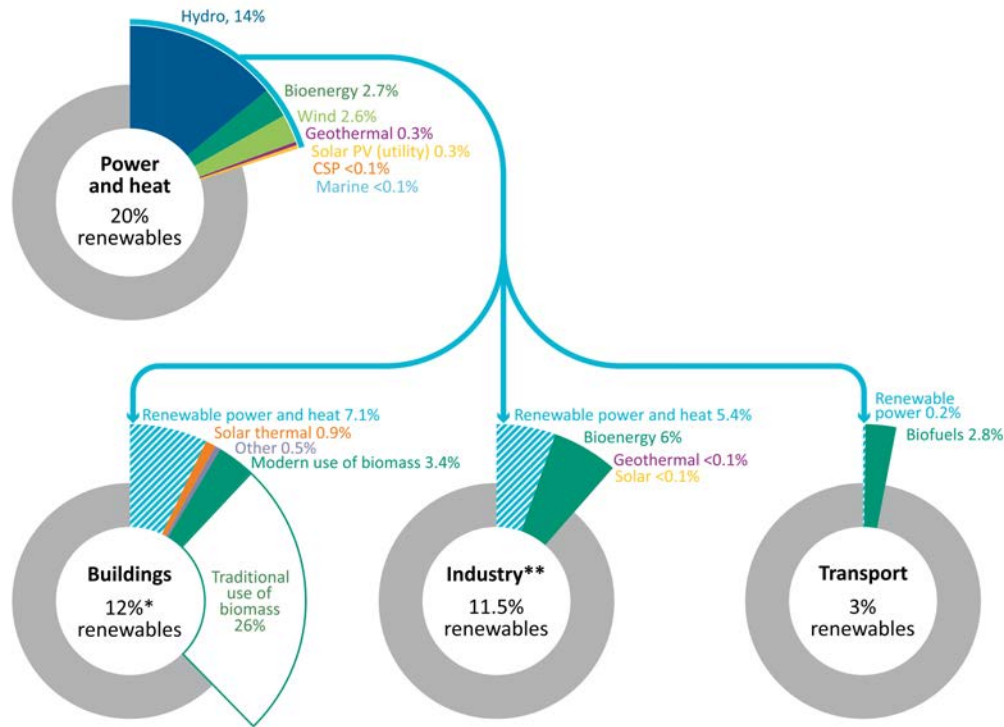


Figure 1.6: World share of renewable energy by sector and type, 2014, [8]

## 1.2 "Paris agreement", COP21

This paragraph has been taken directly from [8], standing on the reliability and credibility of that source.

"The accord reached in December 2015 at the Paris UNFCCC conference (COP21) was the culmination of a long and complicated negotiating process. The agreement, referred to as the "Paris Agreement", was already ratified by a sufficient number of Parties (the threshold of 55 Parties accounting for at least 55% of total global greenhouse-gas emissions) to allow it to enter into force on 4 November 2016, just before the start of the COP22 in Marrakech, Morocco. The Paris Agreement sets out the common goal to limit global warming and identifies ways in which this might be achieved. It aims to strengthen the global response to the threat of climate change, by:

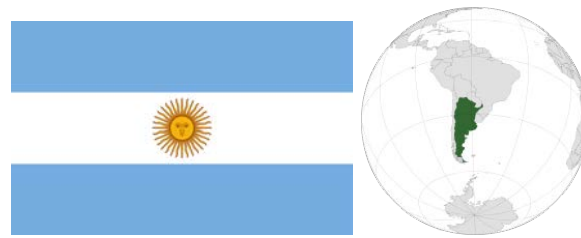
*"Holding the increase in the global average temperature to well below 2 °C above pre-industrial levels and pursuing efforts to limit the temperature increase to 1.5 °C above pre-industrial levels."*. Countries are committed to reach this goal via "global peaking of greenhouse-gas emissions as soon as possible", recognising that this will take longer for developing countries, and then by reducing emissions rapidly to a point - sometime in

the secondhalf of this century - when the world achieves a balance between anthropogenic emissions and their removal by sinks, by means of measures such as afforestation or carbon capture and storage.

How is this goal to be achieved? The main mechanism is via Nationally Determined Contributions (NDCs), the pledges made in advance of Paris that outlined climate ambitions and which, implicitly or explicitly, include commitments relating to the energy sector. The first round of NDCs for the period from 2020 are formalised when countries ratify or accede to the Agreement; subsequent NDCs will be communicated every five years, with the next round set by 2020.

To facilitate implementation of the NDCs, particularly in developing countries, the Paris Agreement established various complementary obligations and mechanisms related to finance (the commitment to mobilise \$100 billion per year in climate-related finance by 2020 was extended to 2025), capacity-building and technology development and transfer. Outside the formal Agreement framework, 20 countries and the European Union also agreed to double their clean energy research and development spending over the next five years as part of Mission Innovation, supported by commitments by 1 companies - like those in the Breakthrough Energy Coalition - to invest capital in early-stage technology development. The Paris Agreement includes provisions on adaptation to climate change, market-based emissions reduction mechanisms (establishing a successor to the Clean Development Mechanism), the roles of non-state actors and the need to achieve universal access to sustainable energy. There is also a unified system to track progress, with all countries reporting regularly on their emissions, progress with implementation of NDCs and adaptation actions."

## 1.3 Argentine country



*Figure 1.7: Argentina position and flag*

Argentina, officially the Argentine Republic, is a federal republic located mostly in the southern half of South America, with a population of more than 42.1 million. Sharing the bulk of the Southern Cone with Chile to the west, the country is also bordered by Bolivia and Paraguay to the north, Brazil to the northeast, Uruguay and the South Atlantic Ocean to the east, and the Drake Passage to the south. With a mainland area of  $2,780,400 \text{ km}^2$  Argentina is the eighth-largest country in the world, the second largest in Latin America, and the largest Spanish-speaking nation. It is subdivided into twenty-three provinces and one autonomous city Buenos Aires, which is the federal capital of the nation.

The maximum north-south distance is 3,694 km, while the maximum east-west one is 1,423 km; the total coast distance is about 5000 km.

### 1.3.1 Climate and biodiversity

Although the most populated areas are generally temperate, Argentina has an exceptional amount of climate diversity, ranging from subtropical in the north to polar in the far south. The average annual precipitation ranges from 150 millimetres in the driest parts of Patagonia to over 2,000 millimetres in the westernmost parts of Patagonia and the northeastern parts of the country. Mean annual temperatures range from  $5^\circ\text{C}$  in the far south to  $25^\circ\text{C}$  in the north. Due to these diverse conditions Argentina is a megadiverse country hosting one of the greatest ecosystem varieties in the world: 15 continental zones, 3 oceanic zones, and the Antarctic region are all represented in its territory. This huge ecosystem variety has led to a biological diversity that is among the world's largest.

In the Argentine territory there are also some large rivers that, as could be seen afterwards, are central players in its energetic mix. The most important rivers, in its flow order, are Río Paraná, Río Uruguay, Río Grande, Río Limay, Río Neuquén and Río Negro.

### 1.3.2 Economy and industry

Benefiting from rich natural resources, a highly literate population, a diversified industrial base, and an export-oriented agricultural sector, the economy of Argentina is Latin America's third-largest, and the second largest in South America. It has a "very high" rating on the Human Development Index and a relatively high GDP per capita (\$959.5 billion, 28th world richest countries by GDP, <http://www.worldsrichestcountries.com/>), with a considerable internal market size and a growing share of the high-tech sector.

2016 (Current)		
Rank	Country	Index score (100=High) (10 = Low)
1	China	100.0
2	United States	99.5
3	Germany	93.9
4	Japan	80.4
5	South Korea	76.7
6	United Kingdom	75.8
7	Taiwan	72.9
8	Mexico	69.5
9	Canada	68.7
10	Singapore	68.4
36	Colombia	35.7
37	Egypt	29.2
38	Nigeria	23.1
39	Argentina	22.9
40	Greece	10.0

Figure 1.8: Global Manufacturing Competitiveness Index: Country rankings, [5]

Historically, however, its economic performance has been very uneven, with high economic growth alternating with severe recessions, income maldistribution and-in the recent decades-increasing poverty. Early in the 20th century Argentina achieved development and became the world's seventh richest country. Although managing to keep a place among the top fifteen economies until mid-century, it suffered a long and steady decline and now it's just an upper middle-income country. Standing on an important global richest country ranking, Argentina took the 28th position in the first part of 2018.

Regarding industry main sectors, in 2012 the leading sectors by volume were: food processing, beverages and tobacco products, motor vehicles and auto parts, textiles and leather, refinery products and biodiesel, chemicals and pharmaceuticals, steel, aluminum and iron, industrial and farm machinery, home appliances and furniture, plastics and tires, glass and cement.

### 1.3.3 Argentine energetic mix

Argentina is South America's largest natural gas producer and a significant producer of oil. The country's electricity generation comes mainly from these thermal sources, while one third of the electricity generated is supplied by hydropower, given the presence of important rivers as exposed before. As reported in [1], the country's power generation mix is the following:

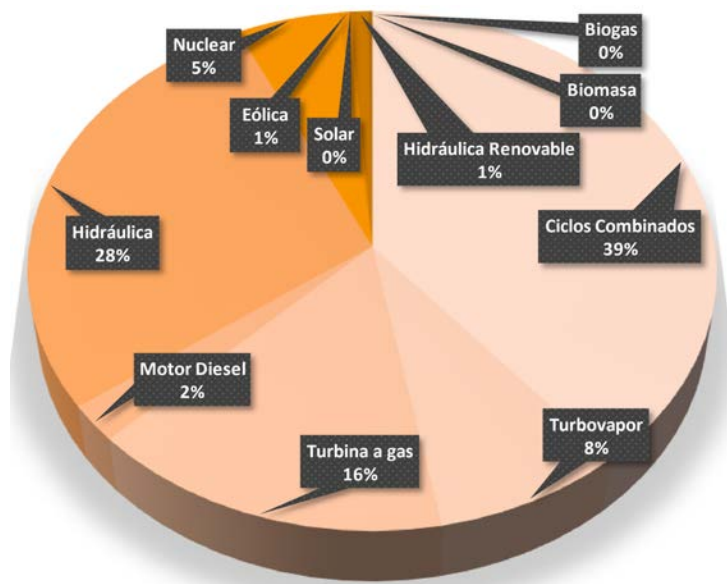


Figure 1.9: Argentina's power generation mix, [1]

The distribution of installed power generation, [1]:

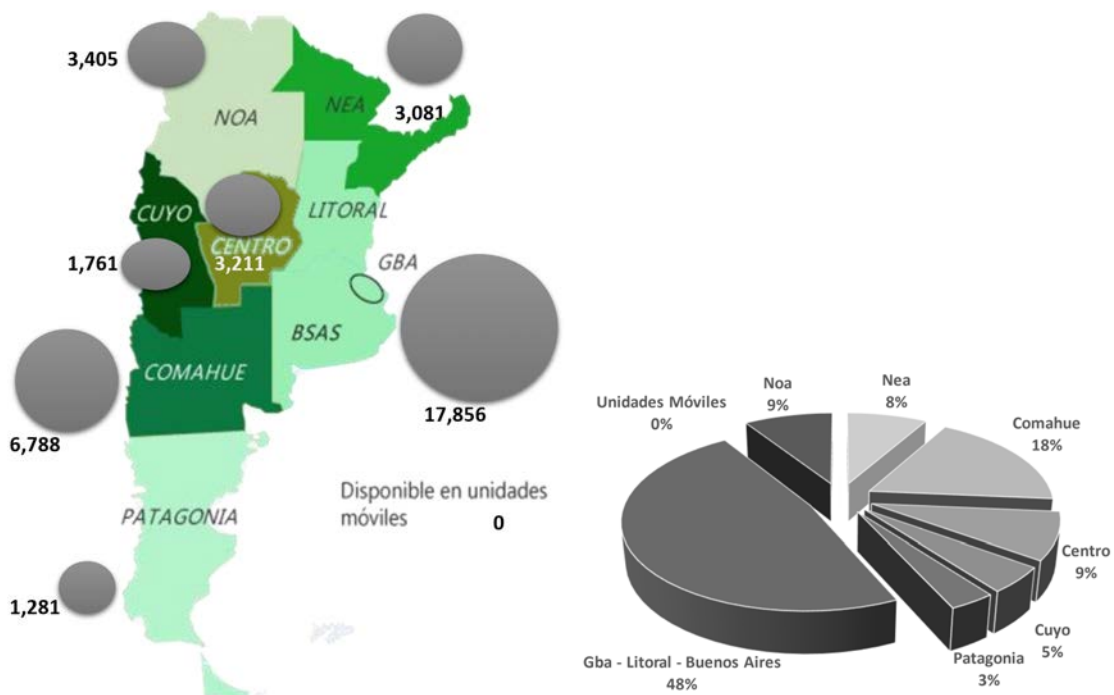


Figure 1.10: Distribution of power generation on Argentine territory

So it's possible to say that the two most important natural resources natural gas and waterways covers the majority of Argentine power demand. In the next Fig.1.11 it's possible to see that in the last 10 years Argentine policy has invested only in combined cycles power, due to the national natural gas reserve.

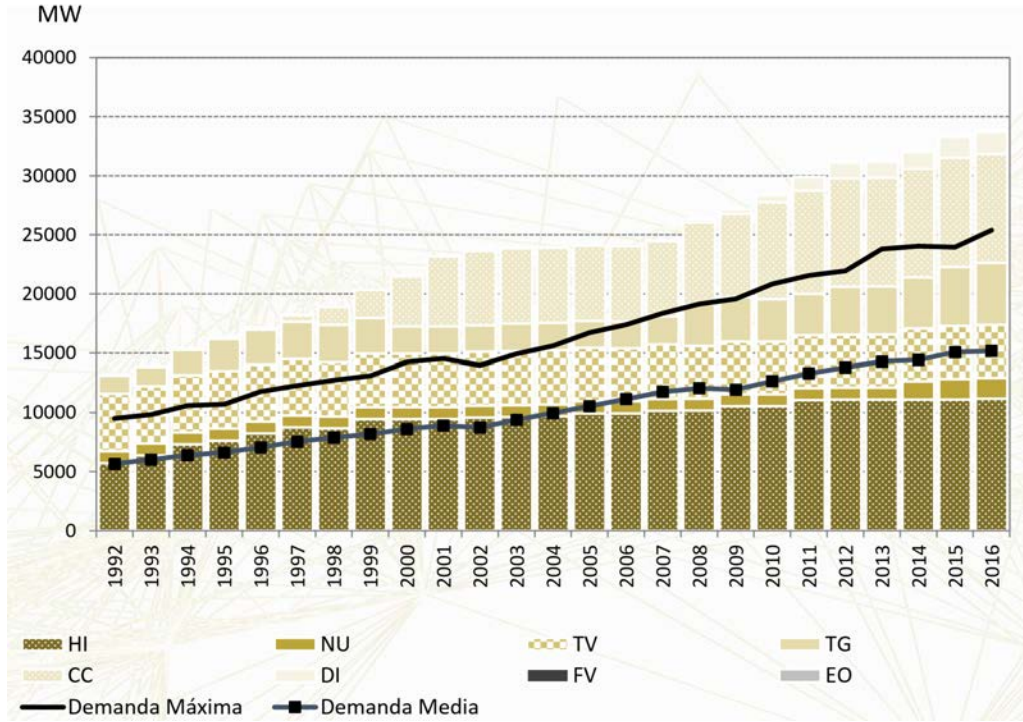


Figure 1.11: Argentina installed power evolution by type, [6]

### 1.3.4 Renewable development

Following what said in several articles and in particular on [26], the Argentine energy system is currently facing a number of challenges: a yearly increasing electricity demand, a strong dependence on fossil fuels and especially Argentina's dependence on their own natural gas reserves which due to the experts' assessments will run out in the next 20 years. In order to address these critical issues a new long-term strategy would be needed. In this context renewable energy systems offer a wide range of development prospects for Argentina: a growing share of renewable energy would reduce the dependence on natural gas imports and at the same time new power generating capacities would contribute significantly to meet the Argentina's ever increasing energy demand. Moreover renewable off-grid-and mini-grid-systems have the potential to enable communities, which will not be connected to the grid in the near future, to access electricity (see Fig.7.3, the southern part is not connected to the national grid at all). Therefore the dissemination of renewable energy would not only help to solve the present energy supply difficulties, but also would be a measure to produce new green industries, jobs and technologies.

According to experts' assessment locations which exceed an average yearly wind speed of 5 m/s offer economically favourable conditions for wind turbines: 70% of the Argentinian territory have an average wind speed of over 6 m/s and therefore the country inherits excellent conditions for wind energy (Fenés, 2015). With wind speeds between 9 and 12 m/s Patagonia is particularly well suited. However also in the coastal regions and in the province of Buenos Aires, which is the main centre of consumption, the average wind speed

is higher than 6,5 m/s (CADER, 2013). The Argentine Chamber of Industry (CIPIBIC) estimates that the theoretical potential of wind power in Argentina amounts to 2,000 GW. This represents a multiple of the installed capacity of 2018, which amounts to 227 MW, [1]. Moreover optimal conditions with solar radiation above  $5 \text{ kWh/m}^2 - \text{day}$  exist in the northwest of the country (west part of Salta, Jujuy, Catamarca, La Rioja and San Juan). Therefore these regions are ideally suitable for large-scale projects (Bariloche Fundacion, 2009). 31,7 Million hectares of the Argentine surface is used for agricultural crops (soy, wheat, corn, sunflower, sorghum, barley) and on an area covering the size of Germany 50 million cattle and 4,7 million pigs are bred (Budzinski & Barlatey, 2014). The Bariloche Fundacion estimates that the theoretical potential resulting out of the usage of agro-industrial waste like peanut shells, sunflower- and forest waste amounts to 720 MW (Bariloche Fundacion, 2009). The majority of hydroelectric power in Argentina comes from major dams with an installed capacity over 10700 MW, which provided in the year 2018 around 39% of the national energy demand, [1]. In 2009 in order to encourage the construction of hydroelectric power plants, the Secretariat for Energy launched the National Plan for Hydroelectric Projects. In the course of the plan studies and projects for hydroelectric power stations have been presented and until the year 2020 the government aims to improve the hydropower potential. Up to now in Argentina, renewable energy systems are predominantly applied in the form of off-grid systems. Because in Argentina 1,5 Million people in the rural areas don't have access to electricity, renewable energies have a wide range of application possibilities (International Energy Agency, 2014). To increase the rural electrification rate and to promote renewable energy systems in 1994 the Argentine government introduced PAEPRA (Program for the Provision of Electricity for the Rural Population of Argentina), a fee-for-service plan to supply the rural population of the country with electricity (Haselip et al., 2011). Beside the provision of energy one of the motives behind financing renewable energy systems by a subsidized program was the development of the private sector, particularly photovoltaic system, in the rural market (Alazraki & Haselip, 2007).

Standing on 2018 Cammesa report [1], renewable energy covers less than 2% of the demand (1,7%), against the 0,85% of 2011, despite stated political aims to generate 8% of the country's electricity from renewable sources by 2017. The following table shows the evolution of renewable energy generation since 2011, [6].

*Table 1.1: Evolution of renewable argentinian generation since 2011*

Source	2011	2012	2013	2014	2015	2016
<b>Biodiesel [GWh]</b>	32	170	2	2	-	1
<b>Biomass [GWh]</b>	98	127	134	114	155	193
<b>Wind power [GWh]</b>	16	348	447	613	593	547
<b>Hydro [GWh]</b>	1255	1453	1274	1457	1624	1820
<b>Solar [GWh]</b>	2	8	15	16	15	14
<b>Biogas [GWh]</b>	-	36	108	103	84	58
<b>Total [GWh]</b>	1403	2141	1980	2304	2470	2632



## Hydroelectric power plants

Following what said in paragraph 1.3.1, Argentina has many important hydroelectric power plants that, as Fig.1.9, covers an important slice of Argentine power demand. Here above the displacement on Argentine territory and many values about each river annual production (table 1.2).

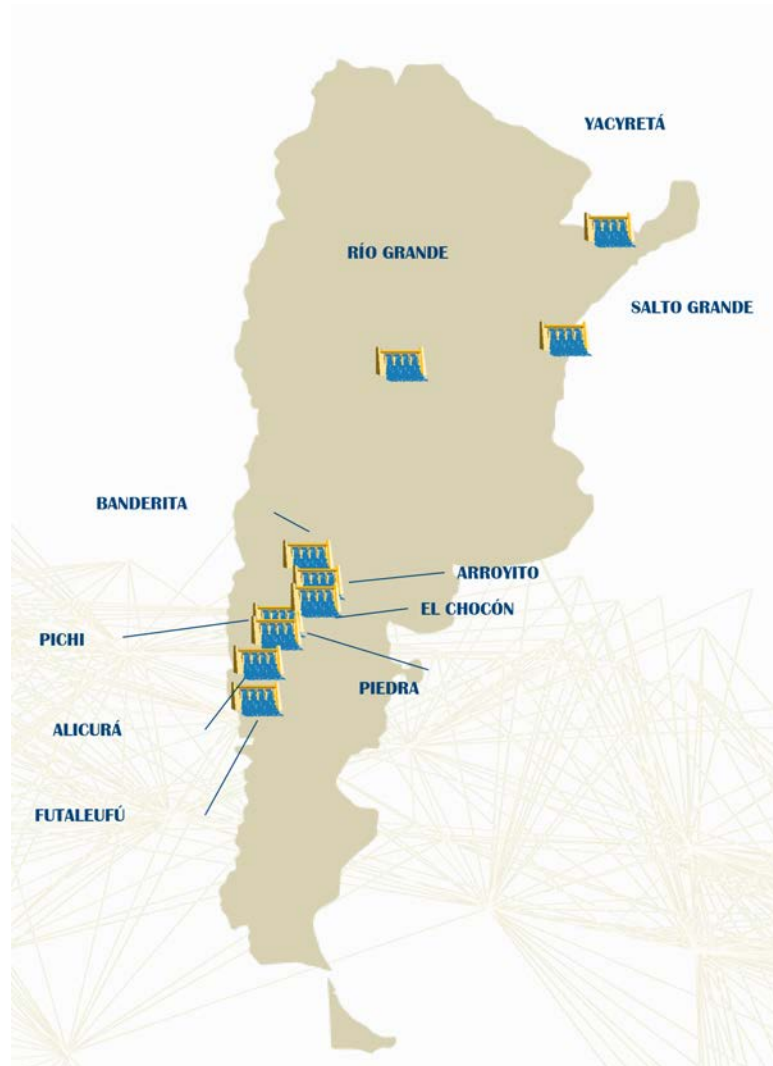


Figure 1.12: Argentine main hydroelectric power plants

Table 1.2: 2017 hydroelectric productivity of main argentinian rivers

River	GWh
Comahue	7205
Salto Grande	4816
Yacyreta	19218
Resto	6773

### 1.3.5 Policy measures relating to climate change and low carbon infrastructure

The Argentine Republic places environmental protection at the highest levels, securing it explicitly within an article in its national constitution (Article 41). According to its basic principles, each Province maintains jurisdiction over environmental issues and its natural resources, whereas the Nation is responsible for shaping the framework of such environmental protection. Besides, Argentina is an active party to the United Nations Framework Convention on Climate Change (UNFCCC), and as such the country reports relevant information regarding the achievement of the commitments established under the Convention framework.

According to Argentina's Third National Communication on Climate Change, GHG (Green House Gas) emissions follow the structure reported in Fig.1.13:

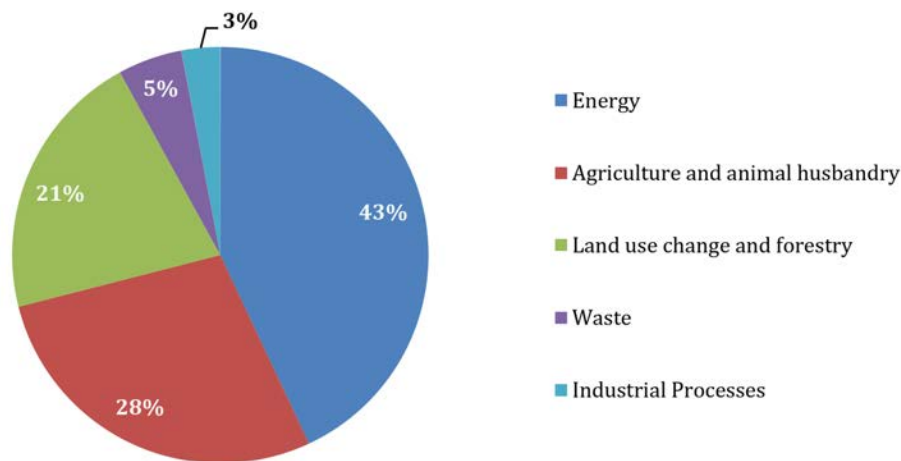


Figure 1.13: Structure of GHG emissions by sector

The energy sector accounts for 43% of GHG emissions. In principle, according to its Third Communication, Argentina's unconditional goal was to reduce GHG emissions by 15% in 2030 with respect to projected business-as-usual (BAU) emissions for that year. The goal includes actions linked to: the promotion of sustainable forest management, energy efficiency, biofuels, nuclear power, renewable energy (the government released *RenovAr.*, a public tendering program which contemplates a series of fiscal incentives and financial support mechanisms, along with regulatory and contractual enhancements aimed at overcoming some of the investment barriers that resulted in the failure of previous government attempts) and transport modal shift (for Buenos Aires' city the goal is to reach 100% penetration of e-buses in the urban bus fleet by 2030).

## Chapter 2

# Wave energy

Harvesting renewable energy from nature is the most prospective route to solve energy crisis, environmental problems and also to achieve the objectives imposed by the targets of  $CO_2$  emissions and world global warming temperature. However, the already developed energy conversion devices including photovoltaics, wind power systems, hydropower stations etc are weather/region-dependent or bring environmental damages, significantly limiting their widespread applications, besides these technologies are affected by a not continue source, think of the sun that can be covered by a cloudy day or the wind that is anything but continuous.

Ocean covers approximate 70% of earth's surface and it keeps moving day and night. In this concept, the capture of wave energy is a more viable technology, especially on off-shore regions. As long as there is wind blowing over the ocean, water waves are always present on the ocean surface, thus offering an infinite source of wave energy. The power that flows in the waves is up to five times greater than the wind that generates the waves, making wave energy more persistent than wind energy [22].

Ocean energy refers to any energy harnessed from the ocean by means of:

- tidal power;
- tidal marine currents;
- wave power;
- temperature gradients;
- salinity gradients.

Tidal and Wave energy represents the two most advanced types of ocean energy technologies, and those expected to become commercially viable in the short-medium term, Fig.2.1. In the EU, the aim is to reach 100 GW of combined wave and tidal capacity installed by 2050 [2]. Standing on a recent study [18], the global wave energy potential (neglecting many islands and the pole) is around

$$2.11 \pm 0.05 TW \tag{2.1}$$

with 95% confidence. Here is reported a chart showing the market point for each technology, highlighting that wave and tidal sources are the most developed.

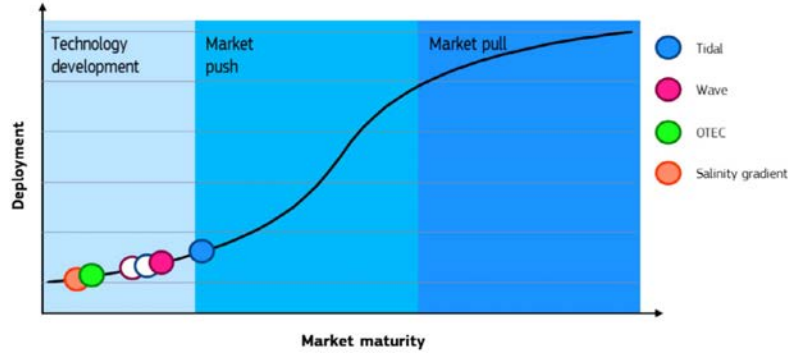


Figure 2.1: Support mechanisms according to market maturity and deployment level. Full circles represent technology frontrunners, hollow circles represent the general market maturity for each technology

The best advantages of wave energy (in general) compared with other renewables sources like solar or wind power are [3]:

- Sea waves offer the highest energy density among renewable energy sources [12]. Waves are generated by winds, which in turn are generated by solar energy. Solar energy intensity of typically  $0.1 - 0.3 \text{ kW/m}^2$  horizontal surface is converted to an average power flow intensity of  $23 \text{ kW/m}^2$  of a vertical plane perpendicular to the direction of wave propagation just below the water surface [20];
- Limited negative environmental impact in use. Thorpe [30] details the potential impact and presents an estimation of the life cycle emissions of a typical nearshore device. In general, offshore devices have the lowest potential impact;
- Natural seasonal variability of wave energy, which follows the electricity demand in temperate climates [12] ;
- Waves can travel large distances with little energy loss. Storms on the western side of the Atlantic Ocean will travel to the western coast of Europe, supported by prevailing westerly winds;
- It is reported that wave power devices can generate power up to 90 % of the time, compared to  $\sim 20 - 30 \%$  for wind and solar power devices [27], [15].

The increased activity in the ocean technologies field at the end of the  $XX^{th}$  Century led to the foundation in 2001 of the Ocean Energy Systems Technology Collaboration Programme (OES), an intergovernmental agency established by the International Energy Agency (IEA) and initially signed by three active countries: Denmark, Portugal and United Kingdom. Main aim of the organization was to coordinate countries in order to advance research, development and demonstration of all the ocean renewable conversion technologies. Every year the IEA-OES Annual Report contains the state of play of the technology development

[10] and inform about the active and expected policies dedicated to the field. In 2012 the European Commission published the Blue Growth communication [7], which contains definitions and indications about the opportunities for marine and a maritime sustainable growth. This document is in general transversely dedicated to all the activities related to sea and coasts economy, and an entire section is dedicated to the wider category of *Blue Energy*. Among these technologies a special mention to the offshore wind energy has to be done. Despite the numerous challenges that it shares with wave power, at the time of the writing this industrial field reached its first commercial installation: the 6 MW Hywind floating offshore wind farm in Scotland. For what concern the Ocean Energies, in the Commission communication it is stated that the challenge is to accelerate its path to commercialization. In the following 2014 Blue Energy communication [16], the parallel with the successful offshore wind sector is drawn, and policies and vision for the field development are more deeply enunciated. The challenges that still need to be faced are nonetheless outlined, underlying in particular the technology cost, the electrical transmission grid infrastructure, the complex licensing and consenting procedures, the assessment of the environmental impacts and the lack of grant and revenue support due to the current economic climate. All these interests and efforts are explained by the nature and size of the ocean resource and the fact that Europe is one of the best spots to harvest this energy. Even if it is difficult to quantify the potential of this resource and data from different authors varies considerably, in table 2.1 it is possible to find some ranges of exploitable potentials of the different physical forms of energy contained into the sea.

*Table 2.1: Potential (TWh) of many ocean resources*

<b>Resource</b>	<b>Potential [TWh]</b>
Tidal energy	300 - 1200
Marine current power	>800
Osmotic power	2000 - 5177
Ocean thermal energy	10000 - 85000
Wave energy	8000 - 80000

Currently, the identified and studied technologies are wave, tidal and ocean currents, the emerging ocean thermal energy conversion and osmotic power (salinity gradient). Tidal current energy is caused by the periodic gravitational pull of the moon and sun on the oceans' water. Tidal technology captures the kinetic energy of the water current motion in and out of the tidal areas. Common installations consist of submerged turbines lying on the seabed. Even if with a lower overall potential, it is more mature with respect to wave energy, and will likely contribute to the energy mix within the 2030 time horizon.

Ocean Thermal Energy Conversion (OTEC) exploits the temperature differential between sea warmer surface and cooler deep water. The heat extracted from the warm seawater is used to produce a vapor that acts as a working fluid for a turbine. On the other hand, the cold water is used to condense the vapor and ensure the pressure difference that drives the turbine. This heat cycle can be realized both in open and close architectures, and it can exploit different working fluids. The power plants can be land-based, moored to the

sea-bed or floating.

Marine current energy is related to the oceans currents, where huge masses of water move below the sea surface. The technologies studied to exploit this motion converts the kinetic energy of the fluxes through axial turbines, analogously to wind energy. Osmotic power, also called salinity gradient power, is the energy present in the difference of salt concentration between fresh and seawater. A common generation station is at the estuary of a river, where the fresh river water is used and then returns to the sea in the form of brackish water.

Another potential resource owned by oceans is that of the waves. Citing two works completely devoted to the wave energy resource [18], the world wave average power resource should be in the range of 2 or 3 TW, meaning a theoretical available energy resource between 17,520 and 26,280 TWh. The relevance of this value is obtained when compared to the overall world energy consumption in 2014, equal to 159,320 TWh [28]. This noticeable value, also coupled with the zero land consumption, makes this resource interesting to be explored.

## 2.1 Wave energy converters classification

One of the problems to be solved in a WEC is the so called "reaction problem": in order to extract power from the sea surface with a force, a reaction to that force must be provided. In his analysis [23], French highlighted that the reaction force can be given in four different ways: reacting on a large structure bigger than the wavelength and therefore hydrodynamically stable, reacting to the seabed, reacting to a mass that is part of the WEC and reacting against a part of the sea. Except from the third choice, the others possibilities have to use mechanical parts in relative motion working immersed into sea water or spray. Those parts can be protected against corrosion, but they could remain a problem in a WEC durability. Following what said in [23] by French, WEC's can be classified in different ways, depending on their distance to the coast, depending on their working principle and finally depending on their dimension related to the wavelength. Here is reported a table that shows the best realization (or prototypes) for each technology, which doesn't take into account the third classification.

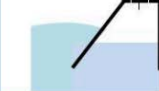
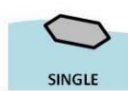
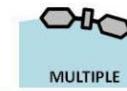
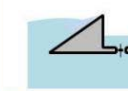


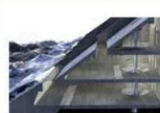



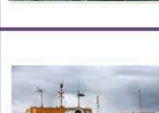


		PRIMARY CONVERSION WORKING PRINCIPLE			
		OWC	WAVE ACTIVATED BODY		OVERTOPPING
					
LOCATION	ONSHORE				
	NEARSHORE 10 - 25m deep				
	OFFSHORE > 40m deep				

Figure 2.2: Proposal of Wave Energy Converter concepts classification, [32].

### 2.1.1 Types

Despite the large variation in designs and concepts, WECs can be classified into three predominant types, following [3]:

- *Attenuator*, attenuators lie parallel to the predominant wave direction and "ride" the waves. An example of an attenuator WEC is the Pelamis, developed by Ocean Power Delivery Ltd;

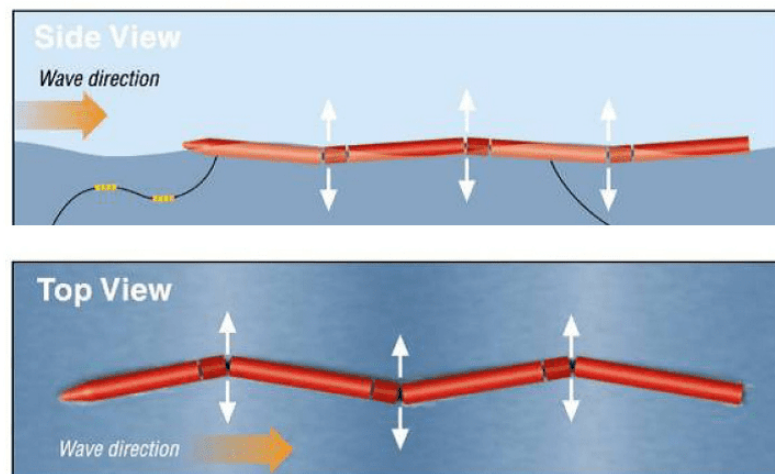


Figure 2.3: Pelamis WEC, side and top view

- *Point absorber*, a point absorber is a device that possesses small dimensions relative to the incident wavelength. They can be floating structure that heave up and down on the surface of the water or submerged below the surface relying on pressure differential. Because of their small size, wave direction is not important for these devices. There are numerous examples of point absorbers, one of which is Ocean Power Technology's Powerbuoy;

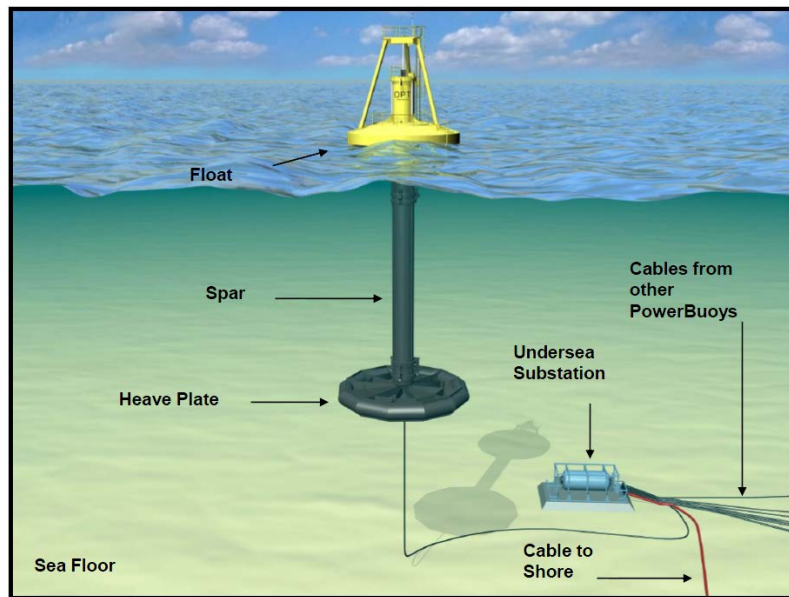


Figure 2.4: Powerbuoy concept image with all the components of an installation

- *Terminator*, terminator devices have their principal axis parallel to the wave front (perpendicular to the predominant wave direction) and physically intercept waves. One example of a terminator-type WEC is the Salter's Duck, developed at the University of Edinburgh, or ISWEC, developed by Politecnico di Torino.

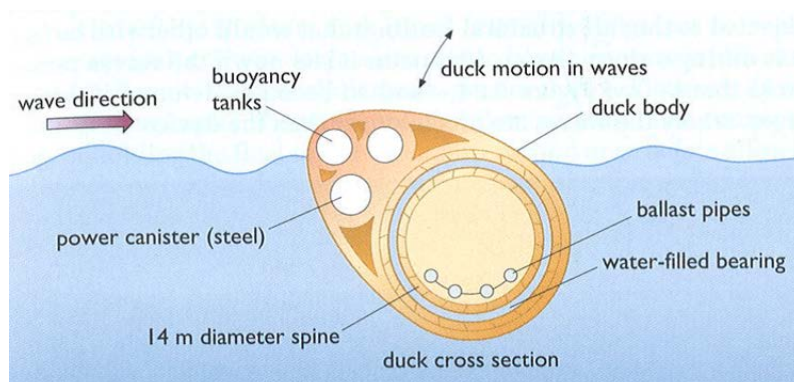


Figure 2.5: Salter's duck concept image with all the components showed



### 2.1.2 Modes of operation

Within the categories identified above, there is a further level of classification of devices, determined by their mode of operation. Some significant examples are given below.

#### Submerged pressure differential

The submerged pressure differential device is a submerged point absorber that uses the pressure difference above the device between wave crests and troughs. It comprises two main parts: a sea bed fixed air-filled cylindrical chamber with a moveable upper cylinder. As a crest passes over the device, the water pressure above the device compresses the air within the cylinder, moving the upper cylinder down. As a trough passes over, the water pressure on the device reduces and the upper cylinder rises. An advantage of this device is that since it is fully submerged, it is not exposed to the dangerous slamming forces experienced by floating devices and reduces the visual impact of the device. Maintenance of the device is a possible issue however. Owing to part of the device being attached to the sea bed, these devices are typically located nearshore. An example of this device is the Archimedes Wave Swing, here represented.



*Figure 2.6: Archimede concept image*

#### Oscillating wave surge converter

An oscillating wave surge converter is generally comprised of a hinged deflector, positioned perpendicular to the wave direction (a terminator), that moves back and forth exploiting the horizontal particle velocity of the wave. An example is the Aquamarine Power Oyster, a nearshore device, where the top of the deflector is above the water surface and is hinged from the sea bed. A prototype of this device has been constructed and here below its representation.

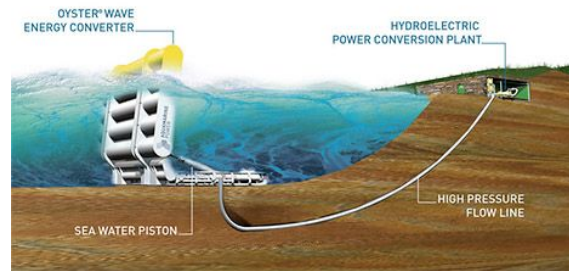


Figure 2.7: Aquamarine Power Oyster system

### Oscillating water column

An OWC consists of a chamber with an opening to the sea below the waterline. As waves approach the device, water is forced into the chamber, applying pressure on the air within the chamber. This air escapes to atmosphere through a turbine. As the water retreats, air is then drawn in through the turbine. A low-pressure Wells turbine is often used in this application as it rotates in the same direction irrespective of the flow direction, removing the need to rectify the airflow. It has been suggested that one of the advantages of the OWC concept is its simplicity and robustness. There are examples of OWCs as point absorbers, as well as being built into the shoreline, where it acts as a terminator. An example of a shoreline mounted device is the Wavegen Limpet, the device is installed on the island of Islay, Western Scotland, and produces power for the national grid.

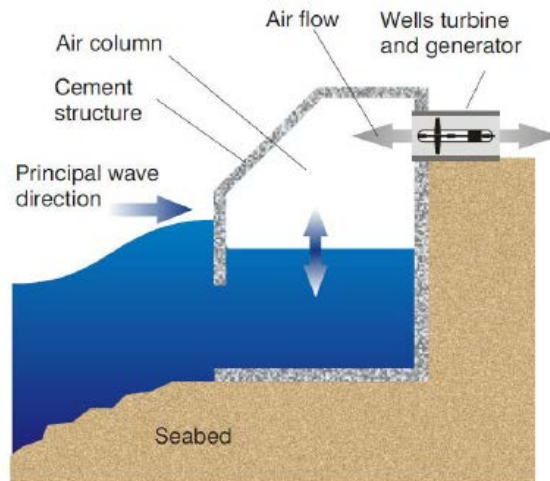


Figure 2.8: Oscillating Water Column scheme

### Overtopping device

An overtopping device captures sea water of incident waves in a reservoir above the sea level, then releases the water back to sea through turbines. An example of such a device is the Wave Dragon. This device uses a pair of large curved reflectors to gather waves into the central receiving part, where they flow up a ramp and over the top into a raised

reservoir, from which the water is allowed to return to the sea via a number of low-head turbines.

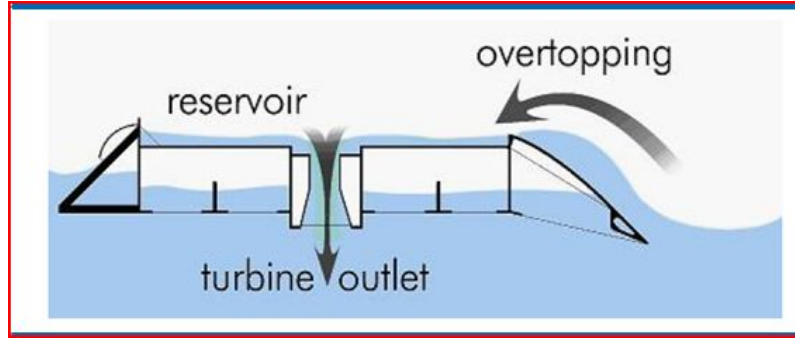


Figure 2.9: Overtopping device principle

## 2.2 Europe state of the art

Now will be given many informations and news about Europe ocean energy contribution, found in [13]. The installation of ocean energy devices is taking place at a slower pace than expected. Europe only accounts for 14 MW of ocean energy installed capacity at the end of 2016, much lower than the expectation set by Member States in their National Renewable Energy Action Plans. According to NREAPs, 641 MW of ocean energy capacity were expected to be operational by 2016, taking into account the 240 MW tidal range currently operational in France. By 2020, if technological and financial barriers are overcome, the pipeline of announced European projects could reach 600 MW of tidal stream and 65 MW of wave energy capacity. Taking into account only projects that have been awarded public funds, 71 MW of tidal stream and 37 MW of wave energy capacity could be operational within the EU in 2020. Although what just said, Europe's technological leadership in the sector has been strengthened. Europe accounts for 52 % of tidal stream and 60 % of wave energy developers of the whole world.

### 2.2.1 Market status

The market for ocean energy technology is still small. A few ocean energy projects are currently being deployed, grid-connected or already operational. According to the NREAPs signed by EU Member States in 2009, the total installed capacity of ocean energy should reach 2253 MW by 2020 [EC 2009]. In 2016, the total ocean energy installed capacity in the EU is only 254 MW based on data made available by Member States in their NREAP progress reports. The following table presents an overview of the NREAPs targets for ocean energy and the actual capacity and production achieved. Only 14 MW out of the 254 MW of ocean energy capacity installed are related to wave, tidal and salinity gradient technology. The remaining 240 MW refer to the tidal barrage of La Rance operational in France since 1966. Whilst market formation has been slow, the trends of the recent years appear to be changing with a number of projects having been commissioned and

Table 2.2: NREAPs targets for ocean energy, capacity and production

	Capacity [MW]	Production [GWh]
2014 actual	247	483
2014 target	322	752
2016 JRC	254	n.a.
2016 target	641	1789
2020 target	2253	6506

announced in 2016; the majority being tidal energy projects.

The majority of companies developing wave energy devices are based in the EU (Fig.2.10). The United Kingdom has the highest numbers of developers, followed by Denmark. Outside the EU, countries with a larger number of wave energy developers are USA, Australia, and Norway.

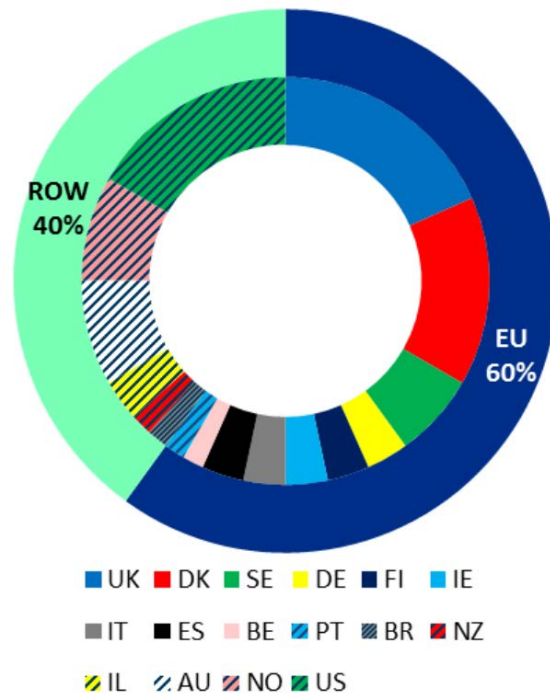


Figure 2.10: Distribution of wave energy developers in the world, [13]

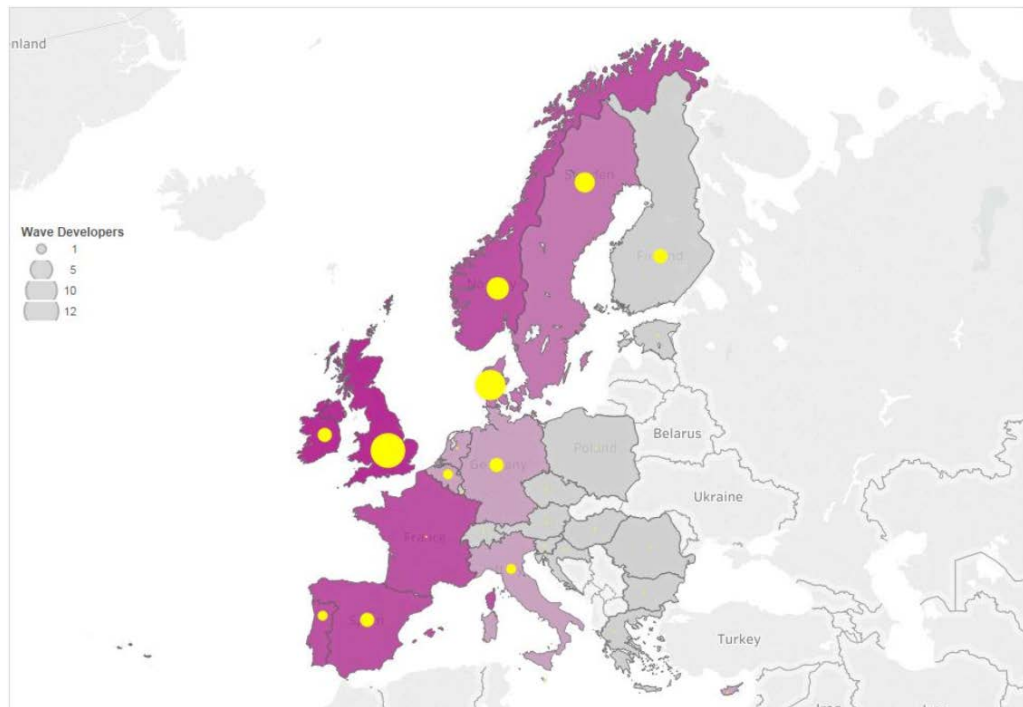


Figure 2.11: Spread of wave developers (in yellow) and resource availability in Europe. Dark purple areas refer to high resources, and light pink areas indicate limited resources, [13]

Here is reported two tables with an hypothetical roadmap for Europe investments until 2050 and then a list of projects for Europe, updated to 2015, [13].

Parameter	Unit	2010	2020	2030	2040	2050
Net electrical power	MWe	1-3	3-10	10	40	75
Max. capacity factor	%	34	41	43	43	46
Avg. capacity factor	%	25	28	31	34	0
Technical lifetime	Years	20	20	20	20	20
CAPEX reference	EUR/kWe	10500	6636	5267	2650	2300
CAPEX low	EUR/kWe	7680	4582	3620	2624	2050
CAPEX high	EUR/kWe	14000	8834	7526	7082	2560
CAPEX learning rate	%	12	12	12	12	12
FOM	% of CAPEX	4.0	4.3	4.2	5.0	5.5
FOM learning rate	%	1-3	3-10	10	40	75

Figure 2.12: 2015 Techno-economic data for wave energy and an hypothetical roadmap until 2050

Project name	Location and country	Capacity (MW)	Companies and devices	Status	Comment
Costa Head	Pentland Firth, Orkney Islands, United Kingdom	200 MW	SSE & Alstom	In planning	Status unclear
Marwick Head	Pentland Firth, Orkney Islands, United Kingdom	50 MW	ScottishPower Renewables	In planning	Scoping report ready
Brittany	La Bretagne, France	1.5 MW	Fortum & DCNS WaveRoller devices	In planning	Development agreement signed
Gibraltar	Gibraltar, United Kingdom	0.5 MW	Eco Wave Power	In construction	PPA signed, construction started in 2015
Sotenäs	Västra Götaland, Sweden	10 MW	Seabased & Fortum	In construction	Completion expected in 2016
Swell	Peniche, Portugal	5.6 MW	16 x 0.35 kW WaveRoller devices	In planning	Entry into operation expected in 2020
Westwave	Killard, Ireland	5 MW	ESB, Device to be selected	In planning	Construction expected in 2016, entry into operation expected in 2018
CEFOW	Wave Hub, Cornwall, UK	3 MW	Fortum Wello Penguin	In planning	Project awarded funding in 2015
Limpet	Island of Islay, Scotland, United Kingdom	0.5 MW	Voith Hydro Wavegen	Commissioned	Current status unclear
Mutriku	Masque Country, Spain	0.3 MW	Ente Vasco de la Energia & Voith Hydro Wavegen	Commissioned	Running as foreseen
Pico	Azores, Portugal	0.4 MW	WavEC	Commissioned	Plant has deteriorated, unclear if still producing electricity
WaveStar 1:2	Hanstholm, Denmark	0.6 MW	Wave Star A/S	Commissioned	Currently under rebuilt
Wello	EMEC, Orkney Islands, United Kingdom	0.5 MW	Wallo Oy Penguin	Commissioned	First deployed in 2012 and after upgrades performed, returned in 2013
Peniche	Peniche, Portugal	0.3 MW	AW Energy WaveRoller	In construction	Installation of first device scheduled for 2015

Sources: [JRC 2014, Eco Wave Power 2015, Fortum 2015, BNEF 2015d]; own analysis

Figure 2.13: List of ongoing leased EU wave energy projects identified by JRC

## Chapter 3

# Mathematical view

Historically, predictions of wave conditions for D-Day (June 1944) are considered the first attempt at operational wave forecasting. The second historical date to mention is the year 1950, in which a parametric relation between the significant wave height and the local wind speed was wrote. In the same year Gelci et al. introduced spectral concepts to the rising numerical wave modeling. After many other models developed with too much assumptions and approximations, community develop *WAM* with explicit treatment to nonlinear interactions, replacing all previous models. In 1994 at NCEP (National Center for Environmental Predictions) *WAM* got the forth evolution with complete operational spectral wave.

In this chapter will be given a view of generally what matters ocean waves and their characteristics and then will be presented a brief view of the *WAM* model just mentioned.

### 3.1 Introduction

The sea state representation is fundamental for description of the wave forces and for the integration with the harvesting machine, but it's a relatively wide topic and for the sake of brevity, in this section a brief overview is given. In particular, the main results here reported are based on the *Guide to wave analysis and forecasting*, *A.K.Laing* [24].

Ocean surface waves are the result of forces acting on the ocean. The predominant natural forces are pressure or stress from the atmosphere, especially through the wind, earthquakes, gravity of the Earth and celestial bodies, the Coriolis forces (due to Earth's rotation) and surface tension (see Fig.3.1). Where the Earth's gravity and the buoyancy of the water are the major determining factors we have the so-called gravity waves. Wind-generated gravity waves are almost always present at sea. These waves are generated by winds somewhere on the ocean, be it locally or thousands of kilometers away: they are very important in the climate processes as they play a large role in exchanges of heat, energy, gases and particles between the ocean and the atmosphere. These waves will be the subject of this chapter. To analyse and predict such waves it need to have a model for them, that is it need to have

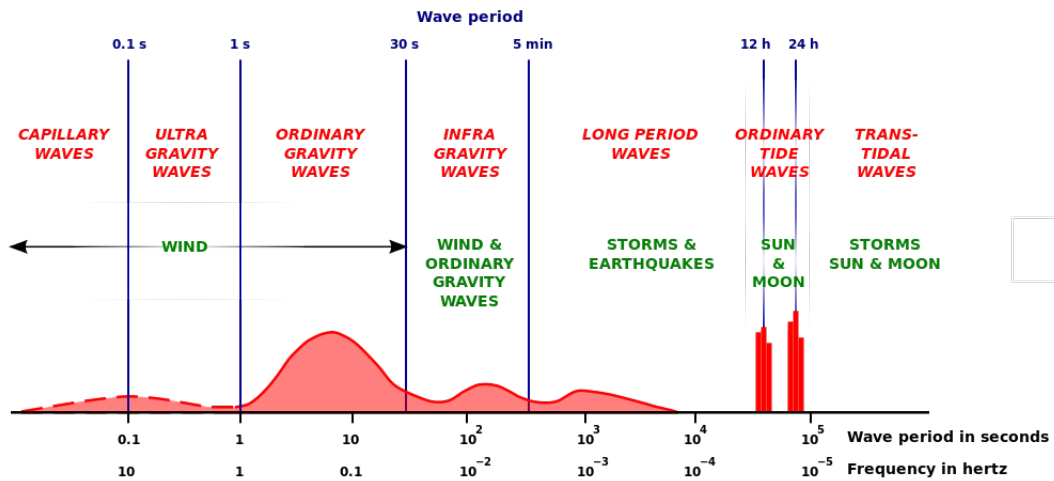


Figure 3.1: Classification of ocean waves by period and by source

a theory that predict how they behave. First of all it's necessary to present three simple mathematical assumptions that opens the next paragraph:

1. Incompressibility of the water: this means that the water density is constant and so it's possible to write a continuity equation for the fluid, expressing the conservation of fluid within a small cell of water;
2. Inviscid nature of the water: this means that the only forces acting on a water particle are gravity and pressure, friction is ignored;
3. Irrotational fluid flow: this means that the individual particles do not rotate. They can move around each other but there is no twisting action. This allows to relate the motions of neighbouring particles by defining a scalar quantity, called the velocity potential for the fluid. The fluid velocity is determined from spatial variations of this quantity.

## 3.2 The simple linear wave

The simplest wave motion may be represented by a sinusoidal, long-crested, progressive wave. The sinusoidal characteristic means that the wave repeats itself and has the smooth form like shown in Fig.3.2. The basic parameters used to describe the ocean wave (not only ocean waves, in generally all the waves, such as electromagnetic waves, sound waves, etc) and presented in figure are:

- *period*  $T$ , it's the time interval (in seconds) between two successive crests;
- *frequency*  $f$ , it's the number of crests which pass a fixed point in 1 second. It's usually measured in Hertz and it's equal to  $1/T$ ;
- *wavelength*  $\lambda$ , it's the horizontal distance between two consecutive crests (in metres);



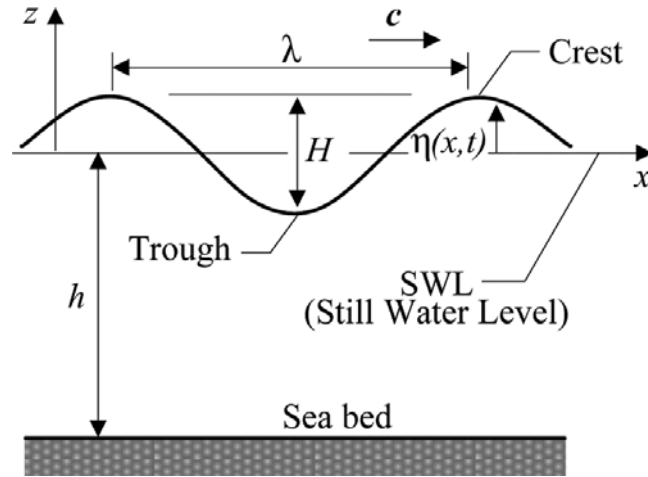


Figure 3.2: Sinusoidal wave parameters

- *amplitude*  $a$ , it's the magnitude of the maximum displacement from mean sea level (in metres);
- *wave height*  $H$ , it's the difference in surface elevation between wave crest and the previous wave trough, equal to  $2a$ ;
- *phase speed*  $c$ , it's the speed at which the wave profile travels, i.e. the speed at which the crest and trough of the wave advance, equal to  $\lambda/T$ , commonly defined as *wave speed*.

The reason for starting with a description of simple waves is that they represent the basic solutions of the physical equations which govern waves on the sea surface and they are the "building blocks" of the real wave fields occurring at sea.

The presented simple wave profile has the form of a sinusoidal wave:

$$\eta(x, t) = a \sin(kx - \omega t) \quad (3.1)$$

in which  $k = 2\pi / \lambda$  is the *wavenumber* and  $\omega = 2\pi / T$  is the *angular frequency*.

### 3.2.1 Influence of water depth

Depending on the wavelength, depth is classified in this way (the classification used in [24], there are many other classifications):

- Deep water:  $h > \lambda/4$ ;
- Transitional depth water:  $\lambda/25 < h < \lambda/4$ ;
- Shallow water:  $h < \lambda/25$ .

Starting from the deep water, when waves propagate into shallow water, for example when approaching a coast, nearly all the characteristics of the waves change as they begin to feel

the bottom, only the period remains constant, the wave speed decreases with decreasing depth and standing on the relation  $\lambda=cT$  the wavelength also decreases. Summarily, the main relations (considered in the following chapters) depending on the water depth are reported in the following table:

A further feature of changing depth is changing wave height: as a wave approaches the

*Table 3.1: Wave property for each depth interval*

Wave property	Shallow water	Intermediate water	Deep water
	$h < \lambda/25$	$\frac{\lambda}{25} < h < \frac{\lambda}{4}$	$h > \frac{\lambda}{4}$
Dispersion relation	$\delta^2 = gK^2h$	$\delta^2 = gK \tanh(Kh)$	$\delta^2 = gK$
$\lambda$ -T relation	$\lambda = T\sqrt{gh}$	$\lambda = \frac{g}{2\pi}T^2 \tanh\left(\frac{2\pi h}{\lambda}\right)$	$\lambda = \frac{g}{2\pi}T^2 \approx 1.56T^2$
Group velocity	$c_g = c$	$c_g = \frac{1}{2}c \left(1 + \frac{2kh}{\sinh 2kh}\right)$	$c_g = \frac{1}{2}c$

shore its height increases. This is a result of the changes in group velocity (for a more detailed description see [24]). It is important to underline that when the depth of water is greater than  $\lambda/2$  the influence of the bottom on the movements of water particles can be considered negligible [25].

*Note: in the next sections it could be seen that in a real sea state there are many wavelengths and waves with close wavelengths combine to form group of waves, since this the group velocity.*

Another fundamental concept to be noted in this context is the one called *Wave breaking*: according to a theory of Stokes, waves cannot attain a height of more than one-seventh of the wavelength without braking.

$$H_{max} \approx \frac{1}{7}\lambda \quad (3.2)$$

### 3.2.2 Orbital motion of wave particles

As stated in [22], " *The motion of the waves sets the water particles in orbital motion. A water wave has both longitudinal and transverse motions. In a longitudinal motion, the particles oscillate back and forth parallel to the direction of wave propagation. In a transverse motion, the particles oscillate up and down in their positions, orthogonal to the direction of wave propagation. These two motions combine to provide the overall orbital motion* ", in fact, during one cycle of a simple wave (i.e. wave period) the particles describe a circle in a vertical plane, the vertical plane is the plane on which the Figure 3.2 has been plotted.

These movements of water particles results from the longitudinal and transverse oscillations and create the orbital path, which is present in deep water waves (depth  $h > \lambda/4$ ) as well as in shallow water waves ( $h < \lambda/25$ ). However, while the orbit is circular in deep water, it is elliptical in shallow water [22], as shown in Figure 3.3.

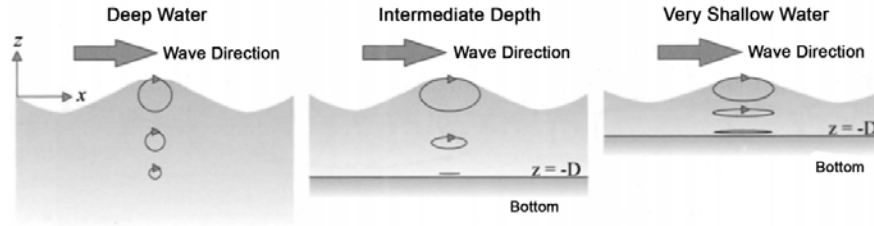


Figure 3.3: The orbital motion depending on the water depth

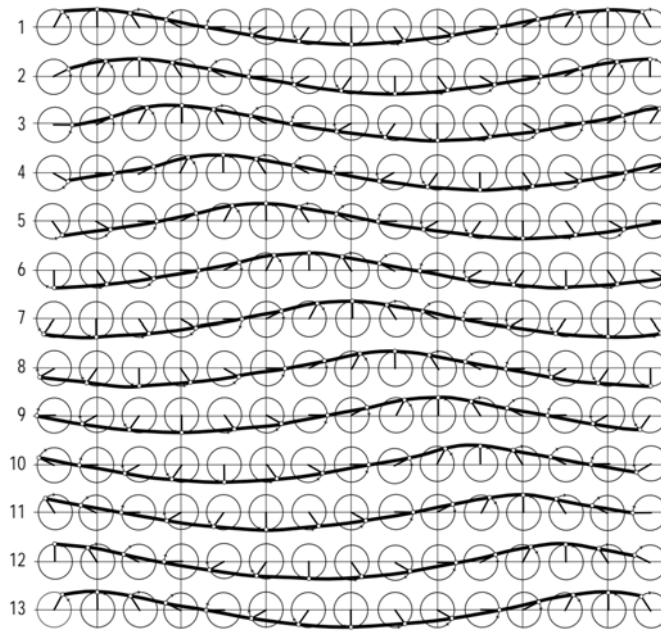


Figure 3.4: Progression of a wave motion. Thirteen snapshots each with an interval of  $1/12$ th period (derived from GrÅlen and Dorrestein, 1976)

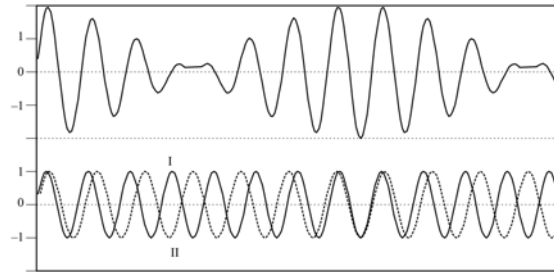
As stated in Fig.3.3, in deep water conditions, the particles describes vertical circles that become progressively smaller with increasing depth. When waves propagate into shallow water, for example when approaching a coast, the motion becomes elliptical.

### 3.3 Superposition theory: real ocean waves

Actual sea waves do not looks as the profile shown in Fig.3.2, with their irregular shapes they appear as a confused and constantly changing water surface, since waves are continually being overtaken and crossed by others. As a result, waves at sea are often short-crested. This is particularly true for waves growing under the influence of the wind. A more regular pattern of long-crested and nearly sinusoidal waves can be observed when waves are no longer under the influence of their generating winds.

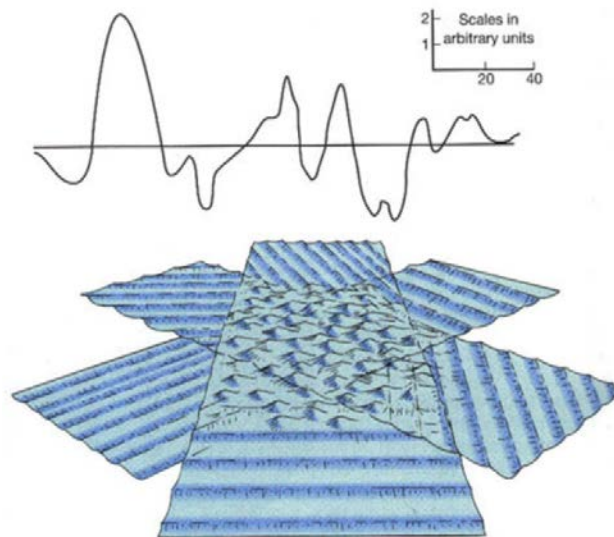
The simple waves presented before can be combined to compose the observed patterns. To put it differently, any observed wave pattern on the ocean can be shown to comprise a

number of simple waves, which differ from each other in height, wavelength and direction, as presented in the figure below:



*Figure 3.5: The upper complex profile presented as a composition of two simple waves, bottom profile.*

Taking this idea one step further, we can see how an irregular pattern of wind waves can be thought of as a superposition of an infinite number of sinusoidal waves, propagating independently of each other. It can be shown that, as the number of different sinusoidal



*Figure 3.6: The sea surface obtained from the sum of many sinusoidal waves*

waves in the composition is made larger and larger, the heights are made smaller and smaller and periods and directions are packed closer and closer together, the result is a sea surface just like the one actually observed in the bottom of Fig.3.6.

### 3.4 Wave records

A typical wave record (like the one measured by a wavemeter buoy) of a real sea state just like the one exposed in Fig.3.6 is the following:

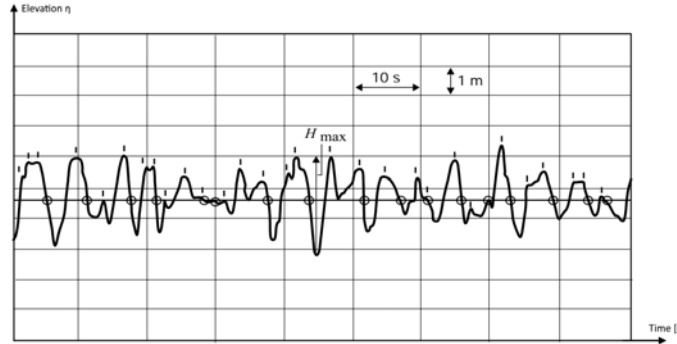


Figure 3.7: Sample of a wave record

Compared with Fig.3.2 it's completely different but can be made two assumptions: on one hand a measured wave record never repeats itself exactly due to the random appearance of the sea surface, but on the other hand if the sea state is "stationary" the statistical properties of the distribution of periods and heights will be similar from one record to another. Just from this idea it can be understood that the most appropriated parameters to describe the sea state from a measured wave record are therefore statistical.

### 3.5 Wave spectrum

We have noted in Section 3.3 that a sea surface with a random appearance may be regarded as the sum of many simple wave trains. A way of formalizing this concept is to introduce the *wave-variance spectrum* whose general ocean expression is reported in Equation (3.3).

$$S(f) = \frac{A}{f^5} \exp\left(\frac{-B}{f^4}\right) \quad (3.3)$$

The above dependence is a general form of the ocean wave model and it indicates the level of energy transported by the different frequency components  $f$ , in which the real sea has been decomposed.

On conducting the studies carried-out worldwide at various water areas, scientists worked out more detailed models elaborating that relation, each model fits with many environmental conditions. While selecting the wave model to apply in the research process, it is necessary to take into consideration also the following aspects and questions:

- Is the considered water area limited with any coastline which prevents full development sea?
- Are the sea waves under a process of formation or degradation?
- The water area depth, waves on deep water areas differ from those on shallow waters;

- Surface currents affecting waves' characteristics.

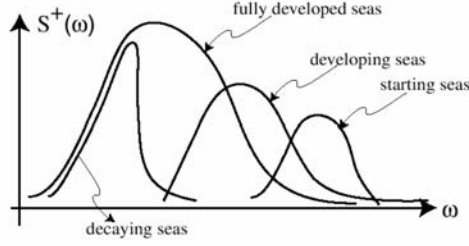


Figure 3.8: Typical form of equation (3.3) for different seas

To work out wave's spectrum for limited and shallow water areas (this thesis' case), at the beginning of the seventies the *Joint North Sea Wave Project*, **JONSWAP** was performed. In view of its characteristics it is often used for purpose of studies and analyses referring to coastal navigation at limited water areas (the environmental conditions mentioned before). For that model, Equation (3.3) became the following:

$$S(f) = \alpha g^2 (2\pi)^{-4} f^{-5} \exp \left[ -\frac{5}{4} \left( \frac{f}{f_p} \right)^{-4} \right] \gamma^{\exp \left[ \frac{(f-f_p)^2}{2\tau^2 f_p^2} \right]} \quad (3.4)$$

The spectrum is two-parameter and dependent on two input parameters, which are a modal frequency and amplification coefficient, where:

- $f_p = 2\pi/T_p$  is the spectral peak or modal frequency of Jonswap spectrum;
- $\alpha = 0.0076 \left[ \frac{U_{10}^2}{F_g} \right]^{0.22}$ ;
- $U_{10}$  is the wind speed at 10 meters height;
- $\tau = \begin{cases} 0.07, & f < f_p \\ 0.09, & f > f_p \end{cases}$
- $\gamma$  is the peak enhancement factor.

In practice, it's more useful to work with the *wave energy* spectrum, in which instead of  $S(f)$  it use  $E(f)$ . Going on with the description of spectrum parameters, many physical variables will be introduced: first of all it has to be introduced the energy spectrum  $F$ , defined for a given wavenumber  $k$ , geographical position  $x$  and time  $t$  as  $\mathbf{F}(\mathbf{k}, \mathbf{x}, \mathbf{t})$ : it describes how the wave energy is distributed as function of frequency  $f$  and propagation direction, it's related to energy  $E(f)$  with the following relation:

$$E(f) = \int F(f, \theta) d\theta \quad (3.5)$$

In its continuos form,  $F(f, \theta)$  describes how the wave energy is distributed as function of frequency  $f$  and propagation direction  $\theta$ : integrated wave parameters are computed as weighted integrals of  $F(f, \theta)$ , as will be exposed later.

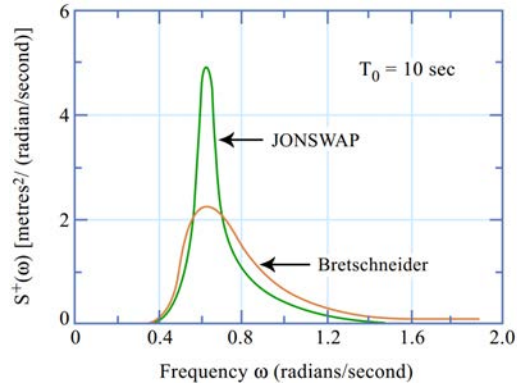


Figure 3.9: Amplitude spectra for Jonswap and another typical spectrum model for significant wave height 4 m

Then, the second parameter to be introduced is the relative radiant frequency  $\sigma$  exposed by the following *dispersion relation*, just seen in Table 3.1:

$$\sigma^2 = gk \tanh(kh) \quad (3.6)$$

with  $g$  gravity acceleration and  $h$  the water depth. The last physical variable to be introduced is the **action density spectrum**  $N$  defined for a given wavenumber  $k$ , position  $x$  and time  $t$ , correlated to the energy spectrum  $F(k,x,t)$  with the following:

$$N = gF/\sigma \quad (3.7)$$

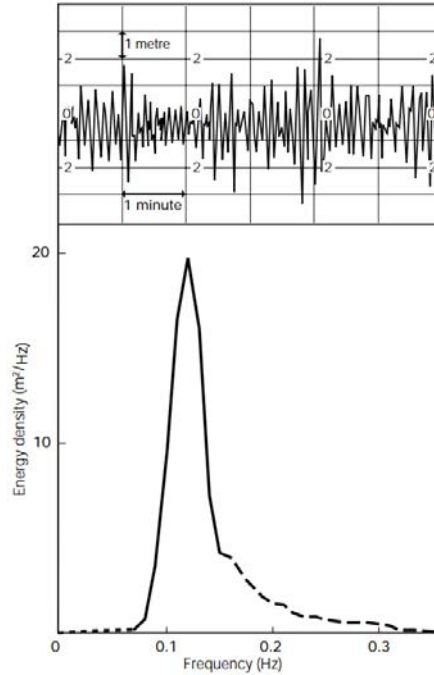


Figure 3.10: Energy density spectrum  $E(f)$  with the corresponding wave sample

The most important variables to describe a wave are computed as moment of the spectrum. The first moment of a distribution (the wave spectrum named before) of  $N$  observations  $X_1, X_2, \dots, X_n$  is defined as the average of the deviations  $x_1, x_2, \dots, x_n$  from the given value  $X_0$ . The second moment is the average of the squares of the deviations about  $X_0$ ; the third moment is the average of the cubes of the deviations, and so forth. When  $X_0$  is the mean of all observations, the first moment is obviously zero, the second moment is then known as the "variance" of  $X$  and its square root is termed the "standard deviation". Thus, the moment of order  $n$  of  $F$  is defined as:

$$m_n = \int f^n F(f, \theta) df d\theta \quad (3.8)$$

Then, the relevant wave integral parameters are calculated as:

- Significant wave height  $H_s$ : the wave energy is defined as  $E_0 = m_0$ , so the definition is

$$H_s = 4\sqrt{E_0} \quad (3.9)$$

- Mean periods: there are many periods to be defined:
  - $T_p$  is the wave period corresponding to  $f_p$ ,  $T_p = f_p^{-1}$ ;
  - $T_{m01}$  is the wave period corresponding to the mean frequency of the spectrum,  $T_{m01} = \frac{m_0}{m_1}$ ;
  - $T_{m-10}$  is the Energy wave period, so-called for its role in computing wave power,  $T_{m-10} = \frac{m_{-1}}{m_0}$ . It is strictly related to the lower frequency band of the spectrum, where most of the power is contained. This parameter is important for the evaluation of the energy transported by the wave  $J$ , with the well known formulation here reported:

$$J = 0.49 H_s^2 T_{m-10} \quad (3.10)$$

### 3.6 Balance equation and WAM model

To predict the behaviour of sea waves the model used in the majority of applications is WAM. The main target of a forecasting model like WAM is to forecast how waves evolve as changing wind fields act on the surface of the ocean. To understand this it need to identify the processes affecting the energy of the waves. In simple terms, wave energy at a given location is changed through advection (rate of energy propagated into and away from the location), the wave energy gains from the external environment and wave energy losses due to dissipation. In wave modelling, the usual approach is to represent these influences as a wave energy conservation equation or the *spectral energy balance* equation, here reported in it's general form:

$$\frac{\partial E}{\partial t} + \nabla \cdot (c_g E) = S \quad (3.11)$$



This form of the equation is valid for deep water with no refraction and no significant currents. If it's specified in a more accurate and specific form (for this thesis' target) it becomes a **spectral action balance equation**:

$$\frac{\partial N(i)}{\partial x} + \nabla_x \cdot (c_g + U) N(i) + \nabla_x \cdot c_i N(i) = \sum S(i) \quad (3.12)$$

where  $c_g$  is the group speed:

$$c_g = \frac{1}{2} \left( 1 + \frac{2 |\vec{k}| d}{\sinh(2 |\vec{k}| h)} \right) \frac{\sigma \vec{k}}{|\vec{k}|^2} \quad (3.13)$$

and  $U$  is the sea current (terms that are not treated in this thesis); the correlation between  $E$  and  $N$  is just exposed in Equation (3.7). The main target of WAM model it has become now to forecast  $\mathbf{N}(\mathbf{k}, \mathbf{x}, \mathbf{t})$ .

The second left term of (3.12) represent the energy advection due to group speed and sea current instead the third left term represent the energy advection in the spectral domain.

The attention has to be focused on the right term of Equation (3.12), indeed  $\sum S(i)$  represent the sum of sources and sinks of energy or action and can be presented as

$$\sum S(i) = S_{in}(i) + S_{nl}(i) + S_{ds}(i) + S_{bot}(i) \quad (3.14)$$

in which the four terms represents respectively: the wind input (linear and exponential), wave-wave interactions (non linear, important for propagation), the dissipation due to whitecapping and finally the process of bottom friction.

### 3.6.1 Sources and sinks description

- Wind input  $S_{in} = \gamma N$ , with  $\gamma$  the *growth rate* computed with the following relation (by Jansenn, 1989):  $\gamma = \delta \epsilon \beta \chi^2$  in which the terms represent respectively: the angular frequency, the air-water density ratio, the *Mile's parameter* and  $\chi$  is a term that relate the friction velocity  $u^*$ , the wind direction and the wave propagation direction;
- Dissipation due to Whitecapping: as waves grow, their steepness increases until a critical point when they break. This process is highly non-linear. It limits wave growth, with energy being lost into underlying currents;  
 $S_{ds} = -C_{ds} \langle \delta \rangle (\langle K \rangle^2 m_0)^2 \left[ \frac{(1-\mu)K}{\langle K \rangle} + \mu \frac{K}{\langle K \rangle^2} \right] N$  (Jansenn, 1989) in which  $\langle \delta \rangle$  is the mean angular frequency,  $\langle k \rangle$  is the mean wavenumber,  $C_{ds}$  and  $\mu$  are constants (equal respectively to 1.33 and 0.5) and  $m_0$  is the total wave variance per square metre just exposed in Equation (3.8);
- Dissipation due to Bottom friction  $S_{bot} = -2C_{bot} \frac{K}{\sinh(2kh)} N$  (Komen et al., 1994) in which  $C_{bot}$  is a constant equal to 0,038/g;

- Wave-wave non-linear interaction for surface gravity waves  $S_{nl}$  is caused by four resonantly interacting waves, whose relation impose that  $\delta_1 + \delta_2 = \delta_3 + \delta_4$ ,  $\vec{K}_1 + \vec{K}_2 = \vec{K}_3 + \vec{K}_4$ . In this way, the computation of  $S_{nl}$  is done computing Boltzmann's integral, which computation take several time so Hasselmann proposed an approximation called *DIA*, (*Discrete Interaction Approximation*) that consider  $\omega_1 = \omega_2$  so  $\vec{K}_1 = \vec{K}_2$  and  $\omega_3 = \omega_+ = \omega_1(1+\lambda)$ ,  $\omega_4 = \omega_- = \omega_1(1-\lambda)$  with  $\lambda = 0.25$ . Hasselmann's relation became the following: 
$$\begin{pmatrix} \frac{\partial N}{\partial t} = S_{nl} \\ \frac{\partial N_+}{\partial t} = S_{nl+} \\ \frac{\partial N_-}{\partial t} = S_{nl-} \end{pmatrix} = \begin{pmatrix} -2 \\ 1 \\ 1 \end{pmatrix} CS_c [N^2(N_+ + N_-) - 2NN_+N_-] \Delta \vec{K}$$
 with  $N_+ = N(\vec{K}_+)$  and  $N_- = N(\vec{K}_-)$

Ignoring the directional characteristics it's possible to construct a diagram for S that gives an idea of the relative importance of the various processes at different frequencies.

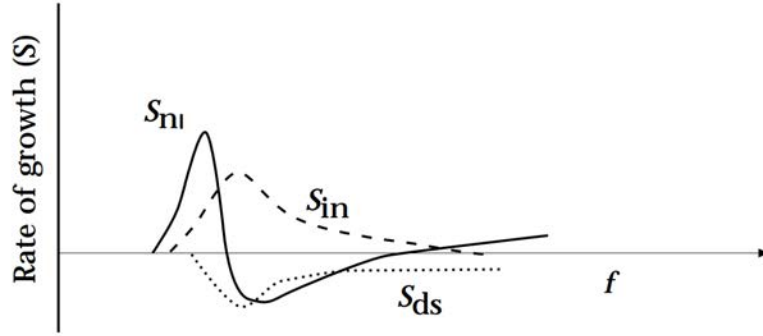


Figure 3.11: Structure of spectral energy growth. The curves shows the components  $S_{nl}$ ,  $S_{in}$ , and  $S_{ds}$

For example the non-linear transfer is the dominant growth agent at frequencies near the spectral peak. Also, for the mid-frequency range the growth is dominated by the direct input of the atmosphere. The non-linear term relocates this energy mostly to the lower frequency range. The dissipation term operates primarily on the mid- and high-frequency ranges.

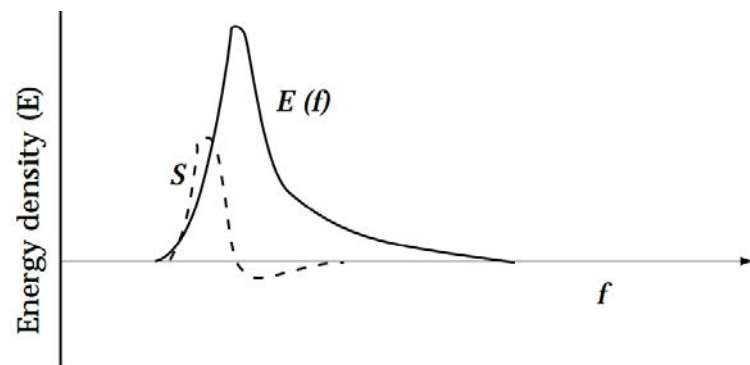


Figure 3.12: Total growth curve compared to the frequency spectrum  $E$



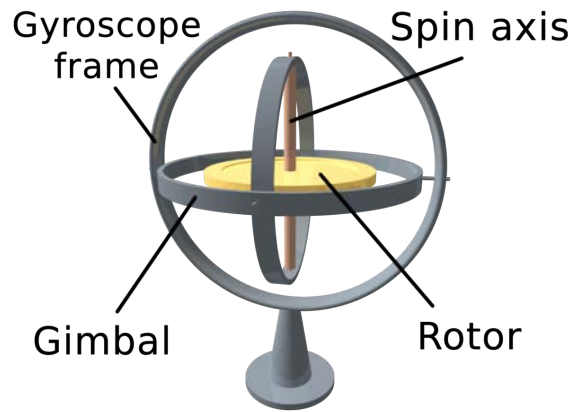
## Chapter 4

### ISWEC device

In this chapter the main characteristics and features of ISWEC device are exposed with also a mathematical section to give a view of the model used later in Chapter 6. All the information exposed here are taken from [32] and [9].

ISWEC is a Wave Energy Converter composed mainly of a single offshore floating body with a slack mooring, the waves tilt the buoy with a rocking motion that is transmitted to an full sealed internal gyroscopic system composed of two units. The first main advantage of a technology like that, compared with those exposed in Chapter 2, is represented by the total absence of any seal, joint or part in relative motion into the harsh sea environment, avoiding problems of corrosion and thus decreasing maintenance expenses, also respecting the sea environment; the only components immersed in the marine environment are the mooring and the electrical cable.

Electricity generation is based on the conservation of the angular momentum of the internal gyroscope (Fig.4.1).



*Figure 4.1: Gyroscopic base system principle*

The integration of a base system presented in Fig.4.1 and the ISWEC device is presented in the figure below (Fig.4.2), in which the rotor is a flywheel, the spin axis is  $\dot{\phi}$ , the gimbal is a 1 DOF (Degree of freedom) platform and the gyroscope frame is a mechanical structure:

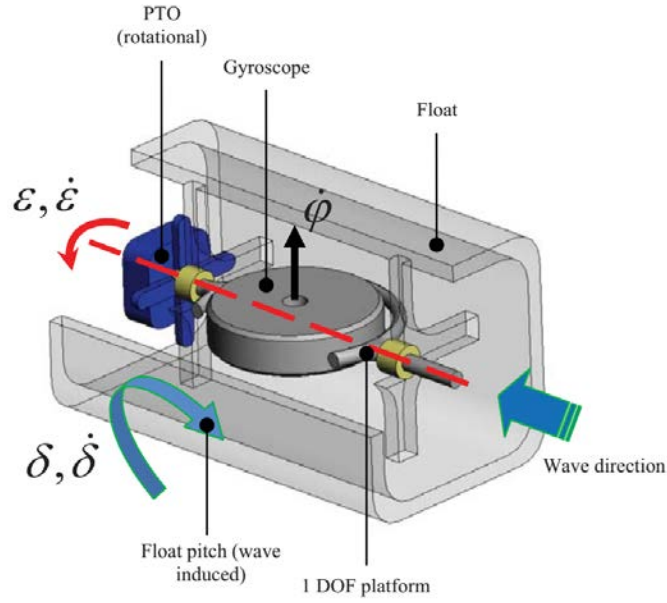


Figure 4.2: Device with main axes and the gyroscope system embedded

In normal energy production operation mode the device is aligned with the wavefront direction and the waves make the floater pitching around the  $\delta$  axis. The floater pitch motion combines with the internal flywheel spinning velocity  $\dot{\psi}$  (Fig.4.3), thus originating an inertial gyroscopic torque acting on the internal precession axis  $\epsilon$ . An electric motor is mounted on this shaft, and electricity is generated braking its motion [32]. Already from here it has to be noted the second main advantage of a device like that: the direct dependence of the angular momentum with the flywheel speed  $\dot{\phi}$  allow a tuning of ISWEC behaviour with the sea state just varying  $\dot{\phi}$ .

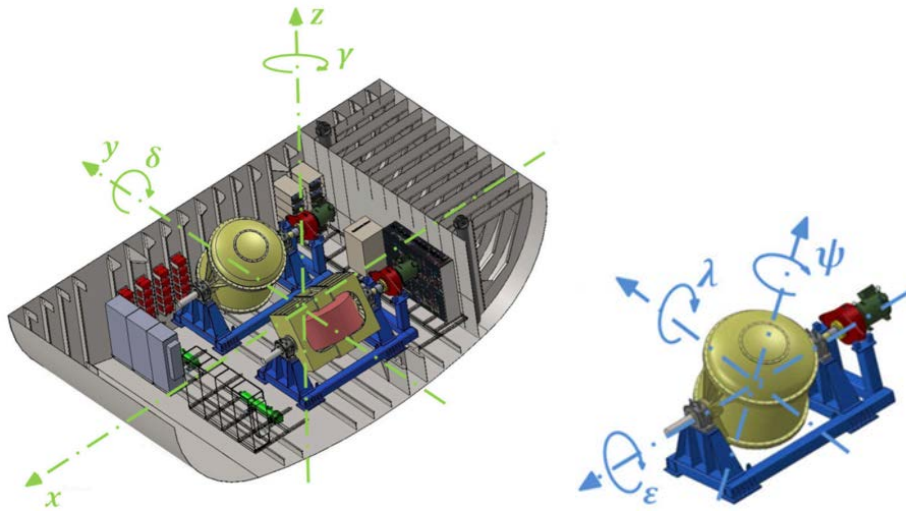


Figure 4.3: ISWEC reference frames

In Fig.4.3 are highlighted the main three components of the conversion: the mechanical structure (blue), the flywheel (red) and the PTO (Power Take Off, green).

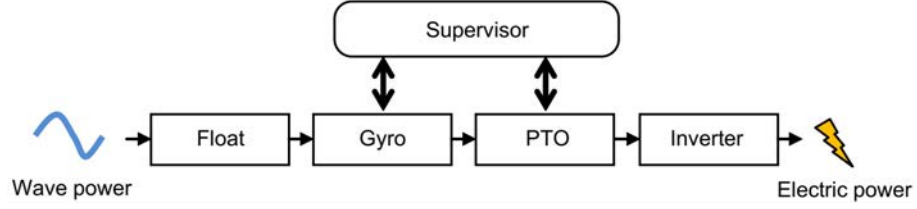


Figure 4.4: ISWEC block diagram

## 4.1 Reference frames

As can be seen in Fig.4.3 there are two different reference frames, one related to the hull (left picture of Fig.4.3,  $x_1, y_1, z_1$  hereafter) and one to the gyroscopic system (right picture of Fig.4.3,  $x_2, y_2, z_2$  hereafter) thus are reported two tables related to the hull movements:

DOF	Name	Comment	Symbol
1	surge	motions in the $x_1$ -direction	$x_1$
2	sway	motions in the $y_1$ -direction	$y_1$
3	heave	motions in the $z_1$ -direction	$z_1$
4	roll	rotations about the $x_1$ -axis	$rx_1$
5	pitch	rotations about the $y_1$ -axis	$\delta$
6	yaw	rotations about the $z_1$ -axis	$\gamma$

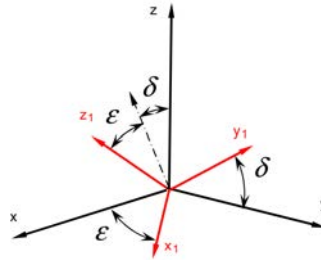


Figure 4.5

and to the gyroscopic system movements:

DOF	Name	Comment	Symbol
1	-	-	-
2	-	-	-
3	-	-	-
4	precession axis	rotations about the $x_2$ -axis	$\epsilon$
5	-	rotations about the $y_2$ -axis	$\lambda$
6	-	rotations about the $z_2$ -axis	$\psi$

## 4.2 Working principle

The mechanical behaviour can be easily explained by starting from the initial position in which  $\delta=0$  and  $\epsilon=0$ , there are no waves and the flywheel rotates around the axis  $z_2$  with constant angular velocity  $\dot{\phi}$ . As effect of the first incoming wave, the system is tilted along the pitch direction  $\delta$  gaining a certain angular velocity  $\dot{\delta}$  along the  $x$  axes. The flywheel is so subjected to the two angular velocities  $\dot{\phi}$  and  $\dot{\delta}$  and the gyroscopic effects produce a torque on the direction  $y_1$  that is perpendicular to both the velocities. If the gyroscope is free to rotate along the  $y_2$  direction with rotation  $\epsilon$ , its behaviour is governed just from the inertia and being the system conservative there is no mechanical power available for generation: the extraction of energy from the system can be performed by damping the motion along  $\epsilon$  coordinate. The damper can be for instance an electric generator directly coupled on the  $\epsilon$  shaft.

During the evolution of the system (damped or undamped) a gyroscopic torque arises on the buoyant too: in fact the two angular velocities  $\dot{\phi}$  and  $\dot{\epsilon}$  combined together produce a gyroscopic reaction on the buoyant along the  $\delta$  coordinate opposing the wave induced pitching motion. Furthermore a second reaction torque arises on the  $z_2$  axes by the combination of  $\dot{\delta}$  and  $\dot{\epsilon}$  angular velocities.

While the devices optimized for the oceans mainly exploit the high height the typical wave of these ecosystems, ISWEC, working on frequency and slope of the wave's side, it is able to extract a high quantity of energy also from short and relatively little powerful waves typical of closed seas. Finally, the hull shape has an important self-aligning feature, that allow to maximize the productivity in a given time period.

## 4.3 Mathematical view

An expression of the conservation of angular momentum for the gyroscopic system can be written as:

$$\vec{M}_e = \frac{d\vec{K}_G}{dt} \quad (4.1)$$

The equation assert that the variation (with respect to the time) of the angular momentum is equal to the applied external torque. If  $\vec{i}_1, \vec{j}_1, \vec{k}_1$  are three versors associated to the reference  $x_2, y_2, z_2$  an expression for  $\vec{K}_G$  is the following:

$$\vec{K}_G = \vec{I} \cdot \vec{\omega}_G = I\dot{\delta}\cos(\epsilon) \cdot \vec{i}_1 + I\dot{\epsilon} \cdot \vec{j}_1 + J(\dot{\delta}\sin\epsilon + \dot{\phi}) \cdot \vec{k}_1 \quad (4.2)$$

in which  $\omega_G$  is the flywheel angular velocity, J represent the moment of inertia of the flywheel around its axis of spinning  $z_1$  and I represent the two moments of inertia of the same flywheel but with respect to the axes perpendicular to  $z_1$ . Time deriving the angular momentum from (4.2) at the end of all mathematical passages the equilibrium of the system



is described by the following vectorial equation:

$$\vec{M}_e = \begin{Bmatrix} I\ddot{\delta}\cos \epsilon + (J - 2I)\dot{\epsilon}\dot{\delta}\sin \epsilon + J\dot{\epsilon}\dot{\phi} \\ I\ddot{\epsilon} + (I - J)\dot{\delta}^2\sin \epsilon \cos \epsilon - J\dot{\phi}\dot{\delta}\cos \epsilon \\ J(\ddot{\delta}\sin \epsilon + \dot{\epsilon}\dot{\delta}\cos \epsilon + \ddot{\phi}) \end{Bmatrix} \quad (4.3)$$

The torque cited before, or better the torque on the PTO (Power Take Off) and the torque on the motor driving the flywheel  $T_\phi$  are given respectively by the second and the third scalar equation of the (4.3):

$$T_\epsilon = I\ddot{\epsilon} + (I - J)\dot{\delta}^2\sin \epsilon \cos \epsilon - J\dot{\phi}\dot{\delta}\cos \epsilon \quad (4.4)$$

$$T_\phi = J(\ddot{\delta}\sin \epsilon + \dot{\epsilon}\dot{\delta}\cos \epsilon + \ddot{\phi}) \quad (4.5)$$

As the device works, an other torque arise:  $T_\delta$  is discharged from the gyroscopic system to the hull along the pitching direction  $\delta$ , this torque can be calculated projecting  $\vec{M}_e$  along the x direction (with versor  $\vec{i}$ ):

$$T_\delta = \vec{M}_e \cdot \vec{i} = \vec{M}_e \cdot (\cos \epsilon \cdot \vec{i}_1 + \sin \epsilon \cdot \vec{k}_1) = (J\sin^2 \epsilon + I\cos^2 \epsilon)\ddot{\delta} + J\ddot{\phi}\sin \epsilon + J\dot{\epsilon}\dot{\phi}\cos \epsilon + 2(J - I)\dot{\delta}\dot{\epsilon}\sin \epsilon \cos \epsilon \quad (4.6)$$

If we consider two important simplifications like  $I \approx J$  and the gyroscope speed constant, the linearized parameters (around the  $\epsilon=0$  position) became the following:

$$\begin{Bmatrix} \tilde{T}_\delta \\ \tilde{T}_\epsilon \\ \tilde{T}_\phi \end{Bmatrix} = J \begin{Bmatrix} \ddot{\delta} + \dot{\epsilon}\dot{\phi} \\ \ddot{\epsilon} - \dot{\phi}\dot{\delta} \\ \ddot{\delta}\epsilon + \dot{\epsilon}\dot{\delta} \end{Bmatrix} \quad (4.7)$$

Now an important concept has to be introduced: if the PTO (Power Take Off) can be imagined as a *spring-damper* group, two more parameters will be used, the system stiffness  $k$  and the damping factor  $c$ .

By giving to the system a sinusoidal input  $\delta = \delta_0 e^{j\omega t}$  and expecting a sinusoidal response  $\epsilon = \epsilon_0 e^{j\omega t}$ , the complex amplitude  $\epsilon_0$  can be linked to the amplitude  $\delta_0$ . The natural frequency on the axis  $\epsilon$  can be defined as  $\omega^2 = k/J$ . So:

$$\bar{\epsilon}_0 = \bar{\delta}_0 \frac{J\phi j\omega}{J(\omega_n^2 - \omega^2) + cj\omega} \quad (4.8)$$

#### 4.3.1 Available power

The non linear differential equation that describe the gyroscopic behaviour is:

$$I\ddot{\epsilon} - J\dot{\phi}\dot{\delta} \cdot \cos \epsilon + (I - J)\dot{\delta}^2\sin \epsilon \cos \epsilon = T_\epsilon \quad (4.9)$$

in which  $T_\epsilon$  represent the mechanical torque exchanged between gyroscopic group and the PTO (Power Take Off), described by the following:

$$T_\epsilon = k\epsilon + c\dot{\epsilon} \quad (4.10)$$

Thus, the main important ISWEC control parameters are:

- $c$  Torsional damping factor on the PTO shaft;
- $k$  Torsional stiffness factor on the PTO shaft;
- $\dot{\phi}$  gyroscope Flywheel rotation speed;

If Equation 4.10 is linearized considering small oscillations on the  $\epsilon$  shaft the average power absorbed from the system by the damper  $P_d$ , considered available for electricity production, is the following:

$$P_d = \frac{c}{2} \omega^2 \epsilon_0^2 = \frac{c}{2} \frac{(J \dot{\phi} j \omega^2 \delta_0)^2}{J^2 (\omega_n^2 - \omega^2) + c^2 \omega^2} \quad (4.11)$$

This equation highlights that the maximum power is absorbed when the system is resonating,  $\omega = \omega_n$ . In resonance conditions the power can be expressed as follows:

$$P_{d,res} = \frac{(J \dot{\phi} \omega \delta_0)^2}{2c} \quad (4.12)$$

From Equation 4.11 the damping coefficient  $c$  is:

$$c = \frac{2P_d}{\omega^2 \epsilon_0^2} \quad (4.13)$$

so the power extracted can be written as:

$$P_{d,res} = \frac{1}{2} (J \dot{\phi}) \omega^2 \delta_0 \epsilon_0 \quad (4.14)$$

Equation (4.14) shows that, for the linearized model, the absorbed power is proportional to the flywheel angular momentum  $J \dot{\phi}$ , to the pitching amplitude  $\delta_0$  and the amplitude of oscillation of the PTO shaft  $\epsilon_0$ . Thus, to increase the extracted power of an ISWEC resonating device it needs to increase the angular momentum, the pitching amplitude of the float  $\delta$  and the  $\epsilon$  amplitude on the PTO shaft. Furthermore, the device can produce more if the incoming wave has a shorter period.

As a first stage it's considered the flywheel speed constant and the friction neglected: since this, during normal operation mode the power absorbed by the motor driving the flywheel is null, it can also be demonstrated rewriting equation (4.5):

$$T_\phi = J \frac{d(\dot{\delta} \sin \epsilon)}{dt} \quad (4.15)$$

Otherwise, the total energy provided by that motor in a time interval  $[t_0, t_1]$  to drive the gyroscope at  $\dot{\phi} = \text{constant}$  is the integral of the instantaneous power, like stated in the following:

$$\int_{t_0}^{t_1} P_M dt = J \dot{\phi} \left[ \dot{\delta} \sin \epsilon \right]_{t_0}^{t_1} \quad (4.16)$$

If  $t_0$  and  $t_1$  are two times before and after a wave, both of them at  $\epsilon = 0$  position, the total energy provided to win the gyroscopic effects on the  $\phi$  axes is thus null. However, in

a real system the relation could not be valid due to friction losses: if power lost for friction is considered, at ambient pressure it's of the same order of the power generated by the device; to reduce it at some percent of the produced power the flywheel needs to be run in a vacuum case.

If the last torque is considered, the one on the gyroscope structure, a connection with the previous device axis is expressed by the following:

$$T_\lambda = -J\dot{\phi}\dot{\epsilon} \quad (4.17)$$

Thus, the radial force  $F_R$ , if  $d_b$  is the distance between the components:

$$F_R = \frac{T_\lambda}{d_b} \quad (4.18)$$

and then the equivalent bearing load:

$$F_{b,eq} = \frac{F_R}{\sqrt{2}} \quad (4.19)$$

The bearings are one of the most critical components in the system, since their life rise many consideration about costs and maintenance intervals. The duration is computed with the constant load conditions equation:

$$L_{10 \ h} = \frac{10^6}{60 \cdot \phi_{nom} \frac{30}{\pi}} \left( \frac{C_b}{F_{b,eq}} \right)^{p_b} \quad (4.20)$$

where  $p_b$  is a bearing type dependent parameter,  $\dot{\phi}_{nom}$  is the flywheel speed at design wave state,  $C_b$  is the dynamic equivalent load coefficient and  $F_{b,eq}$  is the equivalent bearing load.

Finally, the following figure 4.6 gives an overall idea of what said before with equations: the dotted line represents the power density  $P_d$  of the incoming wave, the wave power density is proportional to the wave period while the power absorption capacity decreases with the wave period (see Fig.4.9): so, when there is a bigger power ISWEC can absorb less and viceversa. This leads to two considerations: ISWEC is more suitable to exploit short waves and probably, since short waves carry a smaller power, ISWEC will not be a device with a high rated power [9].

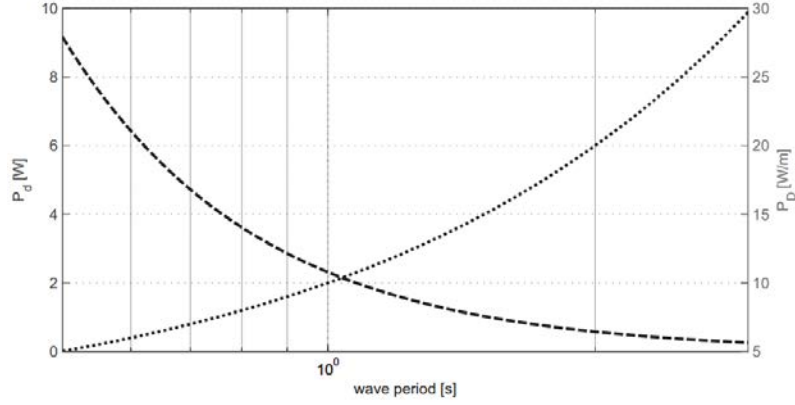


Figure 4.6: Tuned system - dashed line - vs. power density - dotted line - with respect to wave period, [9]

## 4.4 Device control

The main results of a complete analyse done in [17] with a 1:45 scale ISWEC prototype are here reported, the same conclusions can be done for the real-scale ISWEC considering a scale effect.

### 4.4.1 PTO stiffness

The importance of the PTO stiffness component for a proper ISWEC control is highlighted in Fig.4.7: if the PTO has no stiffness (it's free,  $k = 0 \text{ Nm/rad}$ ) the system settles with a damped oscillation to the condition  $\epsilon = 90^\circ$  because in that condition the gyroscopic effects disappear and therefore the torque and the power generated from the PTO are null (continuous line). As the stiffness increase the system oscillates around the  $\epsilon = 0^\circ$  position (dots and dashes lines), as in rated condition.

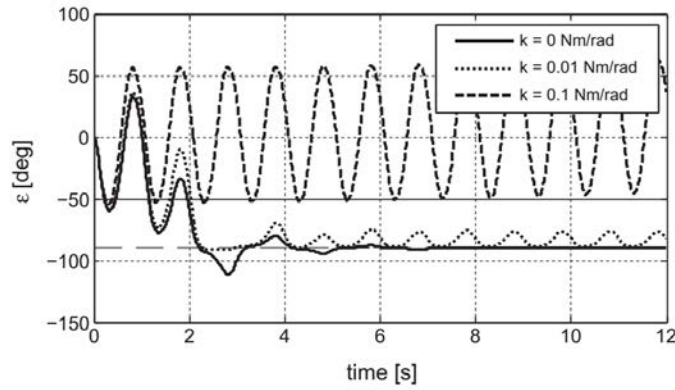


Figure 4.7: ISWEC behaviour at small and null stiffness

#### 4.4.2 Flywheel speed $\dot{\phi}$

As stated before, the flywheel velocity can be used to regulate the power absorption, for instance if the incoming wave generates a pitching angle  $\delta$  too big,  $\dot{\phi}$  can be reduced to absorb the rated power even if the waves are too much powerful. If the waves are so big to be dangerous (like in a stormy sea), then the flywheel can be arrested shutting down the gyroscopic effects and, if the PTO is locked, making the buoy behave like a dead body [9]. Besides, as in Fig.4.8, if the gyro speed isn't correct (equal to the rated speed) it causes an important power drop; if the gyro speed is increased too much the torque on the float increase, so the angle on pitch is small and the hull behaves as a float stabilizer and it's unsuitable for power generation.

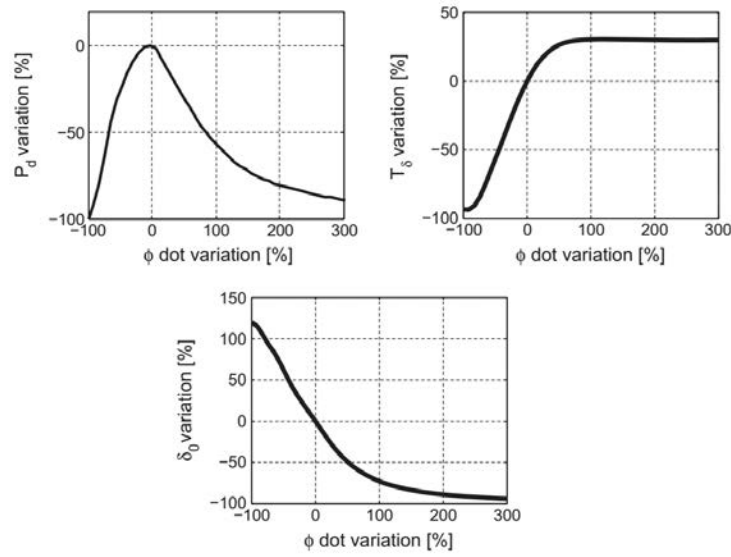


Figure 4.8: ISWEC dependence on  $\dot{\phi}$

#### 4.4.3 Wave frequency

As stated before, the PTO stiffness  $k$  is changed for each incoming wave frequency to maintain the device resonating and therefore maximizing  $P_d$ . As can be seen in Fig.4.9 for each gyroscopic speed there's an optimum point in the corresponding curve, given the resonating ISWEC frequency. If the incoming wave frequency change the power absorption can be kept adjusting the gyroscopic speed  $\dot{\phi}$ .

Besides, as the device works closer to the resonating frequency as lower will be  $\dot{\phi}$  [17].

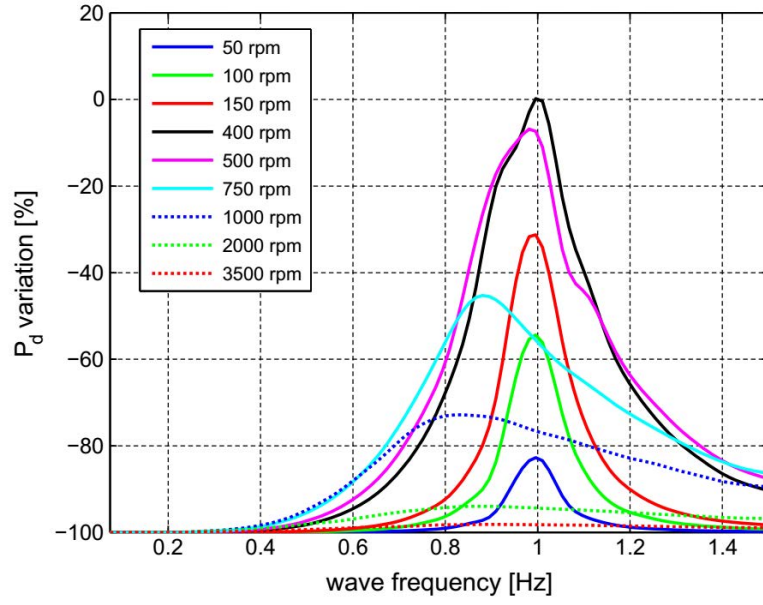


Figure 4.9: ISWEC dependence on the wave frequency

## 4.5 Power matrix

Generally when a renewable source electricity production plant has to be performed, it's important to present the behaviour of the harvesting-system with the environmental source. For example, for a photovoltaic system this concept is represented by a diagram that for each solar irradiance gives the electrical power available for each solar photovoltaic module. The same idea is presented here with the *power matrix*. It represent the power that the device can elaborate for a given sea state, that is for a given wave of  $T_p$  and  $H_s$ .

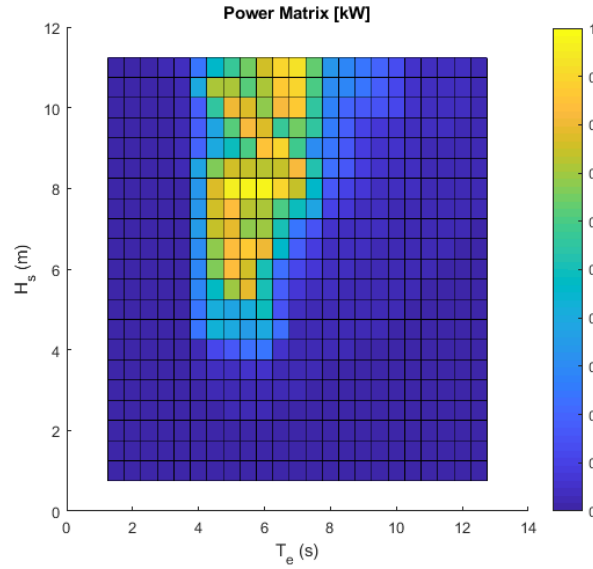


Figure 4.10: Power Matrix associated to a specific Marine site (San Clemente del Tuyu)

The *power matrix* is computed with a set of configuration waves that is then compared with each marine site waves to re-elaborate an "ad hoc" *power matrix* specific for the given marine site. This important part of ISWEC mathematical model allow a simple connection with the sea model, represented by another matrix (explained in Chapter 6): the product of that two matrices gives the device productivity (given a time period).

## 4.6 Mooring system

The mooring system is a vital part of a wave energy converter, regardless of the type of device. Therefore the interaction between mooring and wave energy converters is still an interesting research topic in order to properly design a mooring line with two main features: first of all the mooring has to ensure the maximum device movement with waves (maximize the productivity) but keeping the device still in place and then it has to minimize the interaction with the seabed, in order to respect the submarine habitat. Depending on the WEC's functionality (see Chapter 2), there's many mooring configurations, like the ones reported.

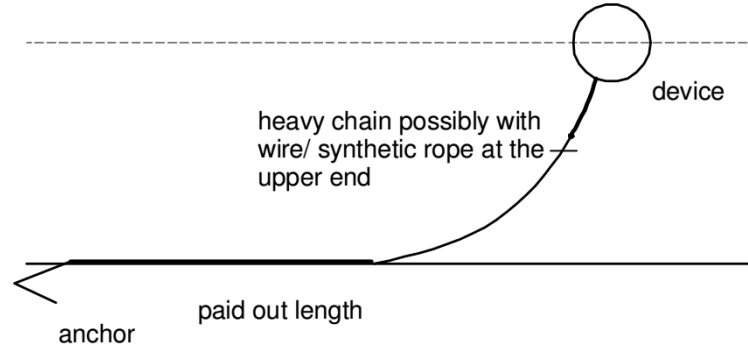


Figure 4.11: Basic catenary with horizontal load anchor

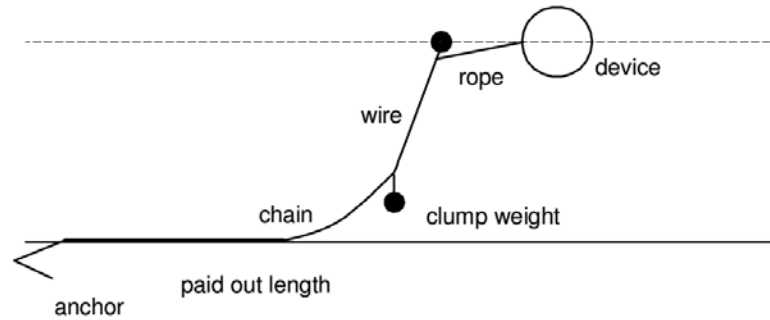


Figure 4.12: Chain catenary with surface buoy and clump weight

Various authors have addressed the design of suitable mooring system for WEC's but there is no specific regulation for WEC moorings and research in the field is still maturing [19]. The ISWEC mooring system has been designed in order to match these characteristics needs:

- ensure device survivability;
- restrain the maximum hull excursion within its reserved sea area;
- assure the hull self-orientation with the incoming wave direction (also guaranteed by the hull shape);
- not interfere with the hull pitching motion which is opportunely controlled to harvest the wave energy.

From bottom to top of Fig.4.13 it is composed as follows: four anchors are positioned on the seabed over a circumference such that the angular distance among them is equal to  $90^\circ$ . From each anchor a chain extends to reach a connection point placed upward with respect to the seabed, identifying a sort of virtual seabed: in this way the seabed abrasion of the chain is avoided and the working angle for the anchors is granted. From the virtual seabed a single chain line goes up vertically to a submerged buoy (a *jumper*) then a second chain links the jumper to a clump weight. A third chain segment, which represent a symmetric bifurcation, links the line to the ISWEC through two hawseholes placed at the hull bow, symmetric to the centerline [19].

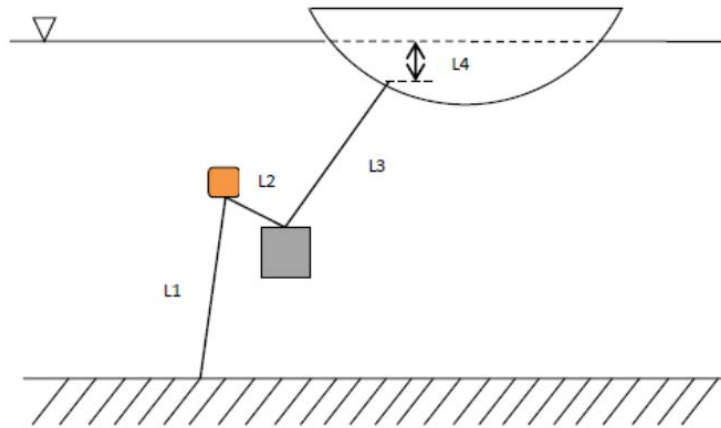


Figure 4.13: ISWEC mooring system concept

This configuration presents different advantages: the load on the main line is distributed among four different lines and so four anchors; the single line system allows the hull rotation around the jumper and its positioning toward the incoming wave direction. However, the most important part is the single line going from the jumper to the clump and then to the hull: this line acts as a spring that increases its restoring force as the hull displacement increases, limiting the hull excursion. On the other hand, it can absorb extreme waves' actions, avoiding snap loads on the mooring line.

#### 4.6.1 Geometry and relation with depth

Here is reported a more accurate scheme that shows better the displacement of all the mooring components for an installation site in which the mean sea level is 31 m from the



seabed:

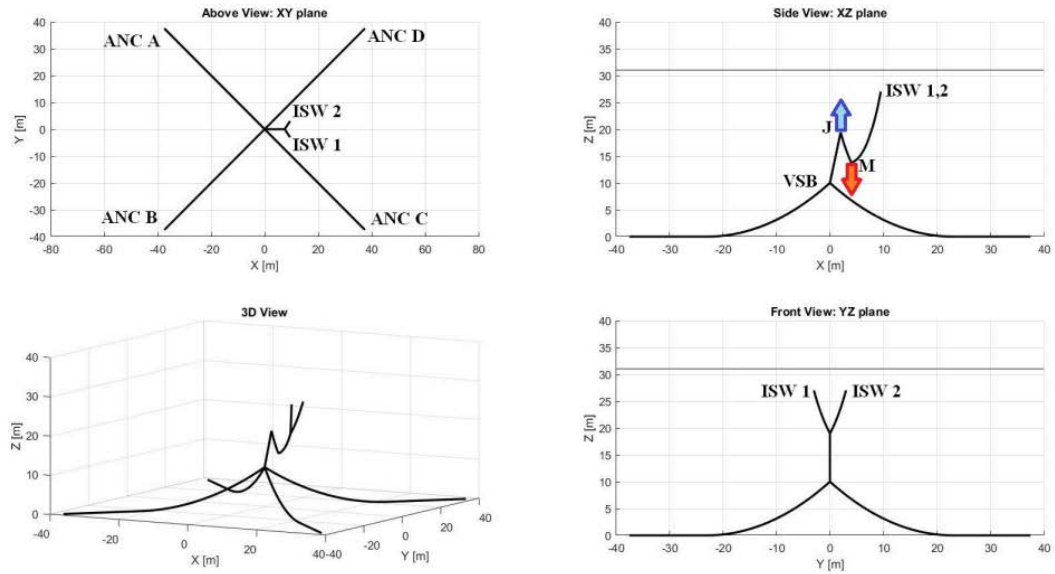


Figure 4.14: Mooring multi-view

and here the numerical characteristics:

Clump Weigth	Volume [m3]	Net Buoyancy [kg]
Steel and concrete element	5.4	-8000
Anchor	Type	Mass [kg]
4 x Italmet - AHN4320	Hall	4000
Jumper	Volume [m3]	Net Buoyancy [kg]
Floatex BOEORM	19.4	12600
Line	Length [m]	Diameter [mm]
1) ANC xx- VSB	55	40
2) VSB - J	9.5	48
3) J - M	6	48
4) M - Bri	6.5	48 / 32
5) Bri - ISW xx	8.8	48

Figure 4.15: Numerical values for each mooring parameter

## Relation with depth

Using that scheme as a reference point, a mathematical connection with sea depth  $d$  is needed for the following chapters (6 and 7). Considering what has been said in the previous paragraph about ISWEC behaviour with the waves and what are the waves that best fit with it's mechanical principle, the depth suitable range for an installation is from 20 m to 80 m (also depending on Politecnico di Torino experience with the device). Due to an absence of literature regarding a mathematical connection with depth, it will be assumed

that in that small depth range the mooring scheme, the anchors dimensions, the floater and the clump weight are the same, only the chain lines changes proportionally with depth. So, a proportion is written for each chain line of Fig.4.15:

- $55 : 31 = x : d \Rightarrow x = \frac{55d}{31}$
- $9,5 : 31 = y : d \Rightarrow y = \frac{9,5d}{31}$
- $6 : 31 = z : d \Rightarrow z = \frac{6d}{31}$
- $6,5 : 31 = k : d \Rightarrow k = \frac{6,5d}{31}$
- $8,8 : 31 = w : d \Rightarrow w = \frac{8,8d}{31}$

So, given a sea depth  $d$ , it's found each mooring line and thus it's possible to connect the sea depth  $d$  with a cost function.

Finally is presented an accurate 3D picture of the mooring scheme:

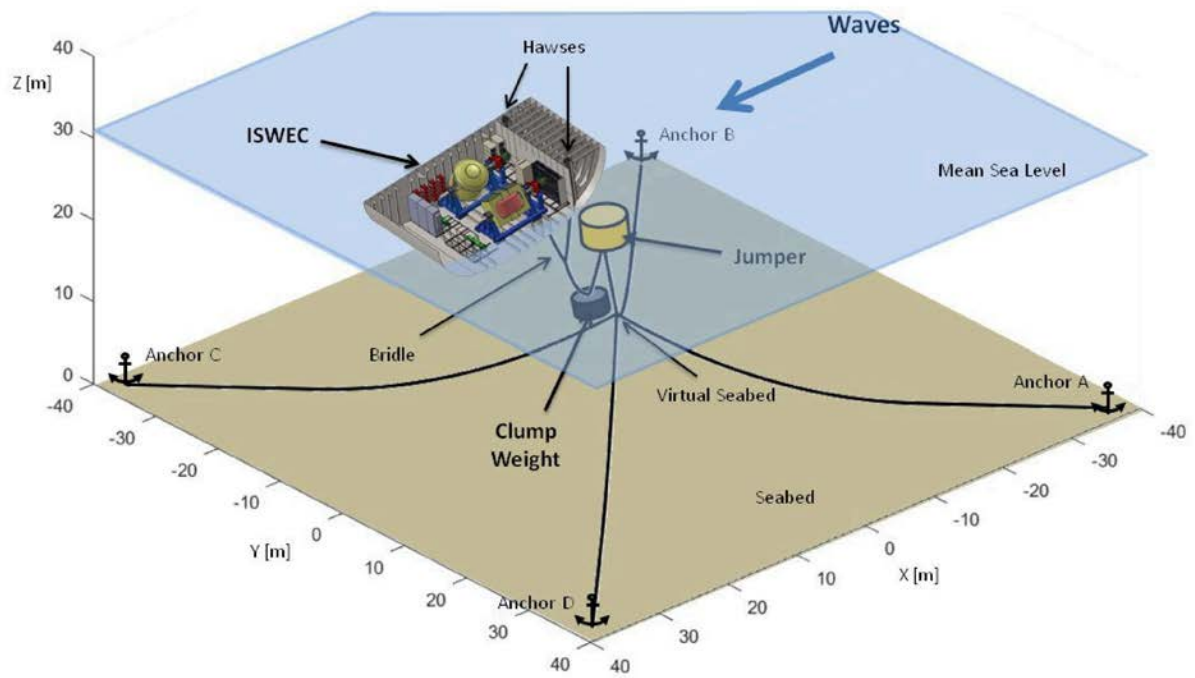


Figure 4.16: The mooring system

## 4.7 ISWEC in numbers

To conclude this chapter are reported many pictures of the device and a table that shows the values of the most important ISWEC parameters exposed in the previous paragraphs with equations thus to create a connection with the real device.

		Prototype	Full scale
$P_d$	[kW]	0.0735	106.4
$P_{d, effective}$	[kW]	0.042	61
$J\dot{\varphi}$	[kgm <sup>2</sup> ·rad/s]	584.3	$6.77 \cdot 10^6$
$\dot{\varphi}$	[rpm]	1005	355
$c$	[Nms/rad]	13.5	$1.56 \cdot 10^6$
$T_\varepsilon$	[Nm]	53.2	$2.18 \cdot 10^6$
$T_\delta$	[Nm]	1860	$7.62 \cdot 10^6$
Crown stress	[MPa]	5.24	41
Wave height	[m]	0.176	1.41
Wave length	[m]	8.8	70.4
$P_D$	[kW/m]	0.0735	13.1

Figure 4.17: Prototype vs real scale main parameters



Figure 4.18: ISWEC in Cantiere Navale F.lli Giacalone S.p.a. shipyard in Mazara del Vallo (Sicily, Italy)



*Figure 4.19: One of either ISWEC Gyroscope groups*

## Chapter 5

# Analysis of the marine resource

To analyze a marine resource, as stated in Chapter 3, wave data like wave height, wave period and wave direction (for example but there are several other data to be considered) are required, because, as said in the same Chapter the WAM wave model force the simulation with that data.

So, it is possible to proceed in two ways: if wavemeter buoys are installed along the marine resource to analyze with enough resolution (buoy per km of coast), data are sampled with them, thus data are truthful, only device uncertainty has to be considered.



*Figure 5.1: Wavemeter buoy*

But in most cases these devices are reserved to research purposes, so aren't installed in a developing country like Argentina. Thus the way to proceed is to use a **reanalysis dataset** (retrospective analyses). *"Reanalysis allows for a close monitoring of the Earth's climate system also where direct observations are sparse (such as for rising Arctic surface temperature)"*, by Copernicus Climate Change Service. The following threads are a summary of what reported in [33] and in [14].

## 5.1 Reanalyses dataset

Ocean reanalysis (ORA) combines observations either statistically or with a hydrodynamical model, to reconstruct historical changes in the ocean. Reanalyses are produced via **data assimilation**, a process that relies on both observations and model-based forecasts to estimate conditions for many variables. They have been used to study atmospheric dynamics, to investigate climate variability, to evaluate climate models, as data in which to look for the presence of greenhouse gas fingerprints. Data assimilation can be characterized as a process in which available information is used to estimate as accurately as possible the state of a system (Talagrand 1997). In atmospheric data assimilation this procedure typically includes both observations from a variety of sources (ground based stations, ships, airplanes, satellites and buoys) and forecasts from *numerical weather prediction* models (NWP). Data assimilation is a crucial part of NWP today, it is used to produce the analysis of current conditions that serves as the starting point for the next NWP forecast cycle, the assimilation system delivers a complete gridded state estimate that provides values (initial conditions) for all NWP model variables at all grid points. Since the '90s data assimilation also has been used to construct long-term datasets for use in climate and other research, in a process known as retrospective analysis or *reanalysis*. Reanalysis involves performing data assimilation for past periods, using a current NWP model and data assimilation method and some or all of the data that are now available for those past periods.

### 5.1.1 Differences between measured data and assimilated data

There are many differences that it's important to highlight, in the way to give the correct description of what are reanalyses and why are them used in this context. First of all, it could think that reanalysis datasets are produced via a complex inferential process that involves theory-based calculation, whereas familiar observations and measurements are obtained directly from instrument readings that mirror atmospheric conditions, but it's not correct at all. It's true that reanalysis results are inferred with the help of theory-based calculation: producing the first-guess forecast(s) involves calculating later conditions from earlier ones using NWP models that incorporate approximate laws of atmospheric motion as well as some empirical parameters and relationships. On the other hand, many measured data are also inferred with the help of theory-based calculation, they are not obtained directly from instruments readings that mirror atmospheric conditions.

Furthermore, instruments often must be corrected for interfering factors and this correction is an equation likely to be informed by both theory and empirical data. Results like the one obtained with that procedure are called *indirect observations*.

A second possible difference is that in reanalysis some equations used in the NWP models relate variables in different times, instead theory-based calculation used in classical measurements relate variables as a single time: as a consequence it could be said that reanalysis create a more accurate picture of the time-depending model.

A third possible (and maybe the most important) is the following: an instrument is always joined with a *calibration certificate* that gives confidently the uncertainty value, often very

small, associated to the measurement. The same thing couldn't be said for reanalysis, because accurate estimates of full atmospheric fields generally are not available. But there's a good reason, for specific reanalysis variables like wind characteristics and temperature where there are many assimilated observations (by ground stations or by satellites), to think that the results are quite accurate: this statement will be explained here below.

### 5.1.2 Uncertainty estimation

The importance of an estimation about validation or uncertainty for reanalysis datasets is evident: first of all it's important for drawing appropriate conclusions from those results. Most of articles wrote until today speaks about reanalysis uncertainty on a trend or on a change in a specific weather parameter, like the growing global temperature; in this context uncertainty value is important for give a correct sea state, since that from it depends the yearly production of the ISWEC. Comparing a reanalysis dataset with one another it expect that they will not agree in each value but if all goes well the differences between them should not exceed the differences that are expected, given their respective confidence intervals: a lack of consistency indicates that something has gone wrong. Anyway, the reanalysis results used in this context are known to be determined primarily by observations that it can expect to be rather accurate (explained below).

### 5.1.3 Availables datasets

There are many reanalysis datasets available for many purposes, they may ingest different input data and may be tuned for different objectives; which one is better is often determined by the target of the user. Here it's reported a comparative table (Fig.5.2) with the most important ocean datasets interesting for the target of this thesis. The table has been created comparing the information reported in the Research Data Web Archive (rda.ucar.edu), considering only ocean datasets with resolution from 10 km to 50 km (a lower resolution allow to get maps too less detailed for the fixed purpose).

For choosing the dataset has been considered the following parameters: temporal resolution less than 1 hour and the best grid resolution available. Thus, as can be seen in Fig.5.2 the best option is **ERA5**, a dataset made by ECMWF (European Center for Medium range Weather Forecast). ERA5 is the fifth generation of ECMWF atmospheric reanalyses of the global climate. ECMWF climate reanalyses started with the FGGE reanalyses produced in the 1980s, followed by ERA-15, ERA-40 and most recently ERA-Interim wich is the predecessor of ERA5.

Dataset ID	ds630.0	ds604.0	ds131.2
Title	ERAS	NCAR CFDDA	NOOA, 20th century global reanalysis, version 2C
Data Types	Grid	Grid	Grid
Data Formats	• NetCDF • GRIB1	NetCDF	GRIB1
Platforms	Reanalysis models	• Ground-Based observations • Reanalysis models	Reanalysis models
Temporal Range	2008 to 2018	1985 to 2005	1850 to 2014
Temporal Resolutions	Hourly	1 minute to 1 hour	Hourly to Daily
Gridded Products	• Analyses • Forecasts • Accumulations	Analyses	• Analyses • Forecasts • Accumulations • Averages
Grid Resolution	0.28°, 31 km	0.4°, 40 km	~ 2°

Dataset ID	ds626.0	ds628.4	ds093.0
Title	ERA-20C	JRA-55AMIP The Japanese 55 year reanalysis simulation	NCEP CFSR
Data Types	Grid	Grid	Grid
Data Formats	• GRIB1 • GRIB2	GRIB1	GRIB2
Platforms	Reanalysis models	Reanalysis models	• Models • NCEP Climate Forecast System • Reanalysis models
Temporal Range	1900 to 2011	1958 to 2013	1979 to 2011
Temporal Resolutions	Hourly to Daily	Hourly to Daily	Hourly to Daily
Gridded Products	Analyses Forecasts	• Analysis • Forecasts • Averages	• Analyses • Forecasts • Accumulations • Averages
Grid Resolution	~1.1°	2.5°	0.312° (best resolution available)

Figure 5.2: Datasets comparison

So, here are reported the reasons of the choice:

- ERA5 is one of the few datasets of which **uncertainty estimation** is given: information on uncertainties is provided for each parameter at 3-hourly intervals and at a horizontal resolution of 62 km (see also Fig.5.6);
- Periodic release of reports about Forecast validation: although they're unimportant in this context, they're good and has to be said that reanalysis are based also on the forecasts (as stated before);
- Periodic release of reports about the quality of observations used in the reanalysis;
- Complete description of each parameter with a well-structured website;

In the previous pages was stated that, for the variables used in this context, there's a good reason to think that they're determined by observations quite accurate: here are reported in Fig.5.3 the ERA5 observations get by Satellites and Buoys that then force the simulation model. That two variables are only an instance to highlight that around Argentina's ocean the observations are enough thick, thus the reason to think that reanalysis are quite accurate is motivated by thick observations.



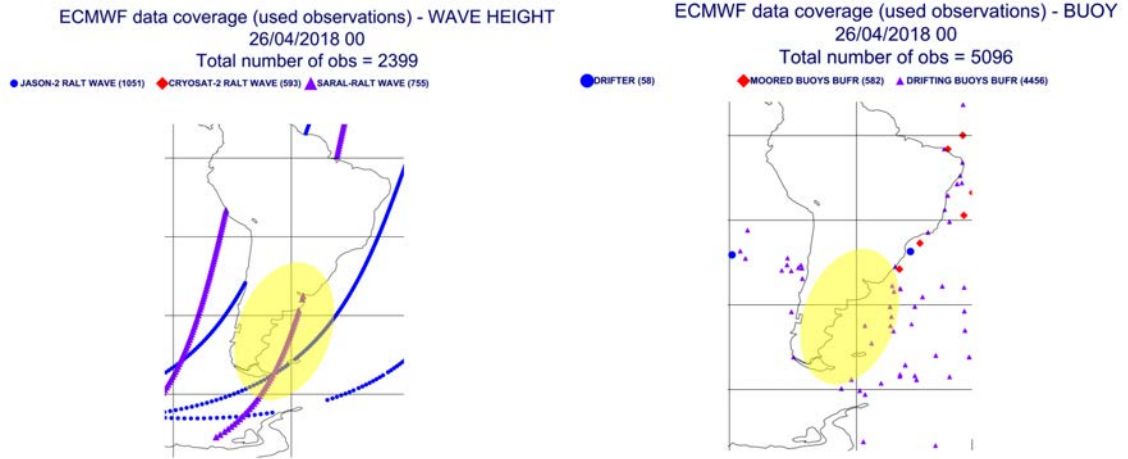


Figure 5.3: ECMWF ERA5 observations on the Argentina's area: Satellites and Buoys

As a further proof of what has just been exposed here below are reported many charts published in an ECMWF article [29] (Note: the Scatter Index in the following figures is the error standard deviation normalized by the mean observed value):

- In Fig.5.4 can be seen that the Scatter index value has got lower with the years, in particular for the forecast at time 0 (red line trend);
- In Fig.5.5 can be seen that ECMWF forecasts have the best Scatter Index trend compared with other datasets;
- In Fig.5.6 can be seen the coherence between observations and ERA5 reanalysis;

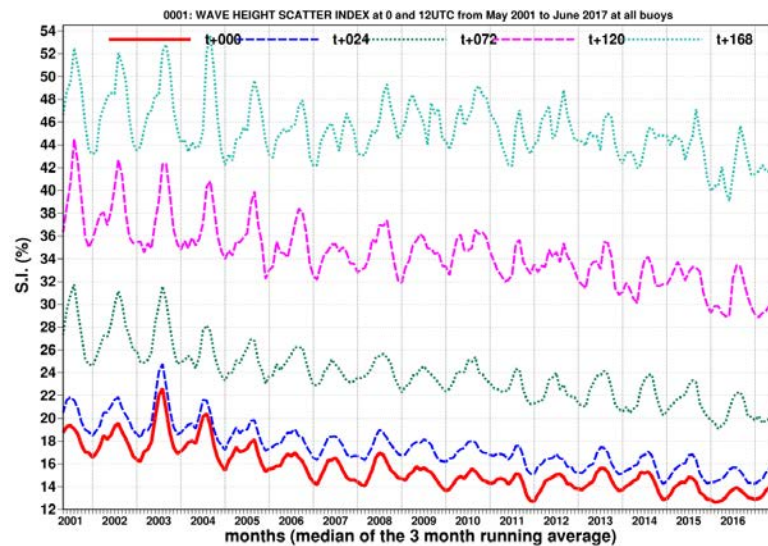


Figure 5.4: Time series verification of wave model forecast verified against buoy observations

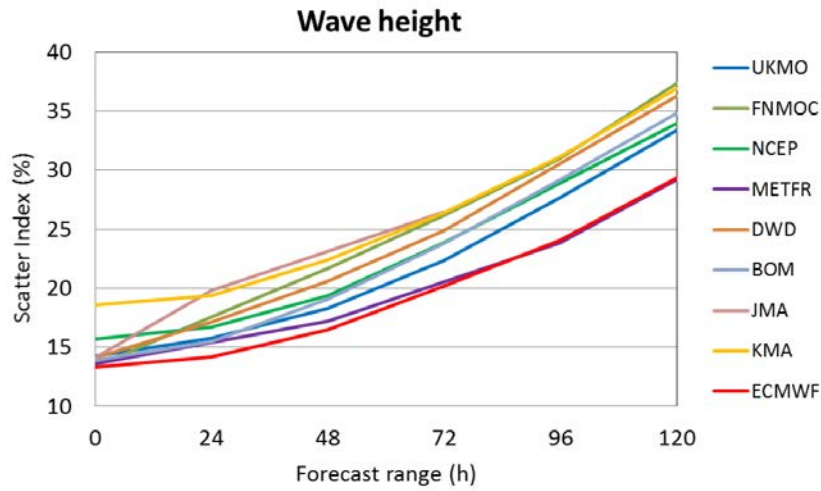


Figure 5.5: Verification of different model forecasts of wave height using a consistent set of observations from wave buoys

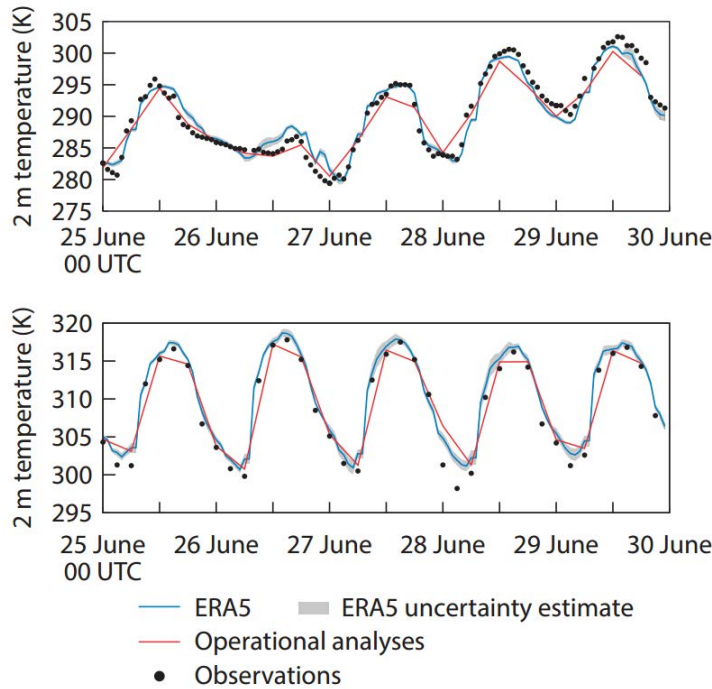


Figure 5.6: Hourly 2-metre temperature data of ERA5 reanalysis compared to in-situ observations with the uncertainty associated

## 5.2 ERA5 brief description

The ERA5 reanalysis is produced with a sequential data assimilation scheme, advancing forward in time using a 12-hourly analysis cycles. In each cycle, available observations are combined with prior information from a forecast model to estimate the evolving state of the global atmosphere and its underlying surface. This involves computing a variational analysis of the basic upper-air atmospheric fields (temperature, wind, humidity, ozone, surface

pressure), followed by separate analyses of near-surface parameters (2m-temperature and 2m-humidity), soil moisture and soil temperature, snow and ocean waves. The analyses are then used to initialise a short-range model forecast, which provides the prior state estimates needed for the next analysis cycle. The forecast model has a crucial role in the data assimilation process. Use of the model equation makes it possible to extrapolate information from locally observed parameters to unobserved parameters in a physical meaningful way, and also to carry this information forward in time. The skill and accuracy of the forecast model determines how well the assimilated information can be retained, better forecasts mean that smaller adjustments are needed to maintain consistency with observations as time involves.

### 5.2.1 Ocean waves

The ocean waves analysis in ERA5 incorporates an optimal interpolation scheme to constrain predicted wave spectra using altimeter wave height observations. ERA-Interim (ERA5 predecessor) used reprocessed ERS-1 and ERS-2 data from ESA, and near-real-time data from ENVISAT, JASON-1, and JASON-2, as received by ECMWF operations. Since ERS-2 and ENVISAT follow the same ground tracks with a separation of only 20 min, ERS-2 data were blacklisted when ENVISAT became available. No observation of wave height were available to constrain the ocean wave spectra prior the introduction of ERS-1 in August 1991. Daily coverage of a single satellite-borne altimeter represents approximately 10% of the number of grid points in the wave model. Consequently, over time, the percentage of the total domain for the wave model constrained daily by observations fluctuates between about 10% to about 20% (when two satellites are available) and so on with more satellites available. Unfortunately, the altimeter only yields significant wave heights and wind speeds over a small footprint.

A more accurate description of the sea state requires the full two-dimensional wave energy spectrum: such observations, albeit neither necessarily fully comprehensive nor independent, are already available with the ERS synthetic aperture radar (SAR). With the launch of ENVISAT, an advanced SAR with a higher spectral resolution operates at twice the current ERS data coverage by providing data every 100 km along the SAR swath over the oceans. Here is reported a table with all the satellites used by ERA5 to measure the wave height (Fig.5.7).

Satellite name	Satellite agency	Measured data
ERS-1 / 2	ESA	Wave Height
ENVISAT	ESA	Wave Height
JASON-1	CNES/NASA	Wave Height
JASON-2	CNES/NOOA/NASA	Wave Height
CRYOSAT-2	ESA	Wave Height
SARAL	CNES/ISRO	Wave Height

*Figure 5.7: ERA5 Satellites for Wave height observations*

### 5.3 IFS quick view

ERA5 is produced using the 4DVar data assimilation of the ECMWF's Integrated Forecast System (IFS) which, for wave elaboration, is based essentially on the WAM model exposed before. Although, the ECMWF version of WAM is basically following the same structure as the original version, there are also important differences to be noted. In particular, the ECMWF version takes full advantage of grib coding and decoding both for the integrated parameters and the two dimensional spectrum. The advantages of grib coding are that the fields are archived in a platform independent form and that the size of the fields reduces by a considerable factor. The second main difference is exposed with Fig. 5.8:

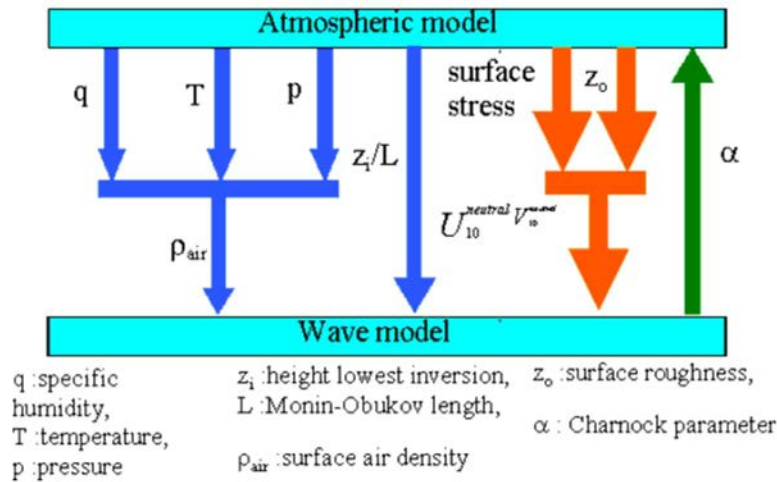


Figure 5.8: IFS ERA5 model

The Figure 5.8 is referred to the integration between two different models for the IFS used to produce the ERA5: in particular, it's known (see Chapter 3) that WAM model needs the friction velocity  $u^*$  but in this context it's available only winds at 10 metres height from the sea surface. A proper solution proposed on the IFS is to transform the surface winds (at 10 metres) into their neutral wind counterparts, using the atmospheric surface stress.

In second instance, it has to be highlighted that there're more degrees of freedom than observations because the altimeter satellites only provides the significant wave height. Thus, in the IFS model, instead of estimate the full state vector, it estimates only the significant wave height  $\mathbf{H}$ , the data vector consists than of the first-guess model wave heights, interpolated to the locations of the altimeter observations: the equation that describe the interpolation procedure so is the following one

$$H_i^a = H_i^f + \sum_{j=1}^{n_{obs}} W_{ij} (H_j^o - H_j^f) \quad (5.1)$$

in which  $H_i^a$  is the analysed significant wave height field,  $H_i^f$  is the wave height field computed by WAM,  $H_j^o$  is the wave height field observed by altimeter satellites and  $W_{ij}$

is the interpolation function.

There are two quantities that are computed at each grid point of the wave model, the *two dimensional wave spectrum*  $F(f,\theta)$  and the total stress  $\tau$  for a given wind forcing.

## 5.4 Considered parameters and how they're obtained

The following list of parameters used during the elaboration has been found on ECMWF website and reported for completeness and consistency with the results exposed at the end of paragraph 3.5.

- $H_s$ : Significant height of combined wind waves and swell, *"Better known as the Significant Wave Height. The significant wave height is defined as 4 times the square root of the integral over all directions and all frequencies of the two-dimensional wave spectrum. The integration is performed over all frequencies up to infinity"*;
- $T_p$ : Peak wave period, *"Reciprocal of the frequency corresponding to the largest value (peak) of the frequency wave spectrum. The frequency wave spectrum is obtained by integrating the two-dimensional wave spectrum over all directions"*.

A comparison test has been done and reported at paragraph 6.4.



## Chapter 6

# Argentinian resource mapping

As can be seen in Figure 6.1 ([18]) Argentina doesn't present a good ocean wave resource, although the south emisphere of global ocean waves presents the higher values of wave power density. This is possibly due to an interruption of the "high energy density flow" that form a stagnation area, but the presence of that higher values in a neighboring area suggested to investigate for a possible influence of the sea state, also for the reasons exposed in Chapter 1.

This country has multiple good reasons for an installation of a wave energy harvesting plant, first of all has several km of coast, for more possible marine sites. Then, its national power mix needs green sources to untie the dependence from natural gas.

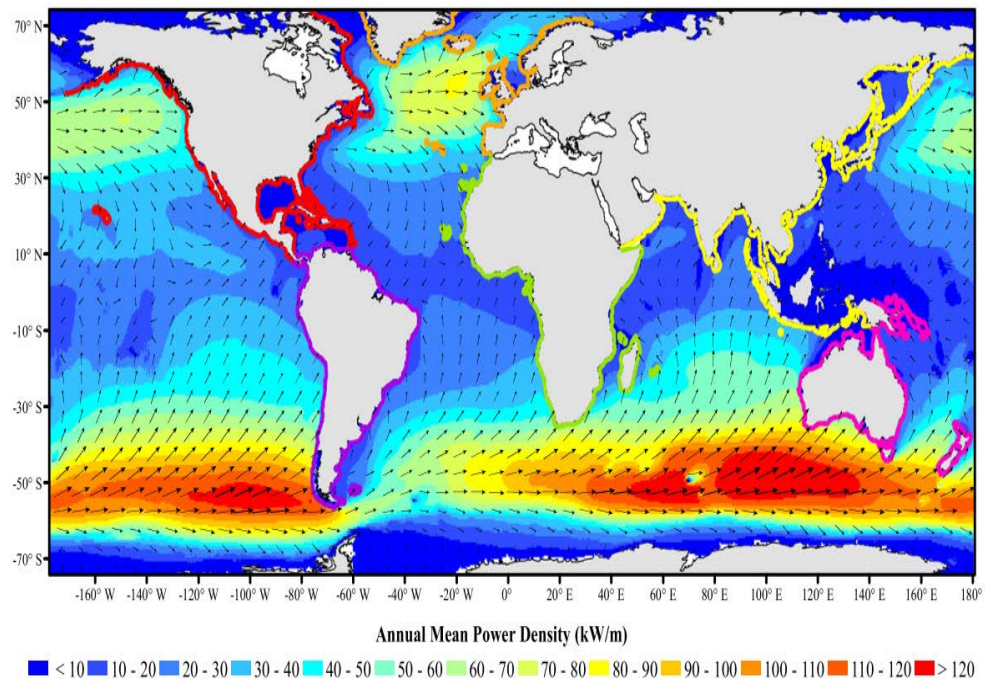
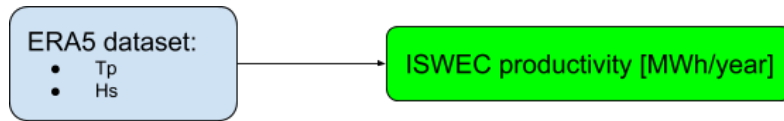


Figure 6.1: Annual Mean Power Density (kW/m), by K.Gunn, C.Stock-Williams [2012]

The main aim of this Chapter is represented by the following scheme:



The left blue block has just been exposed in Chapter 5, now will be presented the procedure to create the right green block.

## 6.1 Introduction

Considering the dimension of the datas to be treated Matlab © is the best choice to treat them using scripts and functions, also for the easy working environment that it offer when big matrices have to be analysed and for many toolboxes available and usefull for the work done here below.

Beginning from the sea state dataset (Chapter 5) it has been followed the following workflow (Figure 6.2) to get Argentina productivity map, starting from the top blocks and ending to the bottom-right block. In green color are showed the main Scripts, in lightblue color are showed the main Functions and in grey color are showed the data input for the following structure (a function or a script).

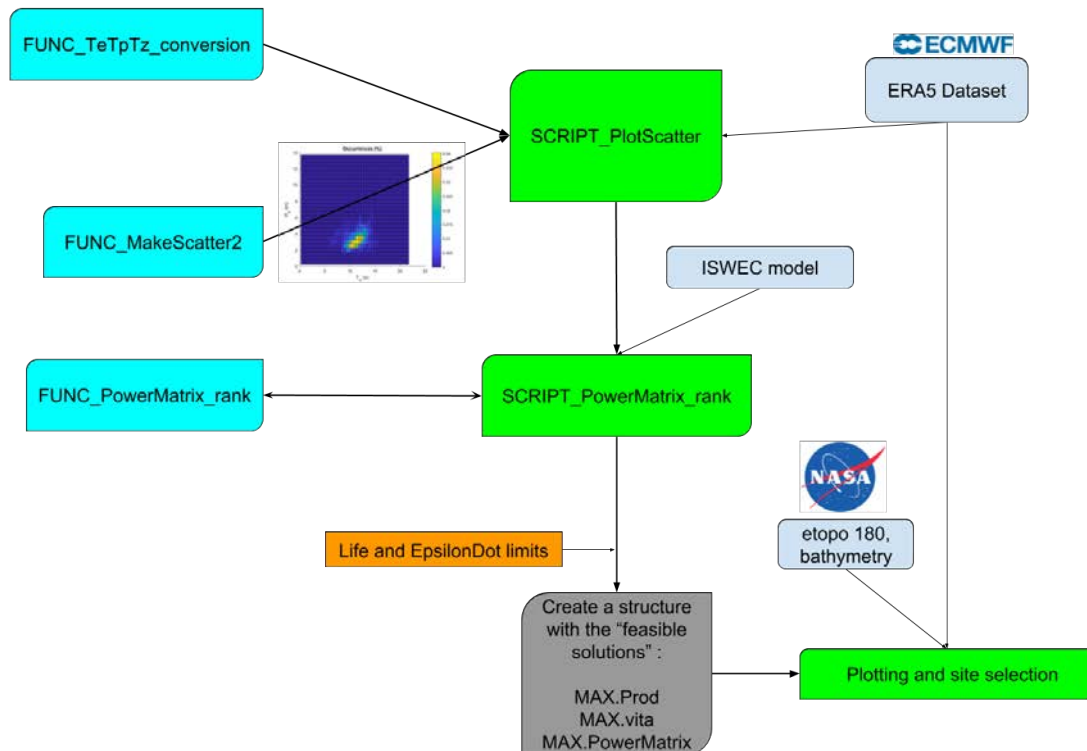


Figure 6.2: Workflow with highlighted the main blocks



## 6.2 Sea state study: wave resource map

It's practice when analyse a given sea spot (or better sea waves) to use a table that describe the sea state in terms of presence of a wave (described with its  $T_p$  and  $H_s$ ) in percentage in a year: this is the *Occurrences matrix*, a matrix in which each element is the sum of hours that a particular sea state (with that  $H_s$  and that  $T_p$ ) happened during the analyzed period (typically a year), the sum of all cells gives 1. An occurrences matrix for wave energy is like a daily solar hours diagram for a photovoltaic system. Here is reported an example for a offshore site near San Clemente del Tuyu (the location on which was plotted the Power Matrix in Fig.4.10):

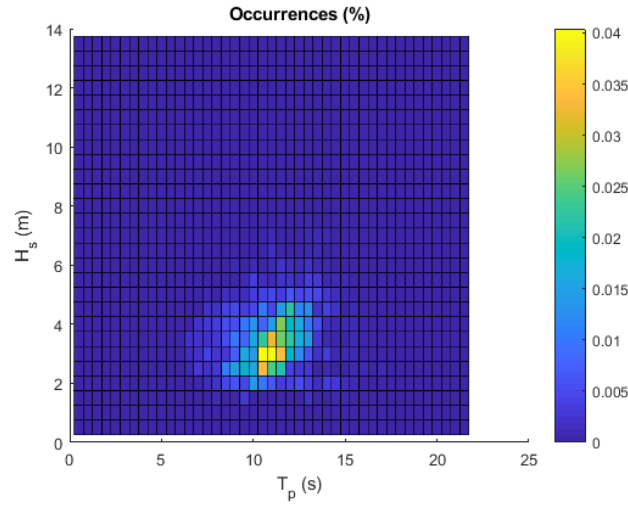


Figure 6.3: Occurrences matrix for offshore site near San Clemente del Tuyu

Looking at the occurrences matrix of a given sea spot it's possible to assess if a device, with its *Power Matrix* can or not harvest energy from waves: for example, standing on what showed in Chapter 4, ISWEC can exploit energy from low period-high elevation waves. Looking at figure 6.2 the first top 4 four main blocks are associated to the elaboration of parameters from ERA5 to create the mathematical structure that allow the interfacing with the ISWEC mathematical model. In detail, they create the structure of the Occurrences matrix for all the Argentinian marine sites using  $T_e$  instead of  $T_p$  as exposed in Fig.6.3 because for energetic calculations it's a more suitable quantity, the conversion is done using the wave spectrum exposed in Chapter 3 and here reported.

### ***FUNC\_TeTpTz\_conversion***

The conversion from  $T_p$  to  $T_e$  can be for first instance computed with the following simple relation:

$$T_e \cong 0.858 T_p \quad (6.1)$$

For a more accurate evaluation of the sea state it's preferable to use the frequency spectrum, just exposed in Chapter 3: JONSWAP spectrum allow to convert that two quantities with a "conversion matrix" that trivially use relation 3.8 specified for Energy and Peak

periods (Chapter 3), implemented in *FUNC\_TeTpTz\_conversion* script.

Furthermore it's computed the *Power density matrix* that show the well known wave measure kW/m instead of percentage in a year, with the following relation for *irregular waves* (just reported in Chapter 3):

$$P_d \cong 0.49 H_s^2 \cdot T_e \quad (6.2)$$

and it depends on the propagation conditions of the wave: *deep water* or *shallow water* [25]. The sum of all cells gives the *yearly average power density*, that is the totality of the available resource in an year. Here in Fig.6.4 is reported that matrix for the same marine site exposed before, it's possible to see that the most powerful wave has a power of more 2 kW/m but it's not the most recurrent, according to the Occurrences matrix of Fig.6.3:

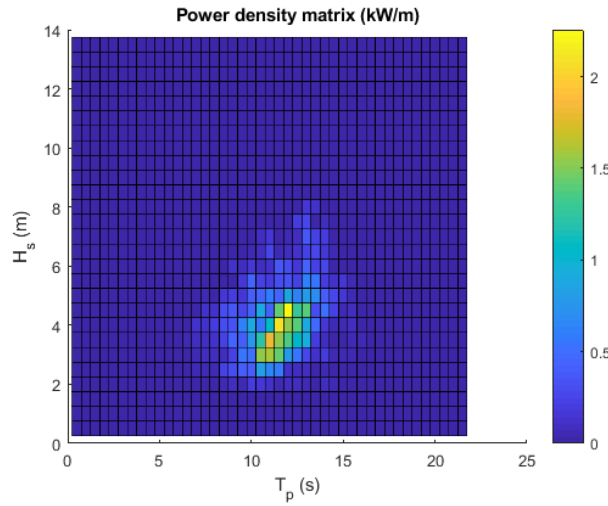


Figure 6.4: Power density matrix for the same spot reported in Fig.6.3

and in Fig.6.8 is reported the yearly average power density for the whole argentinian sea. Looking at Fig.6.1 by K.Gunn, C.Stock-Williams [2012] exposed before it is possible to notice that the resulting data are the same, giving confidence on the procedure done up to this point. A second validation is presented in 6.4.

### 6.3 Device rank on the sea state: productivity map

The second step to be done is to interface ISWEC machine with the mathematical sea model just exposed with that two matrices: as stated in Chapter 4 ISWEC machine is equipped with a mathematical model that easily allow the interfacing with the sea by other matrices. But this operation will not be done directly because in that way it draw a result that hasn't got real engineering base, a cost function is thus the right connection to draw a more accurate result. In a first moment, the interfacing between the sea state and

the ISWEC device can be computed with the following relation:

$$E_{prod,y} = \sum (M_{occ} \cdot P_m) \frac{365 \cdot 24}{1000} \left[ \frac{MWh}{year} \right] \quad (6.3)$$

in which for a given marine site the yearly production is calculated as the product of the sea state matrix  $M_{occ}$  (Occurrences matrix) and ISWEC Power matrix  $P_m$  (Chapter 4). But it's not correct at all, keep reading.

So the main target of this second step is to create a structure that consider a cost function, or better, the machine usury. In this way the best solution found will be computed with an economical model too that consider the following quantities: the mechanical usury, the device useful life and the productivity, the combination gives the best solution.

To consider the ISWEC mechanical usury has been introduced two negative gains,  $G\_Ceq$  and  $G\_TDelta$ , the first one show how much the ISWEC gyroscope bearings are loaded in terms of mechanical torque ( $\epsilon$  axis of Fig.6.5, the one on which is coupled the PTO), the second one show how much the ISWEC mechanical structure is loaded in terms of forces ( $\delta$  axis of Fig.6.5, blue part of Fig.4.3).

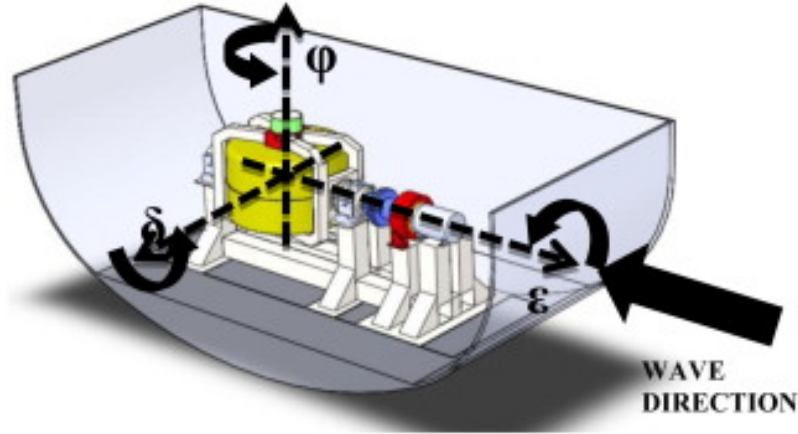


Figure 6.5: ISWEC main rotating axes

These two parameters are implemented in two nested cycles (Fig.6.6) that increase each one of them from zero to 2 for  $G\_Ceq$  and from zero to 0.2 for  $G\_TDelta$ , both of them with step 0.05. For each couple of values ( $41 \cdot 5 = 205$  total couples) there's a further nested cycle that for all ISWEC Power Matrix cells calculates: the Power Gross, Bearing losses, PTO losses, Seal losses, the structure equivalent load so the net power and finally a score called *ranking*:

$$ranking = Power_{netta} \cdot \frac{RankGain(1)}{65K[W]} + C_{eq} \cdot \frac{RankGain(2)}{7 * 10^5[N]} + T_{delta} \cdot \frac{RankGain(3)}{8 * 10^5[N]} \quad (6.4)$$

More the value of  $G\_Ceq$  and  $G\_TDelta$  less the "weight" of that given examination: if  $G\_Ceq$  and  $G\_TDelta$  are equal to zero (first run of the two nested orange cycles, Fig.6.6)

the cycle calculate the maximum ISWEC power value and it doesn't take into account the gains (in this case the gains are "weight zero"), if instead  $G_{Ceq}$  and  $G_{TDelta}$  grow up, the productivity value has to be weighed with both of them. Then, on the maximum score is computed the Mean Net Power ([W]). The maximum score represent the best give-and-take for the device in that given sea state. So once finished the green cycle in Fig.6.6 and so once defined the ISWEC power matrix for that sea state (characterized by latitude, longitude) and for the given gains values, it's computed the productivity with Eq. 6.3.

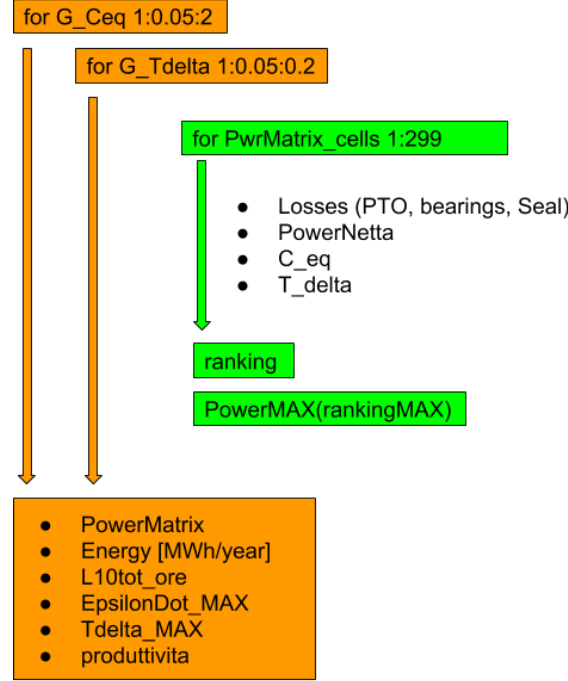


Figure 6.6: Implemented nested cycles

*RankGain* is a vector that carry the gains values for each cycle:

$$RankGain = \begin{bmatrix} 1 & G_{Ceq} & G_{TDelta} \end{bmatrix} \quad (6.5)$$

Once finished the whole process the system create a big matrix (called *OUT* in the code) that for all argentinian ocean sites holds all possible solutions found.

Now this big matrix is filtered applying many limits to find solutions that better fit with the real life engineering, so lower limit of useful life 15 years (with the  $L_{10toth}$  parameter) and upper limit on the gyroscope rotation axis speed 40 rpm (with the  $\epsilon$  parameter), all other tests are excluded for obvious lack of interest.

The productivity map result is reported in Fig.6.8.

## 6.4 Validation for Mediterranean basin

As a further proof of the reliability of the procedure done about the assessment of the wave potential in paragraph 6.2, has been made a comparison with the result presented in Fig.6.8 and the result of a work done by G.Sannino in an important article [21] regarding the Mediterranean basin wave potential.

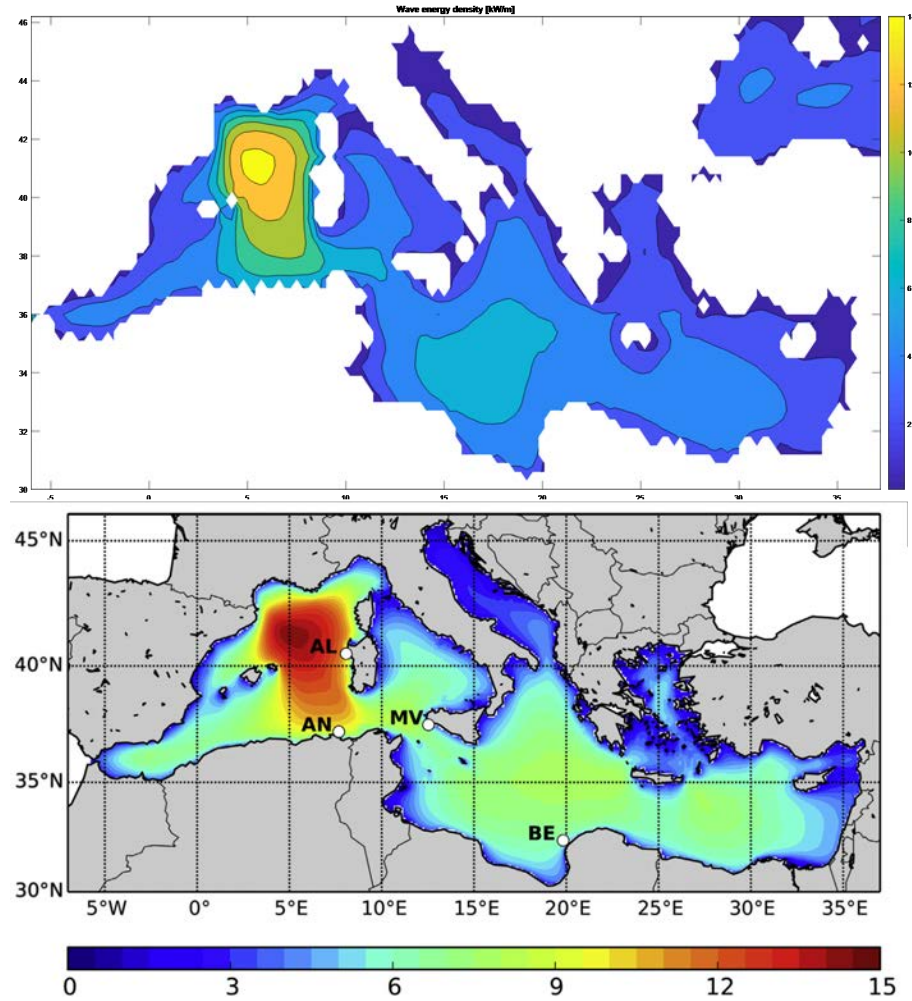


Figure 6.7: Two same results from different studies of wave potential: the top one by this thesis, the bottom one by Sannino [21]

As can be seen there's a high correspondence level, especially for the high intensity area near Sardinia. The only main difference is represented by the resolution of the information: dataset resolution is the same for that two figures but Sannino [21] forced the plotting with a bathymetry model that allow to get a much more higher resolution and to fill empty areas with the nearest value of wave power density.

## 6.5 Results

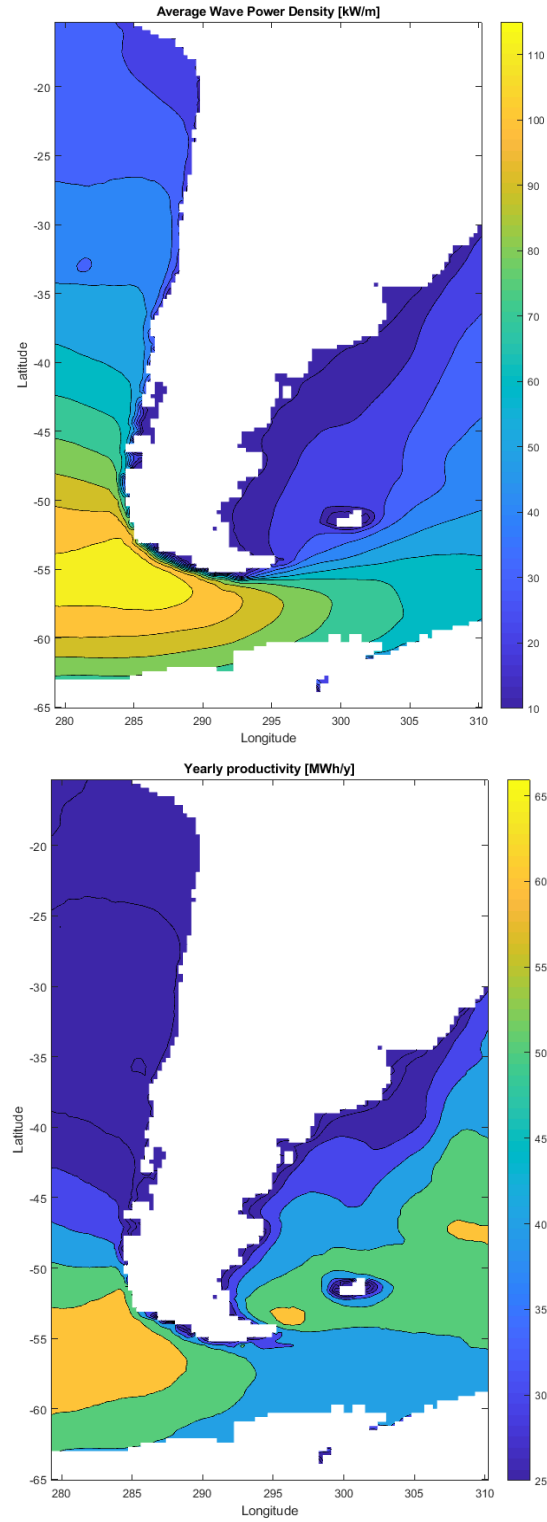


Figure 6.8: Average wave power density for the whole argentinian sea [kW/m] and Yearly ISWEC productivity [MWh/y]

## Chapter 7

# Site selection and tecno-economic evaluation

There are many aspects to be considered when it has to be chosen a site for a power plant installation, such as environmental, economic, technical and socio-political. For this thesis purpose is used an *exclusion siting criteria* ([31]) that consider the following decision parameters: Wave Energy Potential (WEP), Water Depth (WD), Distance from shore (DS), Connection to Local Electrical Grid (CLEG), Population Served (PS), Distance from Ports (DP) and presence of restricted area such as natural parks. *WEP* in this context is replaced by Yearly productivity (YP) that represent a more accurate information considering this chapter aim. For this thesis purpose are not considered environmental impacts such as the presence of a special ecosystem, the most important effects that a system like ISWEC can do are acoustic noise, vibrations and electromagnetic fields. Since that *exclusion siting criteria* becomes different economic scenarios for each installation, briefly represented in the figure below.

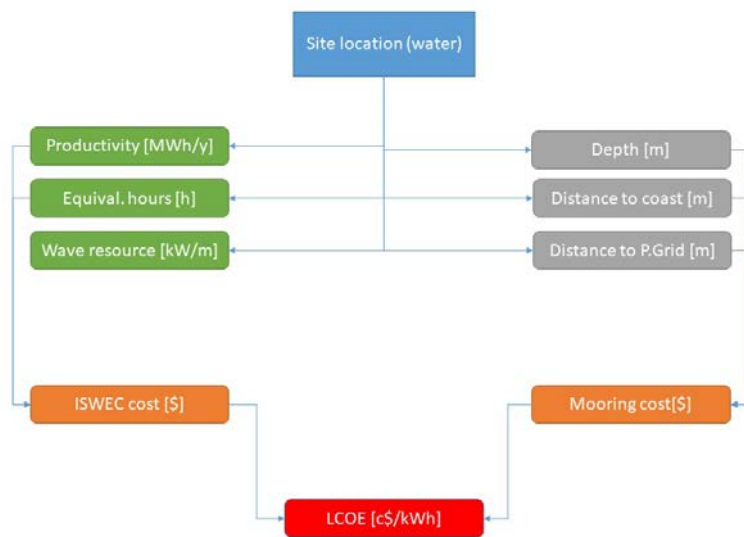


Figure 7.1: Diagram that shows how the LCOE is composed

## 7.1 Bathymetry database

To get the bathymetry information for each site the best solution is presented by a database released by NOAA (National Oceanic And Atmospheric Administration, USA) called Etopo. ETOPO1 is a 1 arc-minute global relief model of Earth's surface that integrates land topography and ocean bathymetry. Built from global and regional data sets, it is available in "Ice Surface" (top of Antarctic and Greenland ice sheets) and "Bedrock" (base of the ice sheets). Interfacing Etopo with the model created before (etopo database is trivially a matrix, the only difficult is due to longitude  $+360^\circ$  correction), it's possible to add the depth information to the productivity map, Fig.6.8.

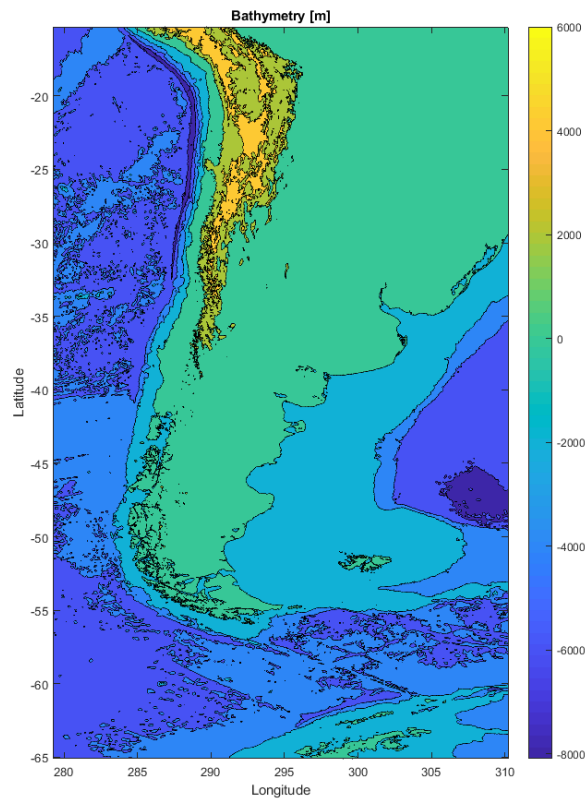


Figure 7.2: Argentina bathymetry plotted with etopo180 database

The integration with this depth matrix allow to determine the depth information for each site with 1 km spatial resolution (much higher than 30 km resolution of ERA5 dataset presented before) and beside, setting the depth in a range from 1 m to -1 m it's possible to find the *coast longitude-latitude matrix*, very important later.

## 7.2 Distance to power grid

To calculate the distance between an hypothetical marine site and the coast has been used a function called *pos2dist*: as reported in Mathworks, "Calculate distance between two points on earth's surface given by their latitude-longitude pair. Choose method 1 or



2. Method 1 uses plane approximation, only for points within several tens of kilometers; Method 2 calculates spheric geodesic distance for points farther apart, but ignores flattening of the earth. Output is in km.”, for the purpose of this thesis has been used method 1 since that the offshore farm will not be too much distant from the coast. So, the distance from ISWEC offshore farm to the onshore power grid has been computed as follows: the first component, from the farm to the coast, the second component from the coast to the power grid.

For the first component, for each sea point it's computed the distance to all the points of *coast longitude-latitude matrix* and then is selected the minimum value. The second component needs the national power grid, here below presented.

### Argentina's power grid

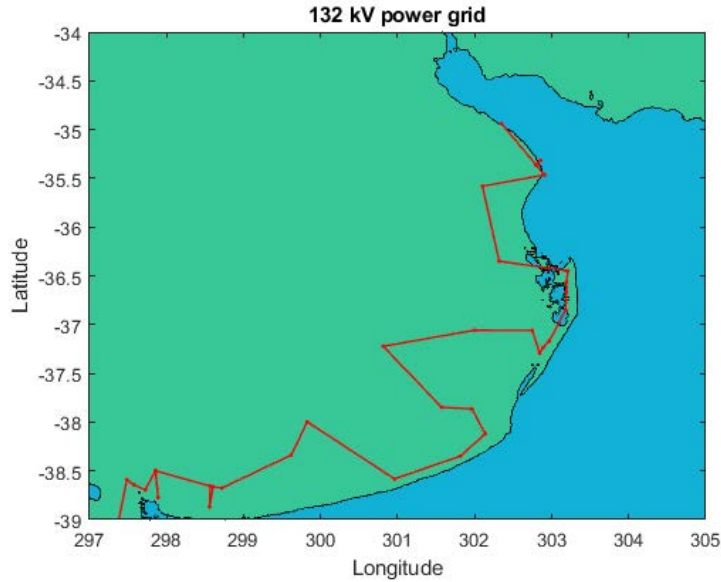
An important information is related to the power grid: indeed, firstly it has to be present near the coast of interest and then it has to be sufficiently close to the coast that receive the cable from the ISWEC offshore farm.



Figure 7.3: Argentinian power grid

To get Argentina's power grid in a matrix points exploitable in Matlab environment has been used a very powerful Matlab tool called *GRABIT* as in Mathworks. *GRABIT* convert

a jpg image in a matrix by setting a reference x-y system and selecting the interest points. The difficulty in this step is due to the terrestrial curvature that distorts a vertical line in a plane. So, once downloaded the power grid jpg image from *CAMMESA*, the Argentinian society for electrical market, has been created the matrix of interest choosing the 132kV stations along the coast. Here is reported the result for Buenos Aires area:



*Figure 7.4: 132kV grid, Buenos Aires area*

### **Focus on Patagonia's region: possible development**

As can be seen in Fig.7.3 the whole southern part of the country is disconnected from national electrical grid and so it isn't suitable for an ISWEC farm installation. It can be rather suitable for a stand-alone farm that covers the electrical demand of that Patagonia's countries (nowadays these countries are fed with a combination of 42% hydroelectrical plants, 45% thermal plants and 13% wind farms, [11]), solution that is out of this thesis purpose.

### 7.3 Presence of Natural Parks or Marine Protected areas

To find a list of all natural national parks on the coast and marine protected areas (MPAs) has been used online resources that plots in a map both of them. In detail, for natural parks the source is <https://tools.wmflabs.org/geohack/geohack.php> and the result has been summarized in the following table.

Table 7.1: List of the most important coastal National Parks

Name	Latitude	Longitude	Area [ $km^2$ ]
R.d.B. Parque Costero del Sur	-35.3207	-57.2209	235
R.N. de Bahia de Samborombon	-36.0469	-57.3665	93
R.d.B. Peninsula Valdes	-42.5349	-64.1739	28000
R.d.B. Patagonia Azul	-44.5298	-65.8109	31000
P.N. Monte Leon	-50.3218	-68.9886	620

Analysing the national grid map and the natural coastal parks map can be noted that the national 132 kV grid is obviously installed close to natural parks but not inside, so when the algorithm calculate the distances from the marine site to the national power grid already avoids the natural parks.

Regarding Marine Protected Areas an integration with the algorithm was necessary, as what has been done for the national power grid. *Atlas of marine protection* [4], the online source that shows the most important marine protected areas around the world, unfortunately doesn't allow to download a high-resolution image to use in Matlab GRABIT, so once finished the overall siting selection procedure has to be compared with Fig.7.5 to avoid restricted areas (however they're few, so this step is quick).

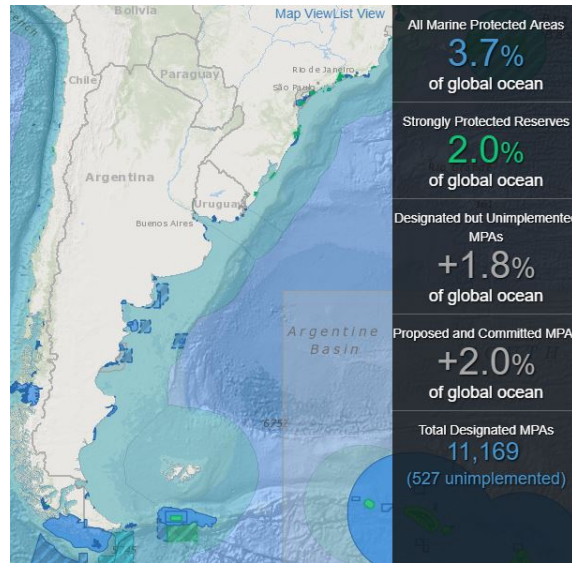


Figure 7.5: Marine protected areas of argentinian basin, <http://www.mpatlas.org/map/mpas/>

## 7.4 Cost of kWh for a 10 device farm

When the LCOE (Levelised Cost Of Energy) of an energy plant has to be computed, the classic relation used in several context is the one proposed by NREL (National Renewables Energy Laboratory) and called *simplified*, here reported:

$$sLCOE = \frac{\text{overnightcapitalcost} * CRF + \text{fixedO\&Mcost}}{8760 * \text{capacityfactor}} + \text{variableO\&Mcost} \quad (7.1)$$

in which:

- CRF, capital recovery factor, is the ratio of a constant annuity to the present value of receiving that annuity for a given length of time, computed as

$$CRF = \frac{i(1+i)^n}{(1+i)^n - 1}; \quad (7.2)$$

where n is the number of annuities received, or better ISWEC life;

- overnight capital cost, it's measured in dollars per installed kilowatt (\$/kW) and it allow a comparison with other plants, the relation for that is explained later;
- capacity factor, it's a fraction between 0 and 1 representing the portion of a year that the power plant is generating power, it's computed dividing by each marine site productivity by the maximum productivity (ISWEC power[W] \* 8760); it's important to underline that hydrodynamic interaction between each device has been neglected;
- O&M costs, device operation and maintenance cost, they depends on several factors and in this context, due to a lack of experience for ocean installations, they're assumed equal to Pantelleria's O&M costs;

Looking at Fig.7.1, to compute the left grey blocks costs (depending on the marine site) has been assumed ISWEC CAPEX equal to 1 (or 100%), so each cost is a percentage of CAPEX, for example the cable cost is given in %CAPEX/m; each percentage was kindly provided by Wave For Energy S.r.l. based on their experience with Pantelleria installation. So, once computed the mooring cost, offshore cable cost and onshore cable cost, choosing the marine sites with depth between 30 metres and 100 metres, again depending on Wave For Energy S.r.l. experience, has been computed an overall cost in %CAPEX. This cost is part of *fixed O&M costs*, to which must be added a second O&M cost (€/kWp/y), taken the same as Pantelleria (probably this component should be greater in ocean). The overall process has been done for four hypothetical ISWEC CAPEX value, the results are here reported: in Fig.7.6 are showed all the possible installation points and the related LCOE [€/kWh], the last map of the overall procedure proposed in this thesis; than in Fig.7.2 for 9 marine sites is showed how the LCOE vary with ISWEC CAPEX (from LCOE 1 with the lower ISWEC CAPEX to LCOE 4 with the upper ISWEC CAPEX).

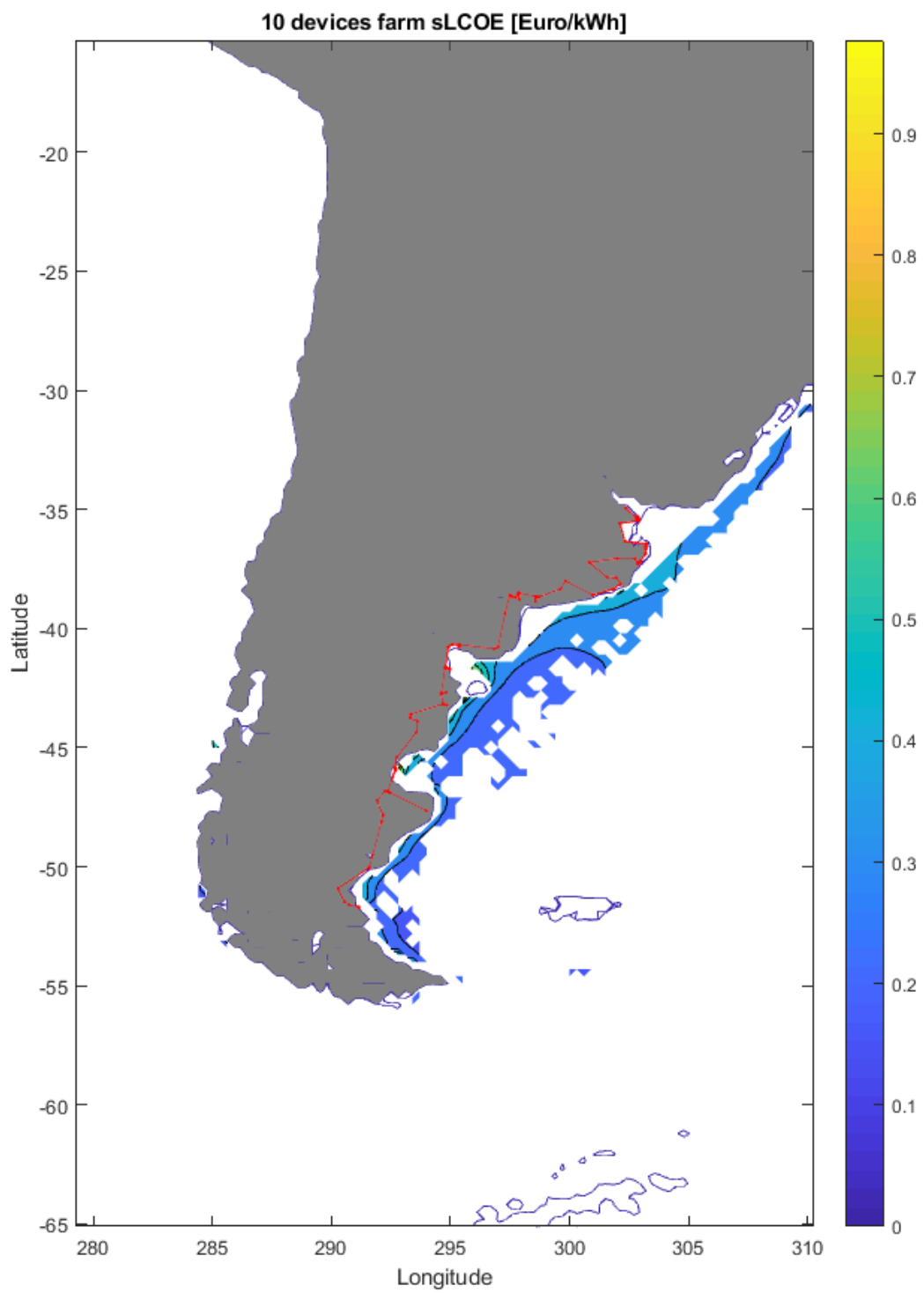


Figure 7.6: 10 devices farm sLCOE [ $c\text{€}/\text{kWh}$ ]

Marine site	Longitude	Latitude	Depth [m]	Wave potential [kW /m]
1	305.1	-36.3	-45	14.5
2	303.6	-38.1	-92	14.5
3	301.5	-40.2	-92	15.13
4	295.5	-45	-100	14.2
5	297.6	-45.9	-94	19.92
6	294.9	-47.7	-82	13.7
7	293.1	-46.2	-98	6
8	293.4	-52.2	-98	14.25
9	293.7	-53.1	-89	14.5

Productivity [MWh/y]	LCOE 1 [€/kWh]	LCOE 2 [€/kWh]	LCOE 3 [€/kWh]	LCOE 4 [€/kWh]
24.43	0.267	0.3278	0.3879	0.448
22.32	0.293	0.3589	0.4246	0.4904
27.04	0.242	0.2962	0.3505	0.4048
35.83	0.183	0.2235	0.2645	0.3055
43.83	0.15	0.1828	0.2163	0.2498
33.92	0.193	0.2361	0.2794	0.3227
18.82	0.347	0.4255	0.5035	0.5815
51.3	0.127	0.1562	0.1848	0.2134
52.27	0.136	0.1532	0.1813	0.2094

Table 7.2: Informations of Fig.7.7 marine sites

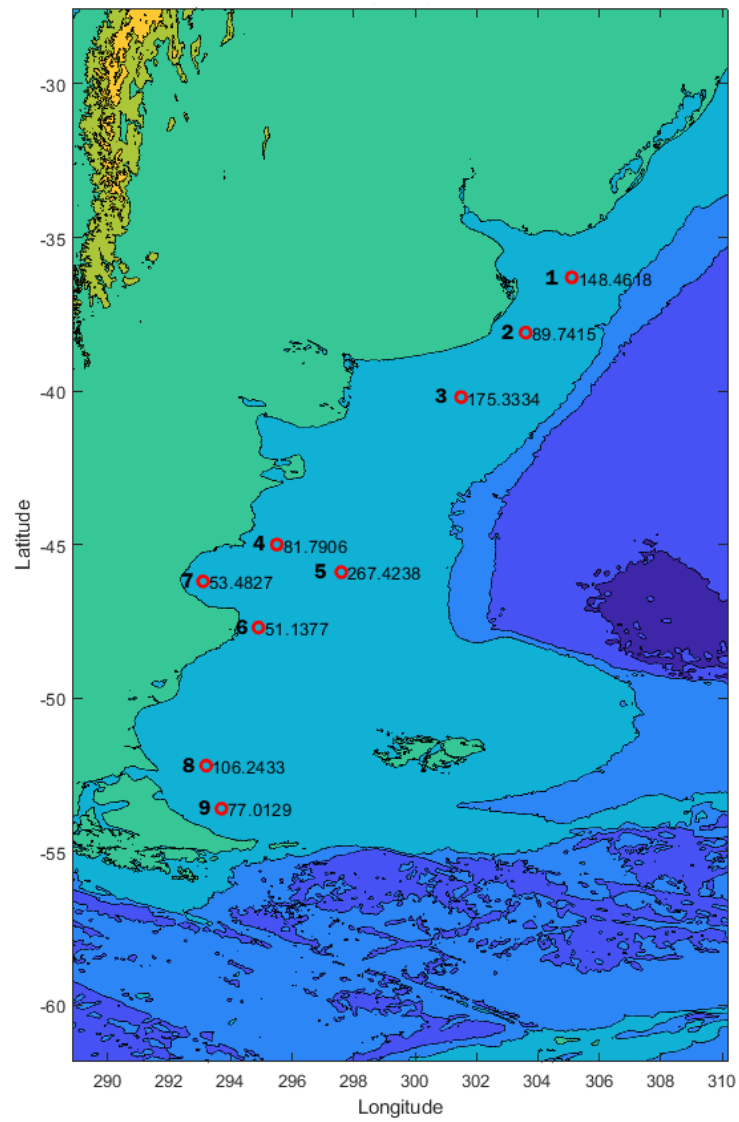


Figure 7.7: Marine sites used for the assessment and the distance [km] to the coastline





## Chapter 8

# Conclusions

This thesis takes place in the context of the renewable energy sources, in particular in the marine field, that is year by year taking more interest due to the enormous potential offered by the waves and also to many advantages compared to other renewable sources: continuity of the source, accurate forecasts and high energy density (kW/m). But as stated this field is nowadays in a development state and the countries that carry this development are few, Great Britain and Denmark first of all. To date, there are several wave energy converters and each one of them has singular characteristics that fits best in a particular environment or in a given sea basin; the commercial phase for many of these is not so far. This thesis purpose is to study the productivity of ISWEC, a wave energy converter that harvest energy by a gyroscope embedded in a pitching hull, on Argentinian sea basin that offer sea state very similar to Mediterranean one. The goal of this thesis is to find and map high productivity Argentinian basin spots related to ISWEC behaviour and to environmental informations.

So the procedure, starting from the sea state and ending on the energy-price map, is the following: once downloaded significant height vector and peak period vector from ERA5 online database, a ECMWF (European Center for Medium-range Weather Forecasts) dataset, the first step was to create the Occurrences matrix for all marine sites of Argentinian sea, having the possibility to understand for each site which is the most recurrent wave in terms of significant height and peak period. Here a bracket has to be opened: the ERA5 dataset is the last release of a dataset series by ECMWF, it's highest resolution dataset and looking at ECMWF forecast validation (the forecast system allow to build the dataset) there a high-correspondence level between the measured data and the re-analysed data (examples done for 2m temperature). A further proof of the reliability of the dataset and the procedure has been done for Mediterranean basin, comparing this work result with Sannino's (the authors of many studies on Mediterranean basin wave potential) result. Then ISWEC model has to be interfaced with the sea state model (represented by the occurrences matrix just exposed) and this is the main advantage carried by this thesis: the procedure will not be done directly but with a ranking cycle that weight each marine site productivity (such as MWh/y) with two gains, the first one represent ISWEC bearing load and the second one represent ISWEC mechanical structure, the whole procedure allow to delete not feasible solutions like high productivity but short bearing life. Now the last step is to integrate the

productivity map obtained before with environmental informations such as bathymetry, distance to the shoreline, distance to electrical power grid, presence of natural parks or marine protected areas. To do this, the model build so far is integrated with 132 kV power grid matrix (get using a Matlab tool), with the bathymetry matrix (get using an online service called Etopo) and with the coastline matrix.

The most interesting marine areas are located in the half southern part of the country, the less densely populated.

## 8.1 Afterwards

With the overall process, starting from the sea state information, it's possible to find the most productive (not only in MWh/y but also considering economic factors like mooring costs, cable costs, etc) sea areas in a coloured map. This process can be done for several part of the World, as long as the wave spectrum respect Jonswap conditions. Since this consideration can be done many possible developments of this thesis: first of all it's possible to apply this method to Mediterranean basin, highlighting most productive areas for possible installations. Then it's possible elaborate on economic analysis, because for this thesis many aspects have been supposed due to lack of experience.

In this thesis context, each ISWEC farm is connected to the national power grid: the most important advantage of a device like that is the possibility to install it (only 4 anchors per device are needed) and feed isolated zones not connected to national power grid, such as Patagonia's countries. Patagonia is totally unplugged from Rio Gallegos to 500 km south; these countries are nowadays fed by diesel generators or worse with old wood systems.

# Bibliography

- [1] Informe mensual, principales variables del mes.
- [2] Ocean energy holds great potential for europeâs low-carbon future.
- [3] A review of wave energy converter technology.
- [4] title.
- [5] Global manufacturing competitiveness index, 2016, 2016.
- [6] Informe anual, 2016, 2016.
- [7] European Commission [2012]. Communication from the commission to the european parliament, the council, the european economic and social committee and the committee of the regions: Blue growth, opportunities for marine and maritime sustainable growth.
- [8] International Energy Agency. World energy outlook 2016. 2016.
- [9] Giovanni Bracco. Iswec: a gyroscopic wave energy converter, 2010.
- [10] A. Brito e Melo and Luis Villate. Oes 2016 annual report, technical report, ocean energy systems (oes), 2016.
- [11] Argentina CAMMESA. Informe mensual, principales variables del mes. 2018.
- [12] McCullen P. Falcao A. Fiorentino A.-Gardner F. Hammarlund-K. Lemonis G. Lewis T. Nielsen K. Petroncini S. Pontes M.-T. Schild B.-O.SjÃ¶strÃ¶m P. SÃ¸resen H. C. ClÃ©ment, A. and T. Thorpe. Wave energy in europe: current status and perspectives.
- [13] A.Uihlein D.Magagna, R.Monfardini. Jrc ocean energy status report 2016 edition, 2016.
- [14] A.J.Simmons P.Berrisford P.Poli S.Kobayashi U.Andrae M.A.Balmaseda-G.Balsamo P.Bauer P.Bechtold-A.C.Beljaars L.van de Berg J.Bidlot N.Bormann C.Delsol R.Dragani M.Fuentes A.J.Geer L.Haimberger-S.B.Healy H.Hersbach E.V.Holm-L.Isaken P.Kallberg M.Kohler M.Matricardi A.P.McNally B.M.Monge-Sanz J.J.Morcrette B.K.Park C.Peubey P. de Rosnay C.Tavolato J.N. Thepaut D.P.De,

- S.M.Uppala and F.Vitart. The era-interim reanalysis: configuration and performance of the data assimilation system. April 2011.
- [15] The Economist. Power buoys.
  - [16] European Commission Directorate General for Maritime Affairs and Fisheries [2014]. Blue energy - action needed to deliver on the potential of ocean energy in european seas and oceans by 2020 and beyond.
  - [17] G.Mattiazzo G.Bracco, E.Giorcelli. Iswec: A gyroscopic mechanism for wave power exploitation. June 2011.
  - [18] Stock-Williams Clym Gunn, Kester. Quantifying the global wave power resource. 2012.
  - [19] M.Hall-M.Raffero G.Vissio, B.Passione. Expanding iswec modelling with a lumped-mass mooring line model. 2015.
  - [20] Falnes J. A review of wave-energy extraction. 2007.
  - [21] G.Sannino L.Liberti, A.Carillo. Wave energy resource assessment in the mediterranean, the italian perspective. Semptember 2012.
  - [22] Krishnil Prasad Young-Jin Cho Chang-Goo Kim Young-Ho Lee M. Rafiuddin Ahmed, Mohammed Faizal. Exploiting the orbital motion of water particles for energy extraction from waves. 2009.
  - [23] M.J.French. On the difficulty of inventing an economical sea wave energy converter: a personal view.
  - [24] Secretariat of the World Meteorological Organization. Guide to wave analysis and forecasting. 1998.
  - [25] Nicola Pozzi. Numerical modeling and experimental testing of a pendulum wave energy converter (pewec), 2018.
  - [26] P.Schaube. The argentine power system: current challenges and perspectives for the development of renewable energy. August 2015.
  - [27] Pelc R. and Fujita R.M. Renewable energy from the ocean. 2002.
  - [28] Paris REN21. Renewables 2017 global status report, 2017.
  - [29] J.Bidlot L.Ferranti F.Prates F.Vitart P.Bauer D.S.Richardson T.Haiden, M.Janousek. Evaluation of ecmwf forecasts, including 2016-2017 upgrades. December 2017.
  - [30] Thorpe T.W. A brief review of wave energy, technical report no.r120.
  - [31] Vagona D.G. Vasileiou M., Loukogeorgaki E. Gis-based multi-criteria decision analysis for site selection of hybrid offshore wind and wave energy systems in greece. June 2017.

- 
- [32] Giacomo Vissio. Iswec toward the sea, development, optimization and testing of the device control architecture, 2017.
  - [33] W.S.Parker. Reanalyses and observations, what's the difference? 2016.